DOE F 241.3
(2-01) p.1 of 2

UNITED STATES DEPARTMENT OF ENERGY (DOE)
Announcement of Scientific and Technical Information (STI)
(For Use By Financial Assistance Recipients and Non-M&O/M&I Contractors)

OMB CONTROL NO. 1910-1400

PART I: STI PRODUCT DESCRIPTION
(To be completed by Recipient/Contractor)

A. STI Product Identifiers

1. REPORT/PRODUCT NUMBER(s)
None

2. DOE AWARD/CONTRACT NUMBER(s)
DE-FC36-97ID13554

3. OTHER IDENTIFYING NUMBER(s)
None

B. Recipient/Contractor

Carnegie Mellon University, Dept. of Materials Science and Engineering, 5000 Forbes Ave., Pittsburgh, PA 15213

C. STI Product Title

Sustainable Steelmaking Using Biomass and Waste Oxides

D. Author(s)

Richard J. Fruehan

E-mail Address(es):
fruehan@andrew.cmu.edu

E. STI Product Issue Date/Date of Publication

09 30 2004
MM DD YYYY

F. STI Product Type (*Select only one)*

☒ 1. TECHNICAL REPORT
☒ *Final* ☐ *Other (specify)* _____

☐ 2. CONFERENCE PAPER/PROCEEDINGS

Conference Information (title, location, dates)

☐ 3. JOURNAL ARTICLE
a. TYPE: ☐ *Announcement Citation Only*
☐ *Preprint* ☐ *Postprint*
b. JOURNAL NAME

c. VOLUME _____ *d. ISSUE* _____
e. SERIAL IDENTIFIER (e.g. ISSN or CODEN)

☐ 4. OTHER, SPECIFY

G. STI Product Reporting Period

04 01 2000 Thru 09 30 2004
MM DD YYYY MM DD YYYY

H. Sponsoring DOE Program Office

Office of Industrial Technologies (OIT)(EE20)

I. Subject Categories *(list primary one first)*

32 Energy Conservation, Consumption and Utilization

Keywords: Steel

J. Description/Abstract

The project concentrated on the development of a productivity model for the Rotary Hearth Furnace (RHF) able to predict changes in productivity according to the type of carbon and iron oxides used as feed materials. This model is required to access the technical feasibility of a new process for ironmaking employing renewable energy in the form of wood charcoal to produce hot metal. The new process combines the RHF and a smelter to produce hot metal and allows the use of wood charcoal as energy source and reductant.

K. Intellectual Property/Distribution Limitations

(must select at least one; if uncertain contact your Contracting Officer (CO))

☒ 1. UNLIMITED ANNOUNCEMENT *(available to U.S. and non-U.S. public; the Government assumes no liability for disclosure of such data)*

☐ 2. COPYRIGHTED MATERIAL: *Are there any restrictions based on copyright?* ☐ *Yes* ☐ *No.*

If yes, list the restrictions as contained in your award document

☐ 3. PATENTABLE MATERIAL: THERE IS PATENTABLE MATERIAL IN THE DOCUMENT.
INENTION DISCLOSURE SUBMITTED TO DOE:
DOE Docket Number: S-
(Sections are marked as restricted distribution pursuant to 35 USC 205)

☐ 4. PROTECTED DATA: ☐ CRADA ☐ *Other, specify*

Release date (required) no more than 5 years from date listed in Part I.E. above ___ ___ ____
MM DD YYYY

☐ 5. SMALL BUSINESS INNOVATION RESEARCH (SBIR) DATA
Release date (required) no more than 4 years from date listed in Part I.E. above ___ ___ ____
MM DD YYYY

☐ 6. SMALL BUSINESS TECHNOLOGY TRANSFER RESEARCH (STTR) DATA
Release date (required) no more than 4 years from date listed in Part I.E. above ___ ___ ____
MM DD YYYY

☐ 7. OFFICE OF NUCLEAR ENERGY APPLICED TECHNOLOGY

L. Recipient/Contract Point of Contact *Contact for additional information (contact or organization name To be included in published citations and who would Receive any external questions about the content of the STI Product or the research contained herein)*

Dr. Richard Fruehan
Name and/or Position
fruehan@andrew.cmu.edu (412) 268-2677
E-mail *Phone*
Dept. of Mat'l Science and Engineering, Carnegie Mellon University, Pittsburgh, PA 15213

UNITED STATES DEPARTMENT OF ENERGY (DOE)
Announcement of Scientific and Technical Information (STI)
(For Use By Financial Assistance Recipients and Non-M&O/M&I Contractors)

OMB CONTROL NO.
1910-1400

PART II: STI PRODUCT MEDIA/FORMAT and LOCATION/TRANSMISSION

(To be completed by Recipient/Contractor)

A. Media/Format Information:

1. MEDIUM OF STI PRODUCT IS:
   ☒ Electronic Document ☐ Computer Medium
   ☐ Audiovisual Material ☐ Paper ☐ No Full-text
2. SIZE OF STI PRODUCT 108 Pages
3. SPECIFY FILE FORMAT OF ELECTRONIC DOCUMENT BEING TRANSMITTED, INDICATE:
   ☐ SGML ☐ HTML ☐ XML ☒ PDF Normal
   ☐ PDF Image ☐ TIFFG4
   ☐ WP-indicate Version (*5.0 or greater)* _____
   Platform/operation system _____
   ☐ MS-indicate Version (*5.0 or greater)* _____
   Platform/operation system _____
   ☐ Postscript _____
4. IF COMPUTER MEDIUM OR AUDIOVISUAL MATERIAL:
   a. Quantity/type (*specify)* _____
   b. Machine compatibility (*specify)* _____
   c. Other information about product format a user needs to know:
   _____

B. Transmission Information:

1. STI PRODUCT IS BEING TRANSMITTED:
   ☒ a. Electronically via E-Link
   b. Via mail or shipment to address indicated in award document (*Paper product, CD-ROM, diskettes, video cassettes, etc.)*
   _____
2. INFORMATION PRODUCT FILE NAME
   ☒ *(of transmitted electronic format)*
   CompiledTRP9902FinalReport.

PART III: STI PRODUCT REVIEW/RELEASE INFORMATION

(To be completed by DOE)

A. STI Product Reporting Requirements Review.

☐ 1. THIS DELIVERABLE COMPLETES ALL REQUIRED DELIVERABLES FOR THIS AWARD
☐ 2. THIS DELIVERABLE FULFILLS A TECHNICAL INFORMATION REPORTING REQUIREMENT, BUT SHOULD NOT BE DISSEMINATED BEYOND DOE.

B. Award Office Is the Source of STI Product Availability

☐ THE STI PRODUCT IS NOT AVAILABLE IN AN ELECTRONIC MEDIUM. THE AWARDING OFFICE WILL SERVE AS THE INTERIM SOURCE OF AVAILABILITY.

C. DOE Releasing Official

☐ 1. I VERIFY THAT ALL NECESSARY REVIEWS HAVE BEEN COMPLETED AS DESCRIBED IN DOE G 241.1-1A, PART II, SECTION 3.0 AND THAT THE STI PRODUCT SHOULD BE RELEASED IN ACCORDANCE WITH THE INTELLECTUAL PROPERTY/DISTRIBUTION LIMITATION ABOVE.

Release by (*name)* _____

Date ___ ___ _____
MM DD YYYY

E-Mail _____

Phone _____

AISI/DOE Technology Roadmap Program

Final Report

SUSTAINABLE STEELMAKING USING BIOMASS AND WASTE OXIDES

By

R.J.Fruehan
Carnegie Mellon University
Pittsburgh PA

September 30, 2004

Work performed under Cooperative Agreement
No. DE-FC36-97ID13554

Prepared for
U.S. Department of Energy

Prepared by
American Iron and Steel Institute
Technology Roadmap Program Office
Pittsburgh PA 15220

Report Documentation Page

Title and Subtitle: AISI/DOE Technology Roadmap Program
Sustainable Steelmaking Using Biomass and Waste Oxides
TRP 9902

Author(s): Richard J. Fruehan, Principal Investigator

Performing Organization Carnegie Mellon University
Pittsburgh, PA

Abstract:

A new process for ironmaking was proposed to employ renewable energy in the form of wood charcoal to produce hot metal. The process was aimed at the market niche of units ranging from 400,000 to 1 million tons of hot metal a year. In the new process, a Rotary Hearth Furnace (RHF) would be combined with a smelter to produce hot metal. This combination was proposed to overcome the technical hurdles of energy generation in smelters and the low productivity of RHFs, and also allow the use of wood charcoal as energy source and reductant. In order to assess the feasibility of the new process, it was necessary to estimate the productivity of the two units involved, the RHF and the smelter. This work concentrated on the development of a productivity model for the RHF able to predict changes in productivity according to the type of carbon and iron oxides used as feed materials. This model was constructed starting with the most fundamental aspect of reduction in composites measuring intrinsic rates of oxidation of different carbons in CO_2-CO atmospheres and reduction of different oxides in the same atmospheres. After that, a model was constructed considering the interplay of intrinsic kinetics and the transfer of heat to and within pellets such as used in the RHF. Finally, a productivity model for the RHF was developed based on the model developed for a pellet and the differences in heat transfer conditions between the laboratory furnace and the actual RHF. The final model produced for the RHF predicts production rates within 30% of actual plant data reported with coal and indicates that productivity gains as high as 50% could be achieved replacing coal with wood charcoal in the green balls owing to the faster reaction rates achieved with the second carbon. This model also indicates that an increase of less than 5% in total carbon consumption should take place in operations using wood charcoal instead of coal.

(RDP Standard Form, Form 298)

DISCLAIMER

TABLE OF CONTENTS

LIST OF TABLES

LIST OF FIGURES

LIST OF FIGURES

Abstract

A new process for ironmaking was proposed to employ renewable energy in the form of wood charcoal to produce hot metal. The process was aimed at the market niche of units ranging from 400,000 to 1 million tons of hot metal a year. In the new process, a Rotary Hearth Furnace (RHF) would be combined with a smelter to produce hot metal. This combination was proposed to overcome the technical hurdles of energy generation in smelters and the low productivity of RHFs, and also allow the use of wood charcoal as energy source and reductant. In order to assess the feasibility of the new process, it was necessary to estimate the productivity of the two units involved, the RHF and the smelter. This work concentrated on the development of a productivity model for the RHF able to predict changes in productivity according to the type of carbon and iron oxides used as feed materials. This model was constructed starting with the most fundamental aspect of reduction in composites measuring intrinsic rates of oxidation of different carbons in CO_2-CO atmospheres and reduction of different oxides in the same atmospheres. After that, a model was constructed considering the interplay of intrinsic kinetics and the transfer of heat to and within pellets such as used in the RHF. Finally, a productivity model for the RHF was developed based on the model developed for a pellet and the differences in heat transfer conditions between the laboratory furnace and the actual RHF. The final model produced for the RHF predicts production rates within 30% of actual plant data reported with coal and indicates that productivity gains as high as 50% could be achieved replacing coal with wood charcoal in the green balls owing to the faster reaction rates achieved with the second carbon. This model also indicates that an increase of less than 5% in total carbon consumption should take place in operations using wood charcoal instead of coal.

Introduction

Conventional Blast Furnace ironmaking consumes approximately 14GJ/ ton of hot metal in energy and is unable to adequately handle wood charcoal as an energy source in units over 200,000 tones of hot metal per year. The low strength and density of wood charcoal limit the use of this renewable energy source to units smaller than 400,000 tons of hot metal per year leaving a market gap for new technologies. A new process was proposed combining a Rotary Hearth Furnace (RHF) and a Smelter such as the AISI or DIOS for the production of hot metal using wood charcoal in that range of production rates. A schematic of the combination process proposed is shown in Figure 1. The combination of these two processes was proposed in order to address the problems of limited productivity of the RHF and excessive demand in energy generation in smelters. Current RHFs suffer major productivity losses in order to produce Direct Reduced iron (DRI) with degrees of metallization higher than 90%. Smelters demand excessive energy generation close to their roofs in order to produce hot metal directly from ores. In the new process, these two problems would be addressed limiting reduction in the RHF to circa 70 to 80% of metallization and feeding the pre-reduced material into the Smelter for the final reduction and gangue separation yielding hot metal. In previous projects, the productivity of the Smelter was studied and models are available to predict production rates according to operating parameters and sizes of units. Thus, the work concentrated on studies pertaining to the metallurgical processing of composite pellets in an RHF.

During the development of the research, three models were developed specifically to address the chemical kinetics of reduction in composite pellets, the interplay of heat transfer and chemical kinetics in large pellets such as used in the RHF, and, finally, a model to predict the change in productivity of the RHF according to the type of feed materials and operating conditions such as reduction temperatures and final degrees of metallization of the DRI produced. In conjunction, these models allow the estimation of RHF productivity in different scenarios paving the way for the analysis of the combination process proposed.

Objectives

The objective of the present work is to assess the feasibility of a new ironmaking process consisting of the combination of a Rotary Hearth Furnace and a Bath Smelter. Since a productivity model already exists to smelting operations, the work concentrated on the development of a productivity model for the RHF. Initially, four main tasks were identified as:

Task I. Develop the fundamental measurements of rates of reduction of iron oxides by carbon in composite mixtures of small grains.

Task II. Develop a reduction model for the composite pellets used in the RHF able to predict the changes in reduction rates due to the replacement of coal with wood charcoal in the green balls.

Task III. Develop a productivity model for the RHF using the pellet model from Task II. The model is used to compute the productivity as a function of pellet size, number of layers of pellets, reductant type, and final degree of metallization of the DRI.

Task IV. Use the model developed in Task III and a pre-existing model developed for the Smelter to assess the productivity and energy demands of the combination process proposed.

Task V. Study the types of wood and the facilities necessary to produce wood charcoal in North America in order to predict the costs of producing wood charcoal in the United States.

Research Results

The work done in this research was organized in three papers according to the specific topics addressed. In appendices A, B, and C respectively are the detailed results for reduction kinetics (Task I), reduction of pellets (Task II), and the productivity model for the RHF (Task III). These publications are given in the appendices. The work done under each task can be summarized as:

Task I. The techniques used for the experimental measurements and data analysis in this task have been thoroughly presented in earlier reports. Figures 2, 3 and 4 summarize the rates measured for wood charcoal and wustite during this task. In here, it was found that reduction in composites at temperatures common to RHF operations can be partially controlled by the reduction of wustite leading to a combined reaction model described in previous reports. Details are given in Appendix A.

Task II. Experimental measurements of reduction rates done with pellets inside of small crucibles showed much slower rates than anticipated from the consideration of chemical kinetics alone. A model considering the transfer of heat to the pellets, pellet shrinkage, as well as chemical kinetics adequately predicted the rates measured as exemplified in Figure 5. Details are given in Appendix B.

Task III. A productivity model for the RHF was developed considering the reduction bed as a stacking of pellets and using the model developed in Task II for a single pellet to compute the reaction rates of each pellet layer. This model achieved a reasonable prediction of productivity (Kg/m^2.hour) for operations using coal. The comparison in terms of projected productivity gains between coal and wood charcoal is summarized in Figure 6. The model also predicted the effects of pellet size which showed that the optimum size is about 0.7 cm. It also showed that the productivity of the RHF with one or two layers of pellets is about the same becoming significantly lower with three layers of pellets. Finally, the model showed that producing DRI only 70% metallized significantly increases the productivity of the RHF.

Task IV. The productivity model for the RHF was also used to compute the amount of carbon required in the process. An energy and materials balance model for the smelter was also developed to determine the coal and oxygen required in the smelter. From this the total carbon (coal and charcoal) required for the combined process was estimated. A summary of the typical results for 70% reduction in the RHF using wood charcoal with 30% of post combustion in the smelter is shown in Table I. The results indicate that the process will be competitive with the Blast Furnace. Work is continuing on this Task.

Task IV. In this task, it was shown that wood charcoal could be produced in the United States using wood from demolition of old houses with prices ranging from U$120 to 150.00 per ton including transport. A major report on this topic was submitted to AISI/DOE in 2001.

References

1) R. J. Fruehan: *Metall. Trans. B*, 1977, vol. 8B, pp. 279-86.

2) Y. K. Rao: *Metall. Trans.*, 1971, vol. 2, pp. 1439-47.

3) E. T. Turkdogan and J.V. Vinters: *Metall. Trans.*, 1972, vol. 3, pp. 1561-74.

4) A. A. El-Geassy and V. Rajakumar: *Iron Steel Inst. Jpn. Int.*, 1985, vol. 25, pp. 1202-1211.

Table I: Estimated consumption of materials in the combination process per ton of hot metal produced with 70% metallizes DRI and 30% post combustion in the smelter.

RHF			
	Inputs		Output
Ore (Kg)	Wood charcoal (Kg)	Smelter gas (Nm^3)	70% metallized pellets, 5% gangue (Kg)
1422	214	158	1148
Smelter			
	Inputs		Output
RHF pellets (Kg)	Coal, 30% volatiles, (Kg)	Oxygen (Nm^3)	Hot metal with 4.5% carbon (Kg)
1148	120	45	1000

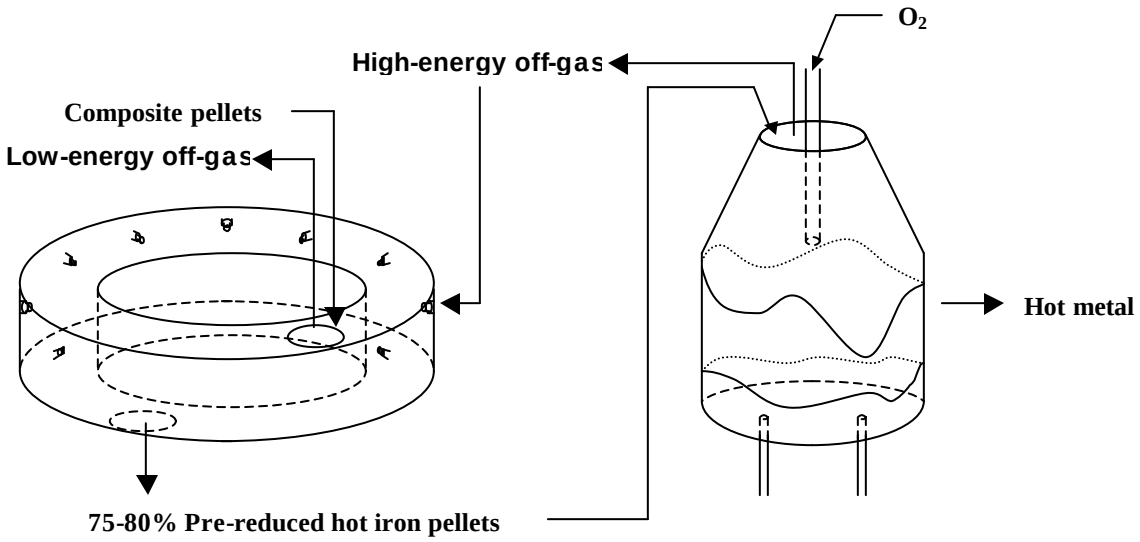

Figure 1: Schematic of the process proposed.

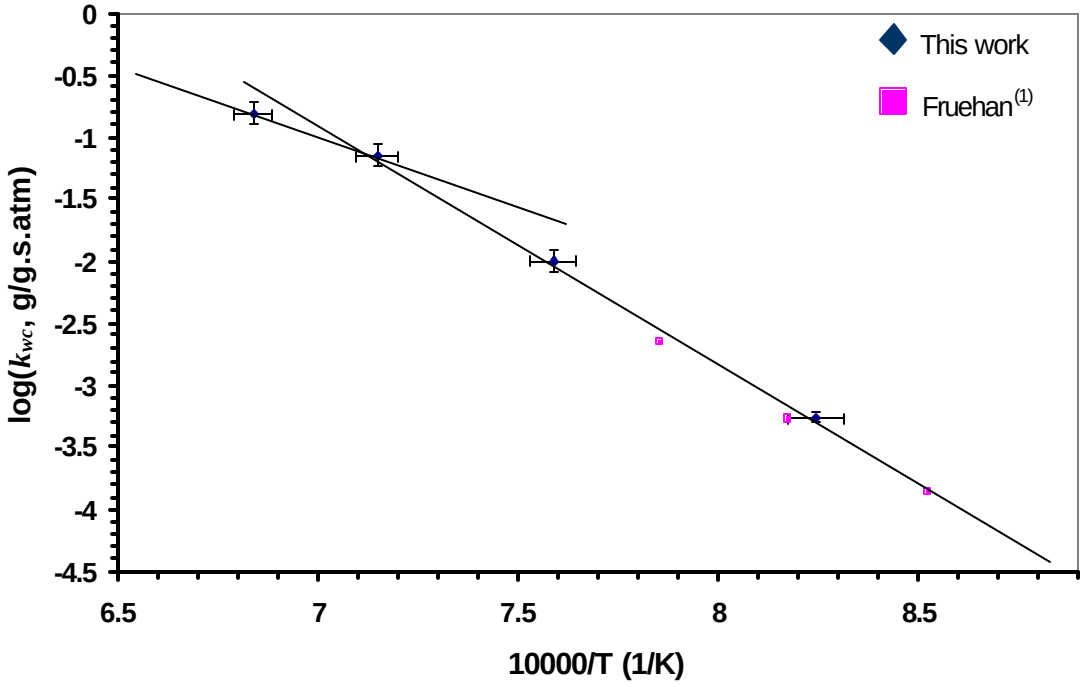

Figure 2: Intrinsic rate constants for oxidation of wood charcoal in composite samples with wustite.

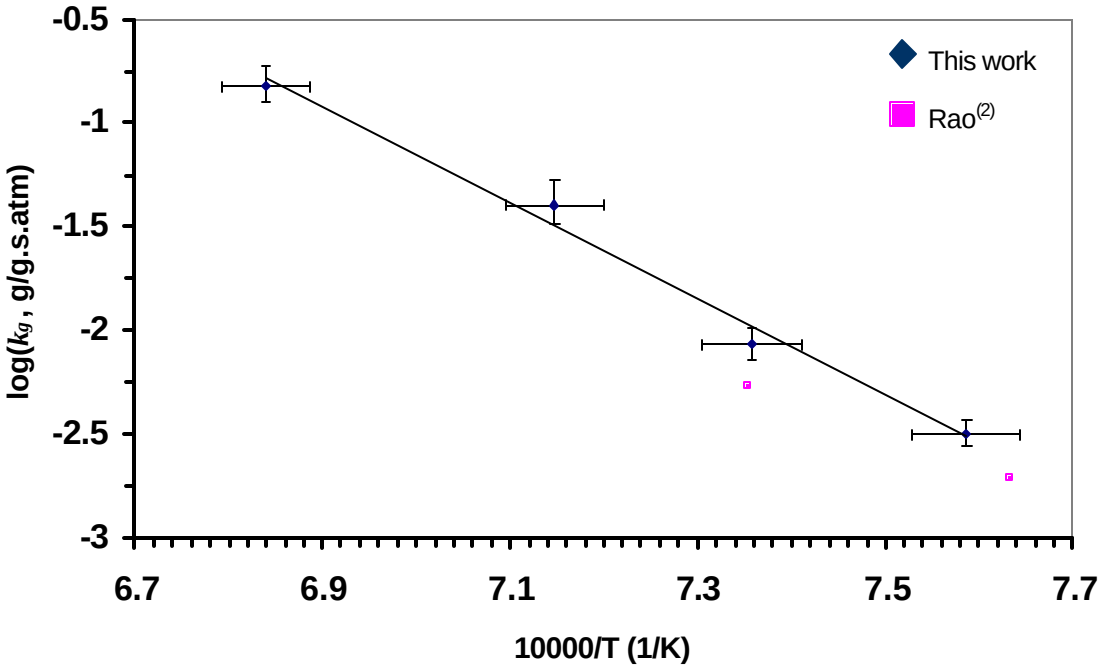

Figure 3: Intrinsic rate constants for oxidation of graphite in composite samples with wustite.

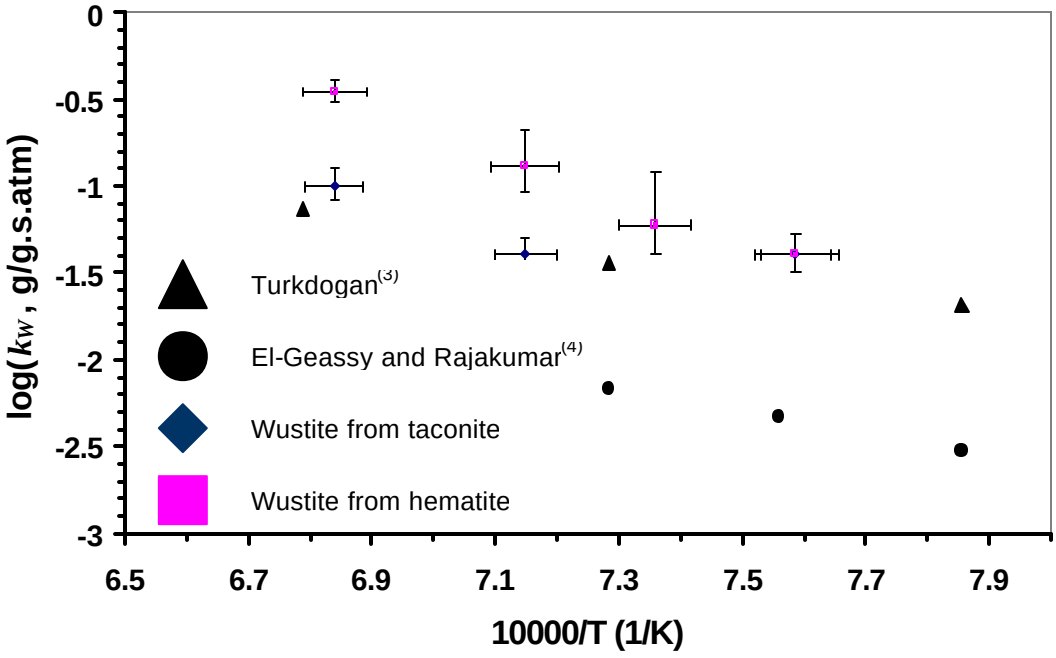

Figure 4: Intrinsic rate constants for reduction of wustite in composites samples with wood charcoal or graphite.

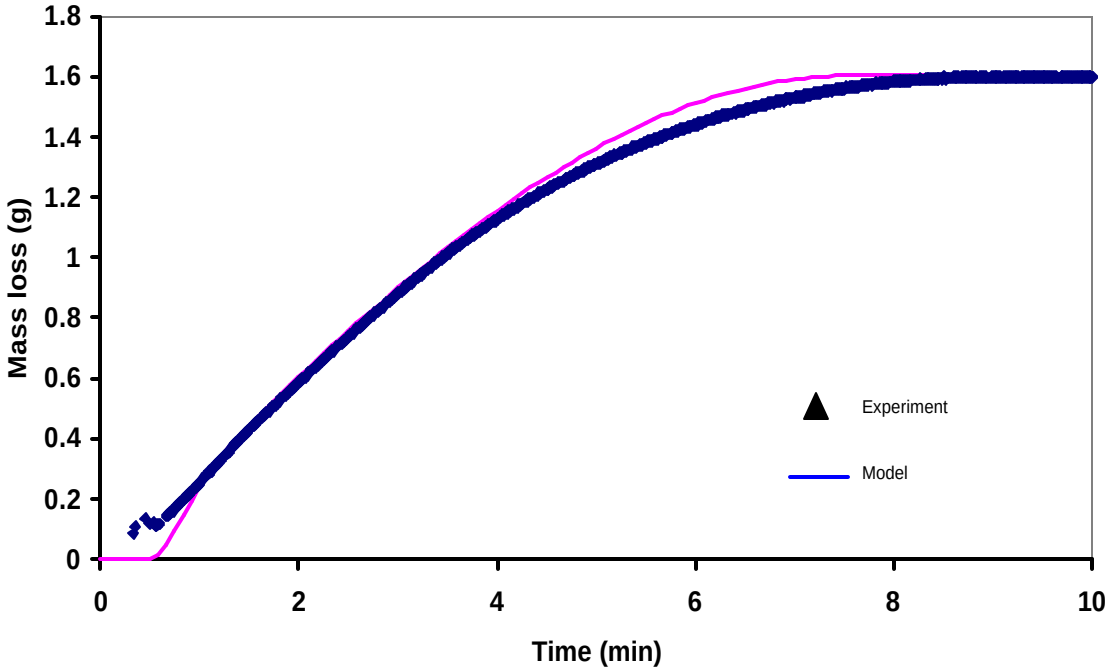

Figure 5: Comparison of experimental rates of reduction of composite pellets of wood charcoal and hematite and results from models with and without heat transfer.

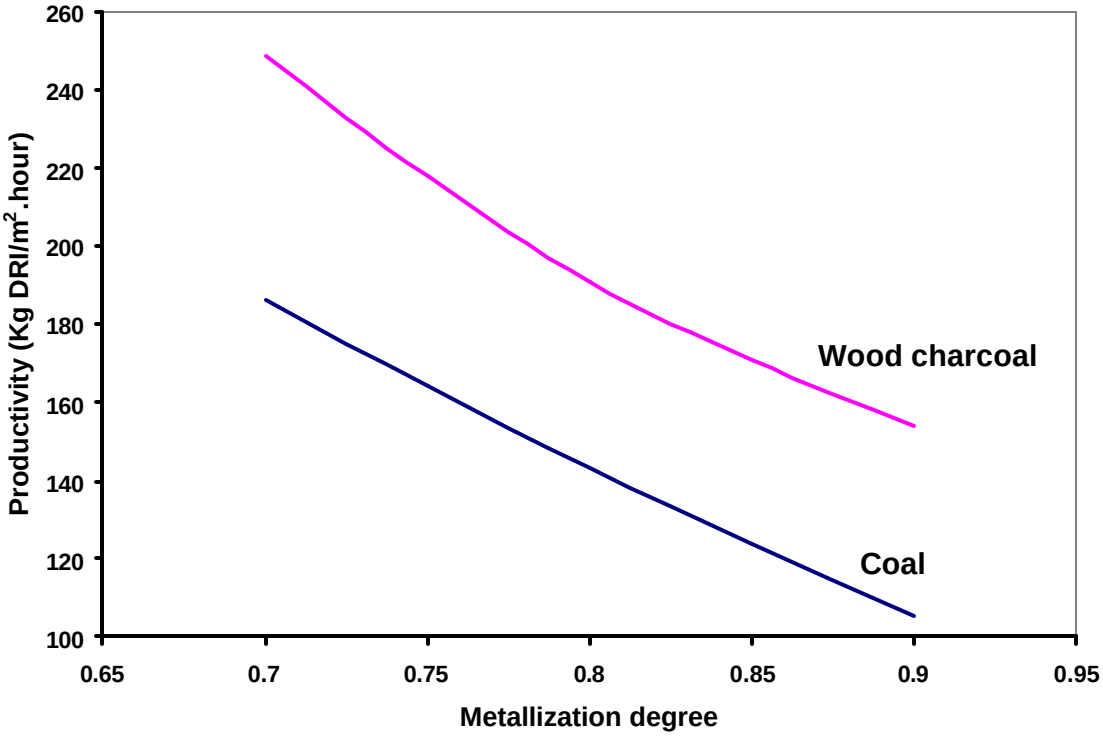

Figure 6: Estimated productivity of the RHF at different final degrees of metallization using wood charcoal and coal as reductant.

Appendix A – Summary of Study on the Intrinsic Rates of Carbon Oxidation and Wustite Reduction

Accepted for publication in Metallurgical Transactions

Rate of Reduction of Ore-Carbon Composites
Part I: Determination of Intrinsic Rate Constants

O. M. Fortini and R. J. Fruehan
Carnegie Mellon University
Pittsburgh, PA

Abstract

A process for ironmaking was proposed consisting of the combination of a rotary hearth furnace and a bath smelter employing wood charcoal as reductant and energy source. This paper examines reactions in composites of iron oxides and carbon at elevated temperatures in conditions developed to minimize the influence of mass and heat transfer to the overall rates. A combined reaction model considering the steps of carbon oxidation and reduction of the iron oxides was developed allowing the measurement of rate constants for carbon oxidation and wustite reduction to be used in a comprehensive pellet model developed in Part II of the current paper. This analysis showed that wustite reduction can have a significant effect on the overall rate of reduction in composites at high temperatures or in the presence of large excess of carbon. Rate constants measured for graphite showed that graphite is as reactive as wood charcoal possibly due to catalysis of graphite or its higher temperature dependence. The poisoning of carbon surfaces by CO is less significant than anticipated from works of previous authors.

I. Introduction

The productivity and energy efficiency of the iron blast furnace has increased significantly in the past thirty years. Energy consumption has been reduced from 40GJ/tonne hot metal in the sixties to less than 20GJ/ tonne in the nineties. However, it still requires coke, produces about 1.5 tonnes of CO_2/ tonne hot metal and is highly capital intensive. If wood charcoal is used for iron production net CO_2 and sulfur emissions can be significantly reduced. CO_2 is converted back to carbon and oxygen during tree growth and wood charcoal contains little sulfur. Wood charcoal is not

appropriate to use in large blast furnaces of high productivity due to its low strength and density; commercial blast furnaces using wood charcoal are limited to 300,000 tonnes/year.

A new process has been proposed using composite pellets or mixtures of wood charcoal and ore fines in a Rotary Hearth Furnace (RHF), which are melted in a smelting unit as schematically shown in Figure 1. In the new process, composite pellets would be pre-reduced up to 75-80% metallization in the RHF and charged into a smelter for final reduction, gangue separation and melting. This process overcomes the RHF drawbacks of low productivity and high gangue in the product by doing final reduction, melting and gangue separation in the smelting unit. It overcomes the drawback of smelters, energy generation, by pre-heating and doing most of reduction in the RHF. In order to fully evaluate and optimize this process, the rate of reduction, energy requirement and gas generation in the RHF must be known.

The overall objective of this research is to develop and verify a model to compute the rate of reduction of ore-carbon pellets or mixtures including wood charcoal. The overall pellet model presented in Part II of this paper includes the rates of oxidation of the carbonaceous materials, reduction of wustite, heat transfer to and within the pellet, shrinkage and other factors. In this paper, the results obtained for determining the two rate constants for different types of oxide and carbon are presented. This model will then be used in a simulation of the RHF to evaluate and optimize the proposed process.

In theory, the rate of oxidation of carbon particles by CO_2 can be determined directly. However, in order to avoid mass transfer effects, high gas velocities are necessary and it is never possible to ensure that such effects did not play a part in a given experiment. Moreover, at the high gas velocities necessary at elevated temperatures, the small powders of carbon and wustite would be carried away with the gas stream. Similarly, the direct measurement of the rate of reduction of the ore by CO would be difficult for the same reasons. Therefore, rate constants of carbon oxidation and wustite reduction were determined from measurements in mixtures and a combined reaction model considering the two steps of carbon oxidation and wustite reduction. The individual rate constants were determined by varying the relative amounts of carbon and wustite in different samples. In addition to preventing the interference of mass transfer

effects, the direct measurement of rate constants in mixtures would take account of possible interactions between reactants such as catalysis by newly formed iron. In Part II of this paper these results are used in a comprehensive model of an ore-charcoal pellet and experimental verification of the comprehensive pellet model is presented.

II. Literature review

A vast amount of work has been done on the subjects of reduction in composites, carbon oxidation by CO_2 and reduction of iron oxides by CO. These three topics are of importance in studies of composites and a thorough review would extend far beyond the possibilities of a single text. Here, only a brief review of the most relevant studies on each subject is presented.

Reduction in composites: A number of researchers have studied reduction in composites of iron oxides and carbon. It became a general consensus that the overall mechanism of reduction consists of two elementary steps of reaction schematically represented by:

$$\left.\begin{aligned} Fe_xO_{y(s)} + CO_{(g)} &\rightarrow Fe_xO_{(y-1)(s)} + CO_{2(g)} \\ CO_{2(g)} + C_{(s)} &\rightarrow 2CO_{(g)} \end{aligned}\right\} \qquad (1)$$

where x = 1, 2 or 3
when y = 1, 3 or 4.

Fruehan[1] and Rao[2] studied reaction rates in composites with different types of carbons and found a good representation of data with a reaction mechanism dominated by the oxidation of carbon at lower temperatures. In the work of both authors, faster rates were measured in the presence of carbon oxidation catalysts such as lithium and slower rates in the presence of inhibitive agents such as sulfur reinforcing the argument of control by carbon oxidation. The studies of Rao[2] were limited to temperatures up to 1086°C and used graphite as the only carbon type. Those of Fruehan[1] extended up to 1200°C and encompassed more varied carbon sources: coal, coke and coconut charcoal. In Fruehan's studies, a considerable slow-down of rates at temperatures above 1086°C was reported and attributed to the possible contribution of wustite

reduction to the overall rate. Later, Sun and Lu[3] developed models for higher temperatures where both steps of carbon oxidation and wustite reduction are given attention.

Carbon oxidation in CO_2: Carbon oxidation is usually dealt with in the literature with complex rate laws with more than one reaction constant. The most widely accepted mechanisms are those proposed by Gadsby[4] and Reif[5], which result in a rate law for carbon oxidation with the form:

$$R = \frac{k_1 P_{CO_2}}{1 + k_2 P_{CO} + k_3 P_{CO_2}} \tag{2}$$

In the expression above, the reaction rate per unit mass of carbon (R) is related to the pressures of carbon dioxide and carbon monoxide (P_{CO_2} and P_{CO}) by means of three constants k_1, k_2 and k_3. The interpretation of the rate constants k_1, k_2 and k_3 depends on the actual reaction mechanism. A number of authors have measured carbon oxidation constants based on a rate law such as equation (2). Selected values can be taken from the extensive compilation of Story[6] and are given in Table I. In composite studies, however, carbon oxidation is usually addressed by means of a single reaction constant as can be illustrated in the work of Sun and Lu[3]. This is reasonable since the gas composition and temperature ranges are relatively small. Therefore, the rate law for carbon oxidation in studies with composites may be written as:

$$R_C = k_C m_C (P_{CO_2} - P^e_{CO_2}) \tag{3}$$

where R_C is the rate of carbon oxidation (g/s), k_C represents the rate constant of carbon oxidation per unit matter of carbon (g/g.s.atm), m_C represents the mass of carbon in the system (g), P_{CO_2} is the pressure of carbon dioxide in the system and $P^e_{CO_2}$ stands for the CO_2 pressure in equilibrium with carbon at the temperature and pressure of the system at hand. Equation (3) implies that the surface area available for reaction is proportional to the mass of carbon so that it should be applicable to limited ranges of carbon burn-off. It should be noticed that the rate laws used in the works of Fruehan[1] and Rao[2] can be obtained from equation (3) in the particular case where a constant pressure of CO_2 is

maintained during reduction. In the light of (3), the temperature dependence or apparent activation energies (E_C) are clearly defined in terms of the change in k_C with temperature:

$$k_C = k_C^0 e^{-E_C / R_g T} \quad (4)$$

where k_C^0 is the pre-exponential Arrhenius factor (g/g.s.atm), R_g is the universal gas constant (atm.L/mol.K), and T is the absolute temperature (K).

Iron oxide reduction: In contrast to the complex laws used for carbon oxidation, the kinetics of wustite reduction seems controlled by the formation of a CO_2 activated complex on the surface of iron. Thus, reduction of wustite may be well represented as a first order process on the local pressure of carbon monoxide by means of a rate law such as given by Turkdogan[7]:

$$R_{FeO} = k_{FeO} m_{FeO} (P_{CO} - P_{CO}^e) \quad (5)$$

where k_{FeO} is a specific rate constant (g/g.s.atm) obeying an Arrhenius relationship with temperature, m_{FeO} is the mass of wustite (g), P_{CO} is the pressure of carbon monoxide in the system and P_{CO}^e is the pressure of CO in equilibrium with iron and wustite. As in the case of carbon, the area is considered proportional to the mass of wustite. Data on the intrinsic rates of reduction of wustite at lower temperatures are abundant in the literature. A temperature dependence of 40Kcal/mol for the reduction of wustite can be estimated from the work of Turkdogan[7] at temperatures below 1050°C. At higher temperatures, however, no reliable data from experiments where intrinsic rates are directly measured is available due to the influence of mass transfer.

III. Model Development

In developing a model for reduction in composites taking into account the steps of carbon oxidation and wustite reduction, rate laws for the two elementary reaction steps were taken as equations (3) and (5). The use of such equations with no corrections for changes in carbon pore surface area available for reaction or more

detailed descriptions for oxide reduction should restrain the use of this model to ranges of carbon burn-off and wustite reduction. Indeed, great changes in porosity may develop during reduction by wood charcoal or graphite seriously affecting measured values of intrinsic reaction rates per unit mass[8, 9]. Nevertheless, this simplistic view may provide some insight into the interplay of carbon oxidation and wustite reduction occurring at high temperatures. The two rate laws in forms (3) and (5) can be used to compute the change in sample mass (*m*) with time (*t*) from the changes in the two solids as:

$$\frac{dm}{dt} = \frac{MW_o}{MW_{FeO}} k_{FeO} m_{FeO} (P_{CO} - P_{CO}^{FeO}) + k_C m_C (P_{CO_2} - P_{CO_2}^{C}) \qquad (6)$$

provided that the local pressures of CO and CO_2 are known. In equation (6), MW_i represents the molecular mass (g/mol) of component *i*. Since the volumes of gas produced are much larger than the volume of gas inside the sample:

$$P_{CO} = \frac{R_{CO}}{R_{CO_2} + R_{CO}} P_t \qquad (7)$$

$$P_{CO_2} = \frac{R_{CO_2}}{R_{CO_2} + R_{CO}} P_t \qquad (8)$$

where P_t is the total pressure inside the sample (atm). The net rates of production of CO and CO_2 in equations (7) and (8) can be related to the rates of the individual reactions of wustite and carbon observing the stoichiometry of the individual reaction steps as:

$$R_{CO} = 2\frac{k_C}{MW_C} m_C (P_{CO_2} - P_{CO_2}^{C}) - \frac{k_{FeO}}{MW_{FeO}} m_{FeO} (P_{CO} - P_{CO}^{FeO}) \qquad (9)$$

$$R_{CO_2} = \frac{k_{FeO}}{MW_{FeO}} m_{FeO} (P_{CO} - P_{CO}^{FeO}) - \frac{k_C}{MW_C} m_C (P_{CO_2} - P_{CO_2}^{C}) \qquad (10)$$

Substitution of (9) and (10) into (7) and (8) allows the pressures of *CO* and CO_2 to be computed as functions of the specific rate constants and moles of reactants present at any instant in time as:

$$P_{CO_2}^2 / P_t + P_{CO_2}(1+f - P_{CO_2}^C / P_t) = P_{CO_2}^C + fP_{CO_2}^{FeO} \quad (11)$$

$$P_{CO}^2 / P_t - P_{CO}(2+f + P_{CO}^C / P_t) = 2P_{CO}^C + fP_{CO}^{FeO} \quad (12)$$

The parameter f in (11) and (12) represents the relative importance of the two elementary steps of carbon oxidation and wustite reduction to the overall rate of reaction. f is defined as the ratio:

$$f = \frac{k_{FeO} MW_C m_{FeO}}{k_C MW_{FeO} m_C} \quad (13)$$

In the following treatment of reaction rates, constants for the two individual reaction steps are determined by simultaneously solving equations (6), (11) and (12). The numerical solution employed a fully explicit scheme to solve changes in number of moles of wustite and carbon with time. Equilibrium pressures of CO and CO_2 with carbon and wustite-iron were computed from Kubaschewski[10] and Darken and Gurry[11], respectively. A total pressure of 1 atm was assumed due to the small sizes of samples used. The question of pressure buildup during reduction is controversial. Rao[12] derived a complex model, which predicted values as high as 20 atm for a sample depth of 2 cm. On the other hand, Tien and Turkdogan[13] argued that such pressure buildup could never be sustained since the powders would be blown away with the outgoing gas. Fruehan[1] measured pressure buildups by means of a manometer inserted into samples of artificial wustite and coke, coal or coconut charcoal and detected no significant pressure buildup. More recently, Lu[14] reinstated the problem as one non-verified hypothesis in many reduction models. Here, the option was taken to rely on the experimental measurements of Fruehan[1] and the argument of Tien and Turkdogan[13].

IV. Experimental

In this work, wood charcoal was used as reductant to represent the class of natural carbons. The wood charcoal used was characterized for ash and volatile content in separate sets of experiments prior to reduction. A volatile content of 21% in mass was determined in experiments of fast heating under argon. Experiments of oblivious burning of wood charcoal under CO_2 and air at temperatures higher than 850°C revealed a very

low ash content of less than 2% in mass. The reagent grade graphite used to represent the class of synthetic carbons had a purity of 99.9% or higher as determined by the supplier.

Wustite obtained from taconite concentrate was used to represent the class of natural wustites. Gangue contents in the taconite concentrate used for preparation of wustite are in the range 4 to 6% in mass as determined by chemical analysis and X-ray fluoroscopy. Wustite was obtained by pre-reducing the original iron oxides at temperatures ranging from 1000 to 1050^{o}C under mixtures of 50%CO-50%CO_2. Pre-reduction to wustite was confirmed by the weight loss of the samples. Artificial wustite was obtained from reagent grade hematite with purity 99.9% or higher as determined by the provider following the same procedure of pre-reduction under CO-CO_2 at temperatures higher than 1000^{o}C.

All reactants used were sized to –200 mesh and thoroughly mixed into master mixtures of 4 - 5g total mass. The masses of reactants used to prepare the master mixtures were measured to a precision of 10^{-3}g. Prior to preparing the master mixtures, all wood charcoal was devolatilized in an induction furnace under argon for 8 hours and complete volatile release confirmed by the total mass loss of the samples. In preparing the mixtures, account was taken of the ash and gangue contents in the wood charcoal and taconite.

In all reduction experiments, samples of 0.10-0.70g from the master mixtures prepared were placed in a small alumina crucible (0.5cm I.D. 2cm high, 2.8g). The mass change after the samples were quickly loaded into a hot furnace was monitored in an apparatus as shown in Figure 2. The furnace temperature was calibrated prior to the experiments with thermocouples placed at several different positions along the hot zone and a safety margin of $\pm 10^{o}$C adopted for the precision in the hot zone. Before each of the experiments, the gas inside the reaction chamber was purged with argon at a total flow rate of 2L/min for one hour to avoid oxidation of carbon or wustite by residual oxygen. During this period, the samples were kept suspended above the furnace tube by means of a secondary chain linked to the crank mechanism shown in Figure 2. The purity of the gas before loading of the samples was confirmed by monitoring the composition with a mass spectrometer at the outlet of gas. After the purging period, the

samples were quickly loaded into the furnace using the crank mechanism linked to the auxiliary chain. The auxiliary chain was released from the main chain once the samples were in the hot zone of the furnace. The balance was linked to a computer to continuously monitor the change in mass with time. This procedure of fast immersion was also used to determine the volatile content of wood charcoal as previously mentioned. The overall precision of the thermo-balance was 0.003g.

Conditions of heat transfer in the experimental furnace were studied using dummy samples of pure alumina powder with an embedded thermocouple in a crucible as used in the reduction experiments. A large variability in heating rates was found depending on the state of the surface of the crucible indicating that most of heat transfer is due to radiation. Results from this analysis were used to estimate the heat supply to the samples during reduction and a maximum change of 5°C in sample temperature induced by reactions was estimated for the sample sizes and furnace temperatures used.

V. Results and Discussion

A brief discussion of the general features of our measurements can be helpful in the interpretation of reaction rate data and meaning of measured rate constants. Typical results of experimental measurements are shown in Figure 3. The measured curves exhibit a behavior quite similar to that described by Kohl[15]. In the most general case, the curves indicate the existence of three distinct periods with respect to the rates of reaction. After an initial period of constant sample weight necessary to bringing the sample up to the experimental temperature, a first onset of reaction at a slow rate can be identified. According to Kohl[15], this period is associated with the buildup of gaseous intermediates at the points of contact between the particles of iron oxides and carbon. In samples with graphite this period may also be associated with the development of porosity in the initially compact carbon as observed by Walker, Rusinko and Austin[9]. After the initial period of slow reaction, a main onset can be identified where the mechanism of gaseous intermediates operates fully. Here, as in most kinetic studies, the discussion is limited to the second and main period of reaction.

An example of determination of intrinsic rate constants is shown in Figure 4 for wood charcoal and wustite from taconite concentrate at a temperature of 940^{o}C. The procedure consists of starting with initial values for the two rate constants and iterates between the two experiments at low amounts of carbon and wustite until a good description of the data is found in both plots. After the initial determination of rate constants in experiments with low amounts of one of the reactants, samples with molar ratios of 1/1 were used for validation as shown in Figure 5. The procedure used for determination of rate constants is schematically shown in Figure 6. Starting with a large excess of wustite the rate of reduction is much faster than the rate of carbon oxidation so that the overall rate will suffer little influence from the rate of reduction of the oxide. Similarly, with excess carbon the rate of carbon oxidation is faster than the rate of reduction and will be strongly influenced by the rate of reduction of the oxides. At temperatures lower than 1086^{o}C, a good agreement could be found within 20% of the base values determined from the experiments with samples of molar ratios 1/5 and 5/1. Moreover, at such low temperatures, rate constants estimated for reduction of wustite from taconite concentrate or hematite are considerably higher than constants measured for wood charcoal and graphite indicating a mechanism controlled mainly by the oxidation of carbon in agreement with Fruehan[(1)] and Rao[(2)]. Intrinsic rate constants for reduction of wustites at temperatures lower than 1086^{o}C should be regarded as a minimum estimate. Since the overall rate under these conditions is primarily controlled by the oxidation of carbon slightly lower values for reduction will not affect the overall rate.

The importance of wustite reduction to the overall reaction mechanism seems to increase at temperatures higher than about 1086^{o}C. By following the same procedure for determination of rate constants as adopted at lower temperatures, larger deviations were found between constants determined in experiments with low amounts of reactants and equimolar mixtures of carbon and wustite as exemplified in Figure 7. Nevertheless, the agreement found is within 30% on average; such agreement is surprisingly good in face of the possible effects of wustite reduction to the overall measured rate. The contribution of wustite reduction may have a twofold effect on the rates of oxidation of carbon. First by limiting the availability of CO_2 for carbon oxidation and second by inducing poisoning of the carbon surface by CO, both factors contributing to a slow down of intrinsic rates of carbon oxidation. In order to cope with this difficulty for the remainder of this analysis,

the characteristic value considered for a given temperature was taken as the average between the experiments with large carbon excess and best fits attained by adjusting the value of intrinsic rates of carbon oxidation in equimolar samples. It should be noted that once wustite intrinsic rates become comparable to intrinsic rates of carbon oxidation, fittings of experiments with excess carbon become quite insensitive to the constants of the latter, thus granting some accuracy to constants determined for wustite. A final note should be put on the measured values of rate constants. In some experiments at low carbon to wustite ratios, it was not possible to attain a reasonable agreement between the measured mass loss and model results due to difficulties in defining the starting point of the second reaction zone discussed previously. In these cases, intrinsic rate constants were determined between the experiments with equimolar mixtures and low wustite. The average values of rate constants measured are shown in Table II. In spite of the broad ranges of apparent rate constants computed, analysis of Table II provides some useful observations. First, measured values indicate that reduction of wustite has a significant role in reduction at temperatures higher than 1086^{o}C and during the later stages of reduction in the presence of excess carbon. In industrial processes, an excess of carbon is most often found so that wustite reduction should play a significant role in the kinetics of reduction. As can be seen from Table II, values of constants measured for wustite from taconite at 1126 and 1186^{o}C are lower than those measured for wood charcoal indicating that a shift in rate controlling step from carbon oxidation to oxide reduction can take place in this type of composites at high temperatures. Second, comparison of the values obtained for graphite and wood charcoal at 1189^{o}C shows that the rates of oxidation of these carbons are comparable at high temperatures. In most of the literature, as exemplified by the work of Turkdogan[16], rates of graphite oxidation in CO-CO_2 mixtures are significantly slower than rates of oxidation of natural carbons such as coconut charcoal. However, Story and Fruehan[19] have previously shown that rates of oxidation of graphite become comparable to rates of oxidation of coke at higher temperatures due to the development of extensive porosity in graphite. Therefore, the measurement of comparable reaction rates at high temperatures could be due to the higher activation energy for graphite oxidation, development of extensive porosity and catalysis of graphite by newly formed iron. The effects of catalysis would be less pronounced in samples with wood charcoal since this is already a more reactive carbon.

The temperature dependence of intrinsic rate constants determined for oxidation of wood charcoal is shown in Figure 8 along with the estimated experimental errors and data from other authors. In Figure 8, the comparison is presented between the values measured by Fruehan[1] for coconut charcoal and those measured here for wood charcoal. As can be seen in the figure, a linear trend is closely followed up to 1126°C but a marked difference is seen between 1126 and 1189°C. This could be an indication of partial control by gas diffusion in the pores of carbon at higher temperatures. Indeed, the temperature dependence of 49Kcal/mol computed with the experimental measurements at 1126 and 1189°C is close to ½ the temperature dependence of 88Kcal/mol computed with the measurements taken at lower temperatures. In the case of limited mixed control, also known as partial internal burn, where the rate of carbon oxidation is controlled by gas diffusion in pores and chemical reaction on the surface of pores, the rate constant k_C for carbon oxidation is given by[17, 18, 19]:

$$k_C = \sqrt{k_S D_e r S} \tag{14}$$

where k_S is the "true" kinetic constant of carbon oxidation per unit area, D_e is the effective diffusivity of reacting gas inside the pores of carbon, r is the bulk density of the carbon and S is the specific area per unit mass of carbon. Since the effective diffusivity is not a strong function of temperature, values measured under partial internal burn usually result in temperature dependences of ½ the "true" temperature dependence of surface kinetics. For the present purpose of developing a model for reduction in composites, the question of determining the "true" temperature dependence of carbon oxidation is of secondary importance since the onset of partial internal burn seems limited to higher temperatures. For the purpose of estimating the magnitude of mass transfer effects on the burning of carbon, the -200 mesh particles can be reasonably assumed as spheres of 2 microns in diameter since this is the largest diffusion distance possible in a given particle grain. Based on the porosity of typical artificial and natural carbons and measurements of gas diffusivity from other authors, a calculation indicates that rates controlled by mass transfer will be at least one order of magnitude faster than the measured rates, to the exception of experiments with natural carbons well above 1100°C as corroborated by the present experimental results. Finally, the temperature dependence of 88Kcal/mol obtained for wood charcoal at lower temperatures is close to

the values of 81.2Kcal/mol and 84.1Kcal/mol estimated from the works of Fruehan[1] and Turkdogan[16] for coconut shell charcoal. Figure 9 shows the temperature dependence of constants measured for graphite. For comparison, values measured by Rao[2] for amorphous graphite are also plotted. A temperature dependence of 106Kcal/mol can be computed over the entire range of temperatures. This value is significantly higher than that measured for wood charcoal as should be expected from the states of graphitization of the two carbons[16]. It is also in good agreement with a value of 102Kcal/mol estimated from the data compiled by Story[6].

A comparison of rate constants measured here for reduction of wustite and literature values is difficult. First, as previously mentioned, most reported values are limited to low temperatures where the current method can provide only coarse estimates. Second, rate constants for reactions of CO and CO_2 on surfaces of iron and wustite are usually reported per unit area of surface such as in the works of Grabke[20], Pettit and Wagner[21], Hauffe and Pfeiffer[22], and Fruehan and Martonik[23] among others. In other parts[24, 25], complex reduction models are used and rate constants fitted from experimental data relying on correlations for rate processes such as sintering and gas diffusion. In broad comparison, the values measured here are somewhat larger than those measured by Turkdogan[7] and El-Geassy and Rajakumar[26] as shown in Figure 10. However, both those authors used methods of direct reaction with a stream of CO-CO_2 so that rates measured may be under considerable influence of mass transfer. The values measured here are more closely related to the conditions required in simulations of reduction in composites.

V. Conclusions

For the evaluation of a new ironmaking process using an RHF and a smelter in series, it is necessary to have a model for the reduction of carbon-ore pellets. This model requires rate constants for reduction of FeO by CO and oxidation of carbon by CO_2. In the present study, these two rate constants were measured under the conditions of interest. In order to avoid the interference of mass transfer effects, measurements were made on small samples of mixtures of fine wustite and carbon. The analysis of data and any reduction model for higher temperatures demands the use of a combined reaction model with due regards to both reaction steps in the mechanism of gaseous

intermediates. The use of this model, however, relies on the assumptions of constant surface area per unit mass of reactants and may be restricted to the initial period of reaction. The main findings of this research can be summarized as:

- Wustite reduction rates become comparable to rates of carbon oxidation at higher temperatures. It is also important in composites with a large excess of carbon.
- Graphite is about as reactive as wood charcoal at higher temperatures. This could be due to a higher temperature dependence of oxidation rates of graphite[19], development of extensive porosity[19] and catalysis by newly formed iron[1, 2].
- CO poisoning of carbon surfaces is less significant than anticipated from measurements of other authors on carbon oxidation. In using a simple rate law for carbon oxidation an average deviation of only 30% in intrinsic rate constants was measured.

In Part II of this paper the results obtained here in terms of intrinsic rate constants as well as the combined reaction mechanism developed are used in a comprehensive model of a pellet where effects of heat transfer become significant. In Part II of the current paper, experimental verification of the comprehensive model is also presented.

Acknowledgements

The author would like to express his deepest gratitude and appreciation to Prof. Klaus Schwerdtfeger for all his many years of careful attention and guidance. Special thanks are also due to the member companies of the Center for Iron and Steelmaking Research, the American Iron and Steel Institute, and the Department of Energy for the financing of this research.

Tables and Figures

Table I: Rate constants measured according to the mechanisms of Gadsby[4] and Reif[5]. After Story[6]. Apparent activation energies E_1, E_2 and E_3 in Kcal/mol).

	Temperature (^{0}C)	k_1^0 (g/g.s.atm)	E_1	k_2^0 (atm^{-1})	E_2	k_3^0 (atm^{-1})	E_3
Coconut charcoal	734 – 839	1.32×10^{8}	58.8	1.26×10^{-8}	-45.5	3.16×10^{6}	30.1
Coke	800 – 1200	3.90×10^{9}	75.7	3.1×10^{-2}	9.70	5.91×10^{-6}	-17.6
Graphite	1060 – 1200	2.0×10^{14}	103.5	3.7×10^{4}	7.01	4.63×10^{7}	31.0
Anthracite coal	800 – 1090	4.37×10^{2}	32.5	4.6×10^{-3}	-16.9	1.8×10^{-3}	-16.6

Table II: Intrinsic rate constants of carbon oxidation and wustite reduction determined by mixed reaction model. Constants in g/g.s.atm.

Temperature (^{0}C)	Wood charcoal	Graphite	Wustite from taconite	Wustite from hematite
940	5.5×10^{-4}	-x-	(5×10^{-3})	-x-
1045	1.0×10^{-2}	3.2×10^{-3}	4×10^{-2}	4×10^{-2}
1086	-x-	8.5×10^{-3}	-x-	6×10^{-2}
1126	7.0×10^{-2}	4.0×10^{-2}	4.0×10^{-2}	1.3×10^{-1}
1189	1.5×10^{-1}	1.5×10^{-1}	1.0×10^{-1}	3.5×10^{-1}

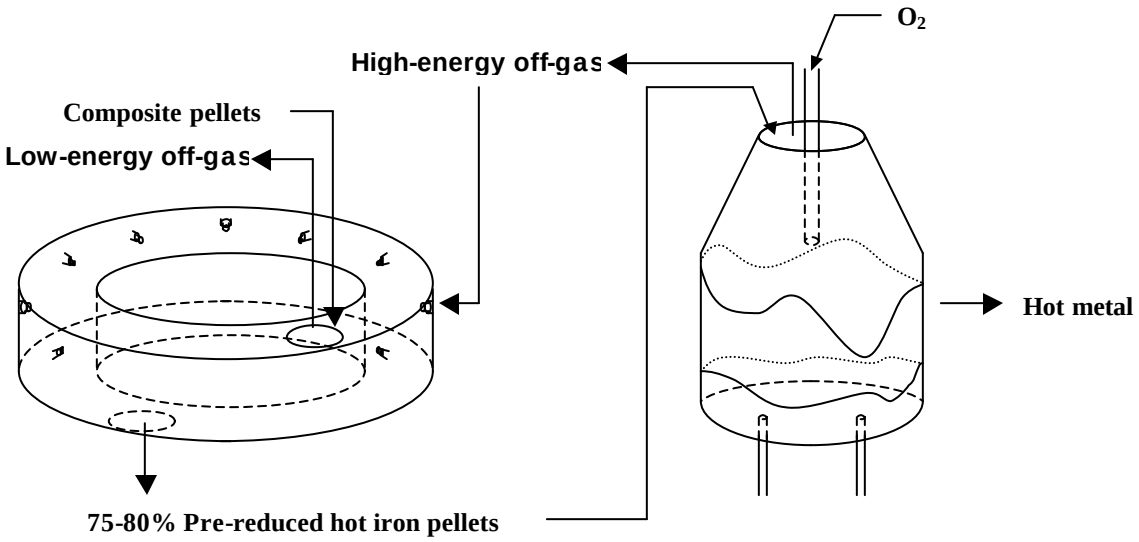

Figure 1: The proposed process.

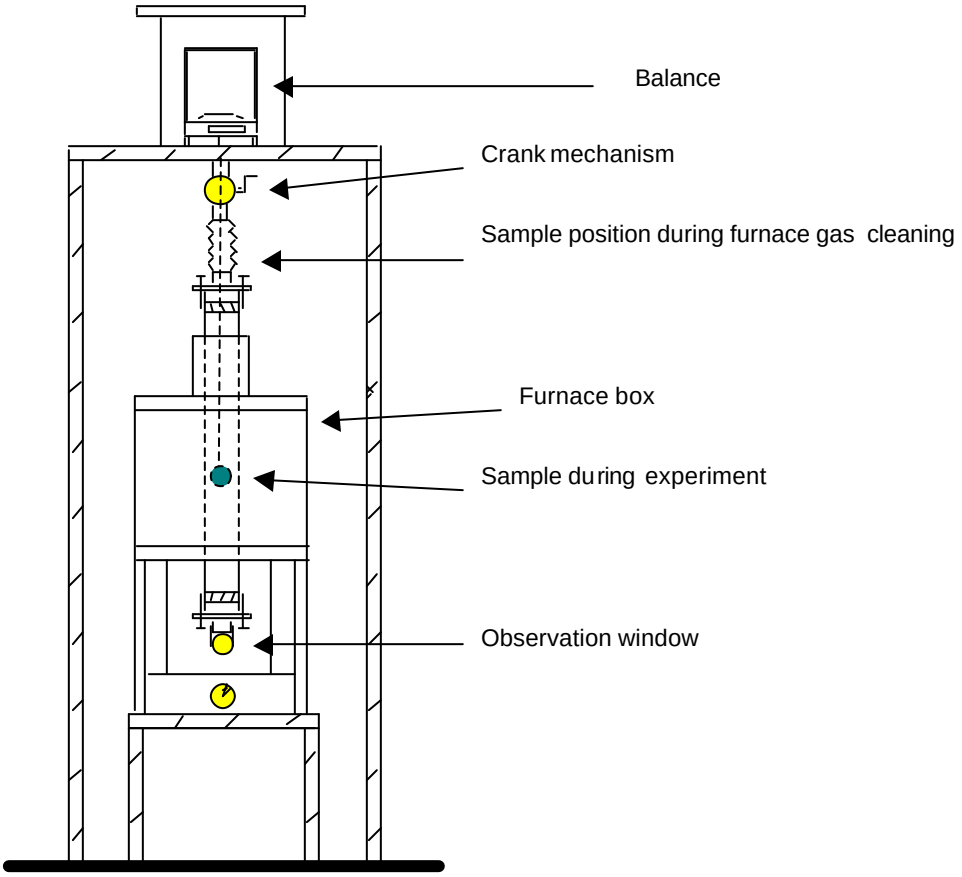

Figure 2: Experimental apparatus.

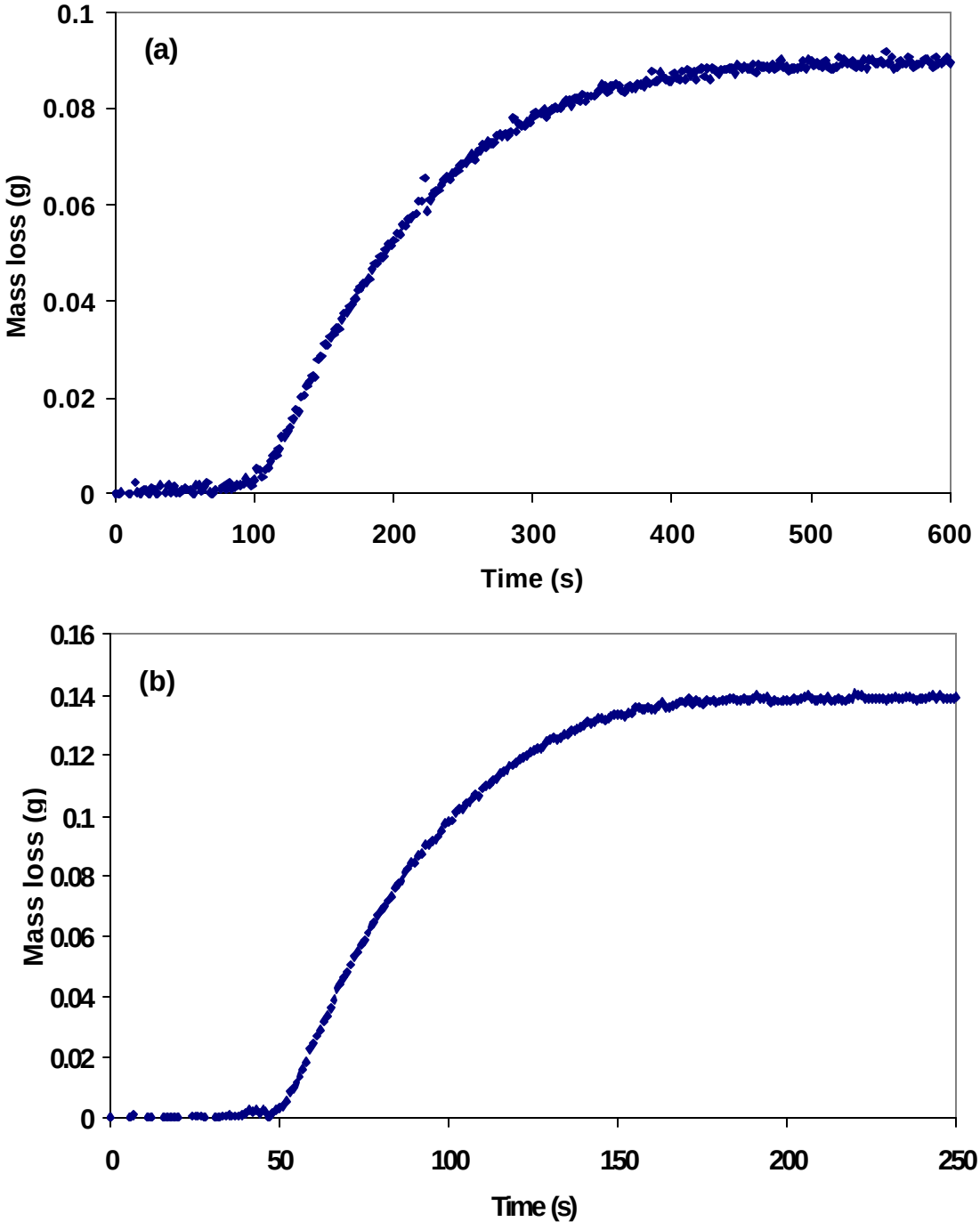

Figure 3: Typical results of measured mass change in samples with (a) wood charcoal and wustite from taconite and (b) graphite and wustite from hematite. 1126^{o}C.

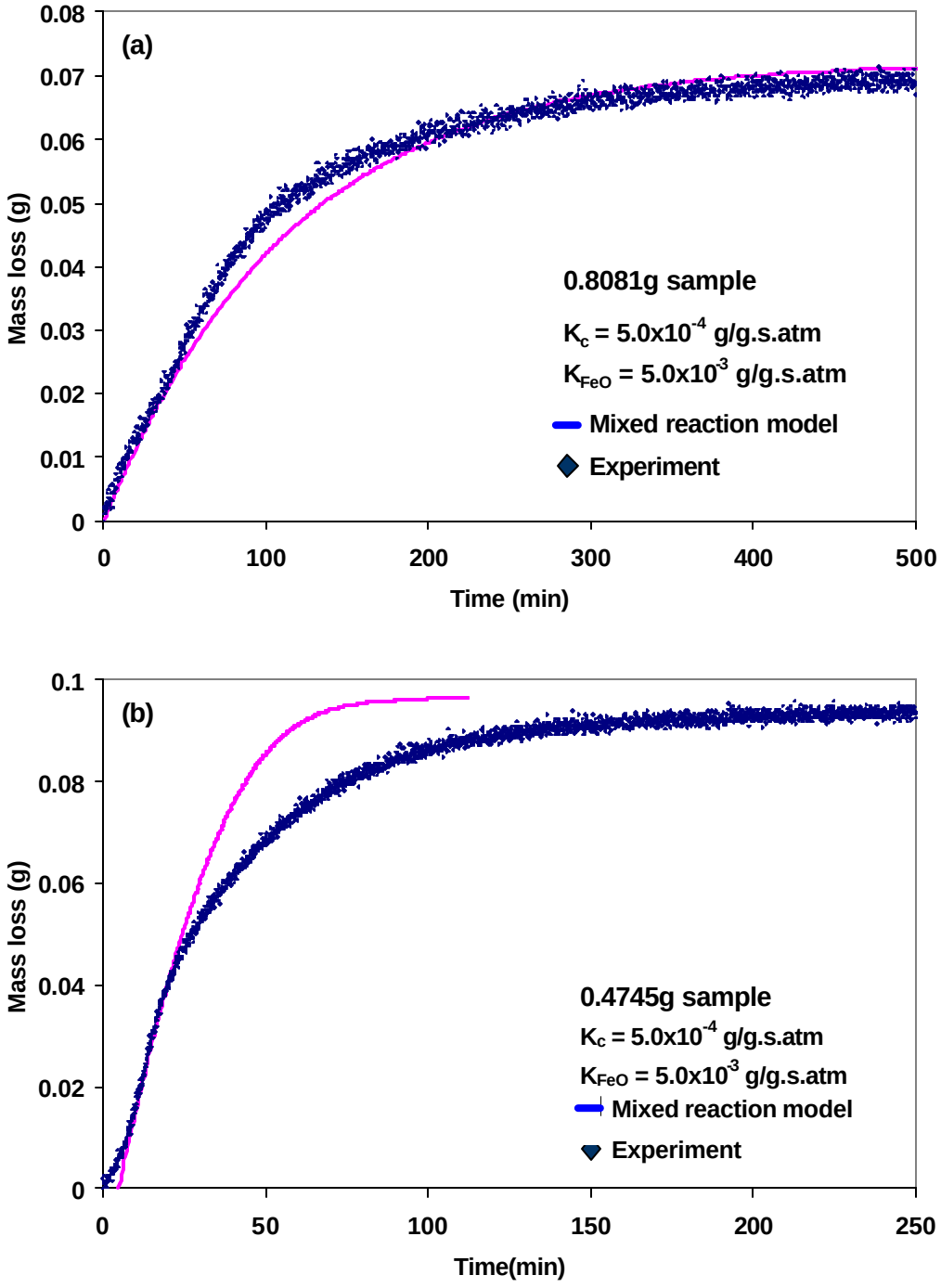

Figure 4: Iterative determination of rate constants by comparison of model results and measured mass losses at 940^{o}C in samples with 1/5 carbon to wustite molar ratio (a) and 5/1 carbon to wustite molar ratio (b). Results for wood charcoal and taconite mixtures.

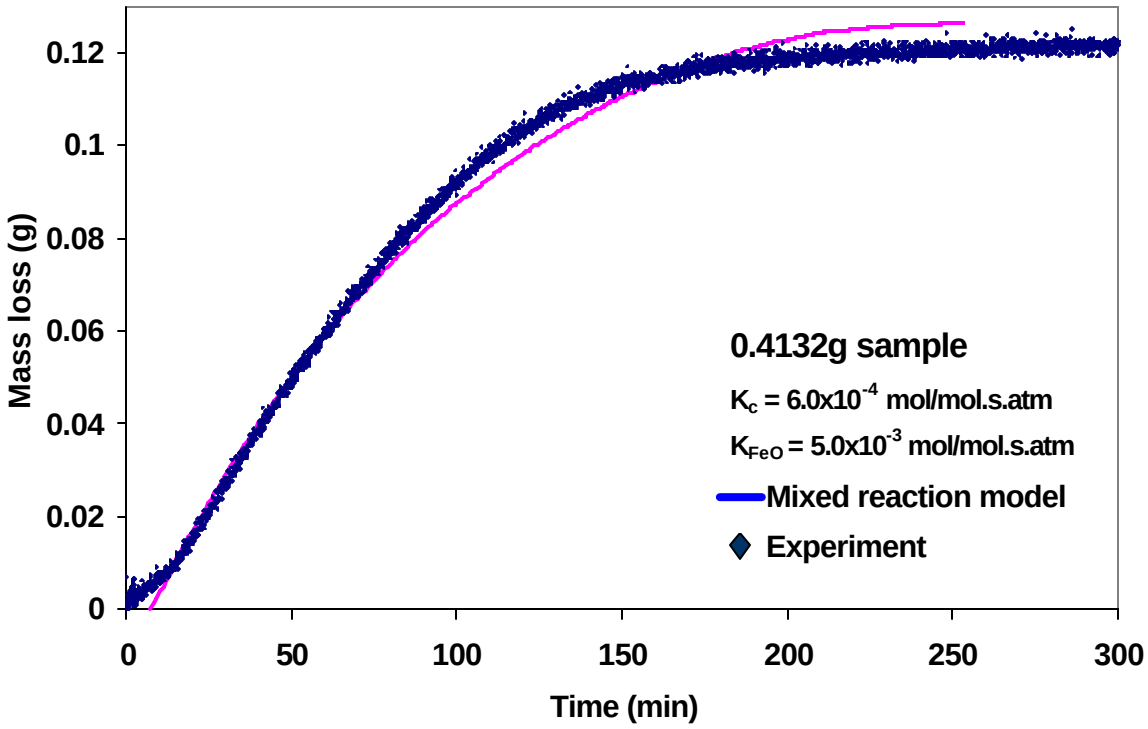

Figure 5: Validation of rate constants determined from experiments with low amounts of reactants using equimolar samples of carbon and wustite. Results at 940^{o}C for wood charcoal and taconite concentrate.

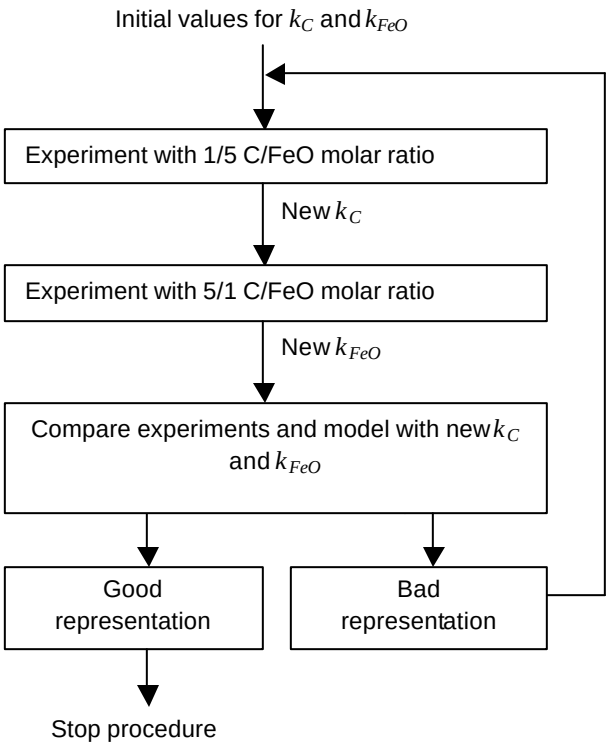

Figure 6: Schematic of procedure for determination of rate constants in mixed control reaction model.

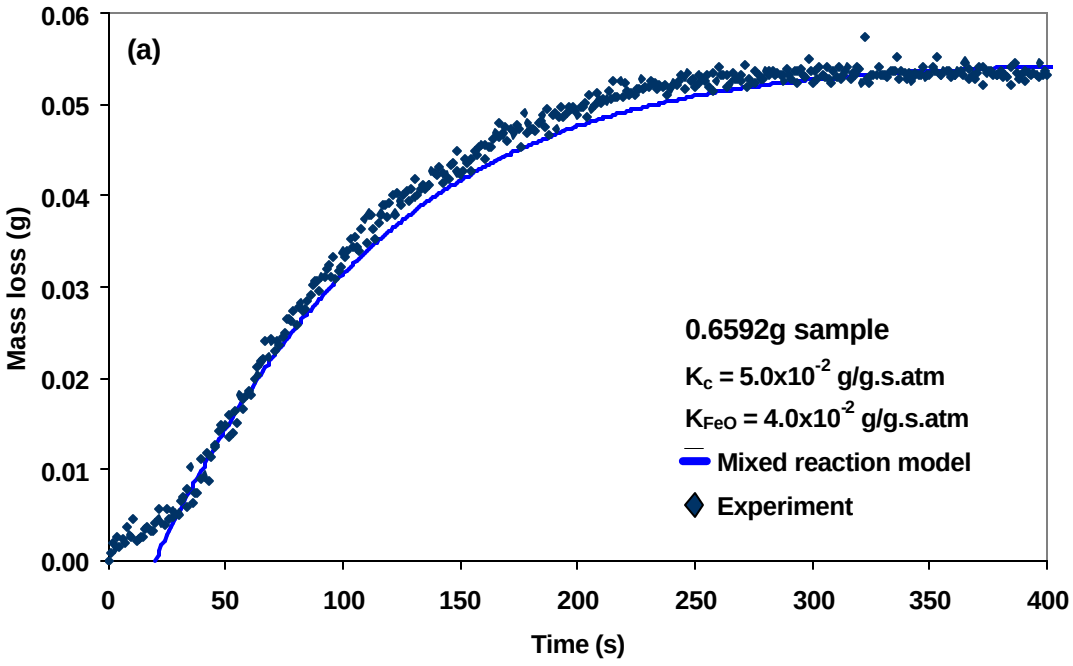
(a)
Mass loss (g)
0.06
0.05
0.04
0.03
0.02
0.01
0.00
0
50
100
150
200
250
300
350
400
Time (s)
0.6592g sample
$K_c = 5.0x10^{-2}$ g/g.s.atm
$K_{FeO} = 4.0x10^{-2}$ g/g.s.atm
Mixed reaction model
Experiment

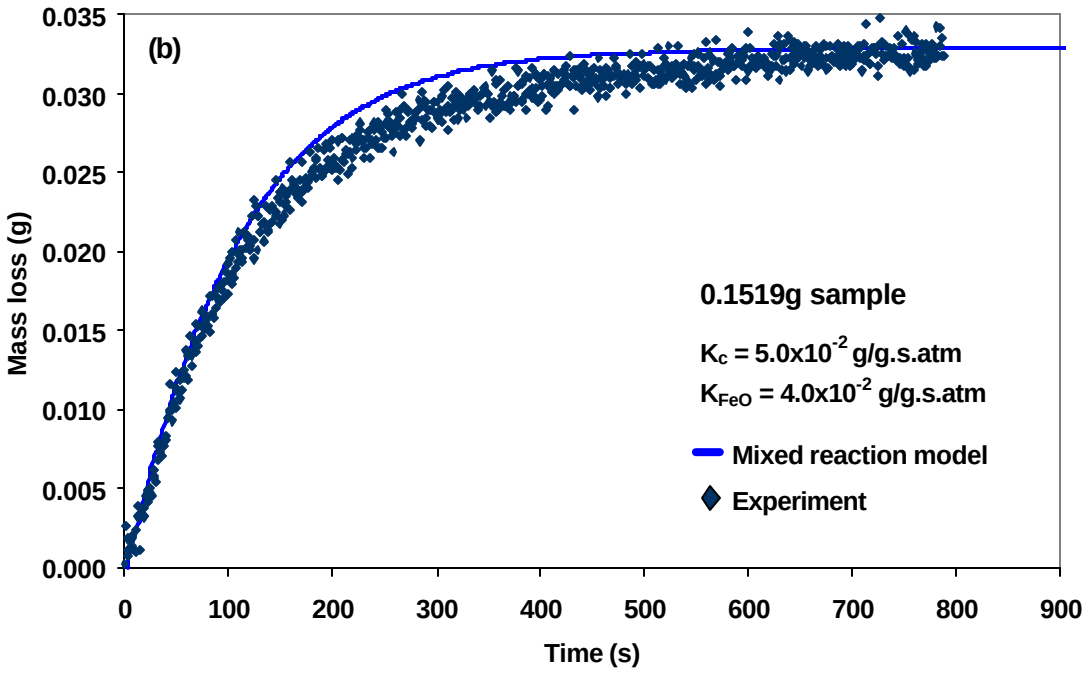
(b)
Mass loss (g)
0.035
0.030
0.025
0.020
0.015
0.010
0.005
0.000
0
100
200
300
400
500
600
700
800
900
Time (s)
0.1519g sample
$K_c = 5.0x10^{-2}$ g/g.s.atm
$K_{FeO} = 4.0x10^{-2}$ g/g.s.atm
Mixed reaction model
Experiment

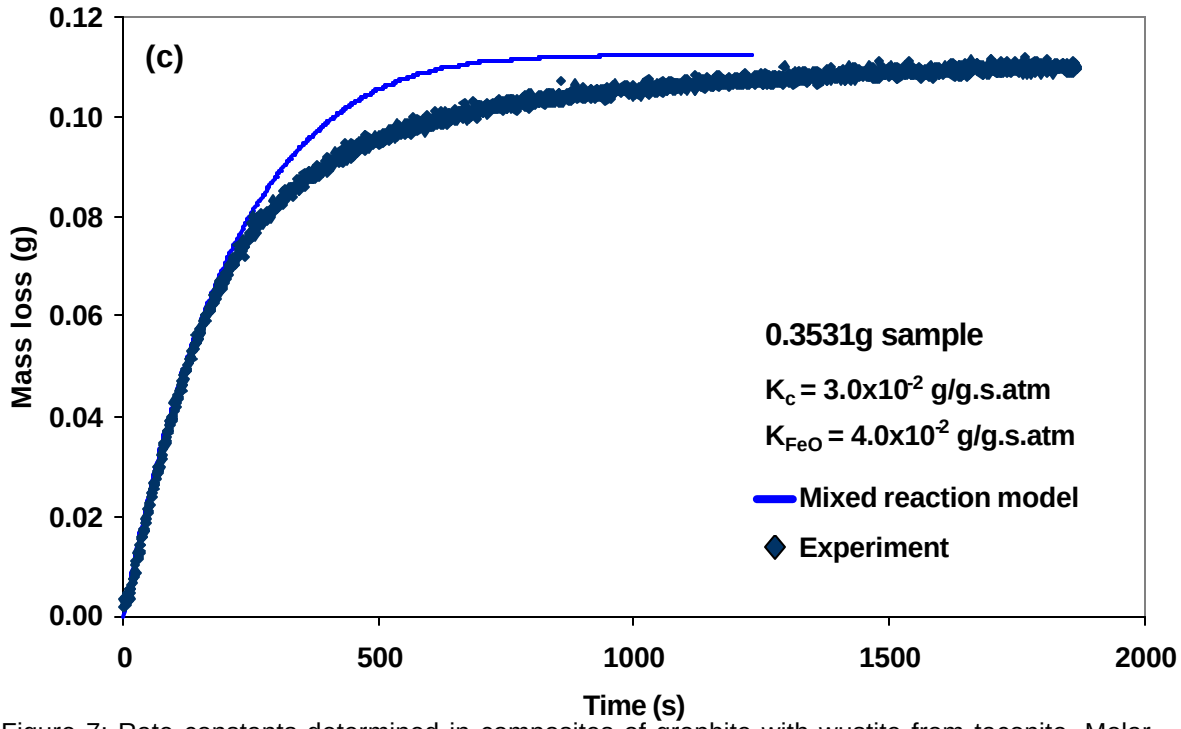

Figure 7: Rate constants determined in composites of graphite with wustite from taconite. Molar ratios of (a) 1/5, (b) 5/1 and (c) 1/1. Furnace at 1126^{o}C.

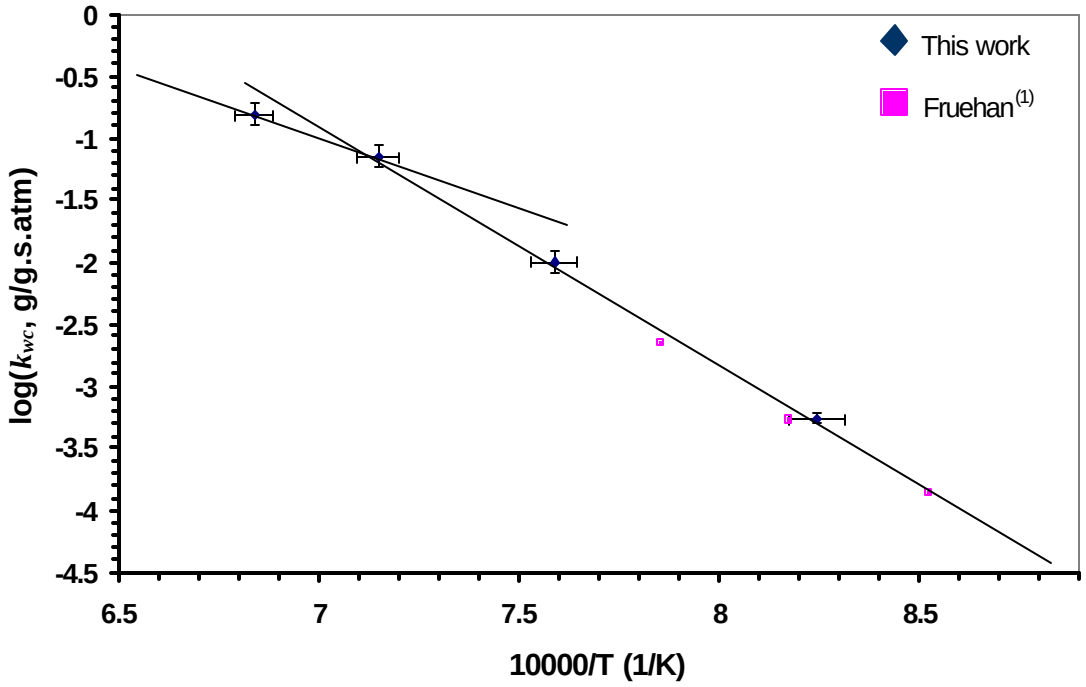

Figure 8: Temperature dependence of rate constants for oxidation of wood charcoal. Rate constants from Fruehan[1] relative to coconut charcoal.

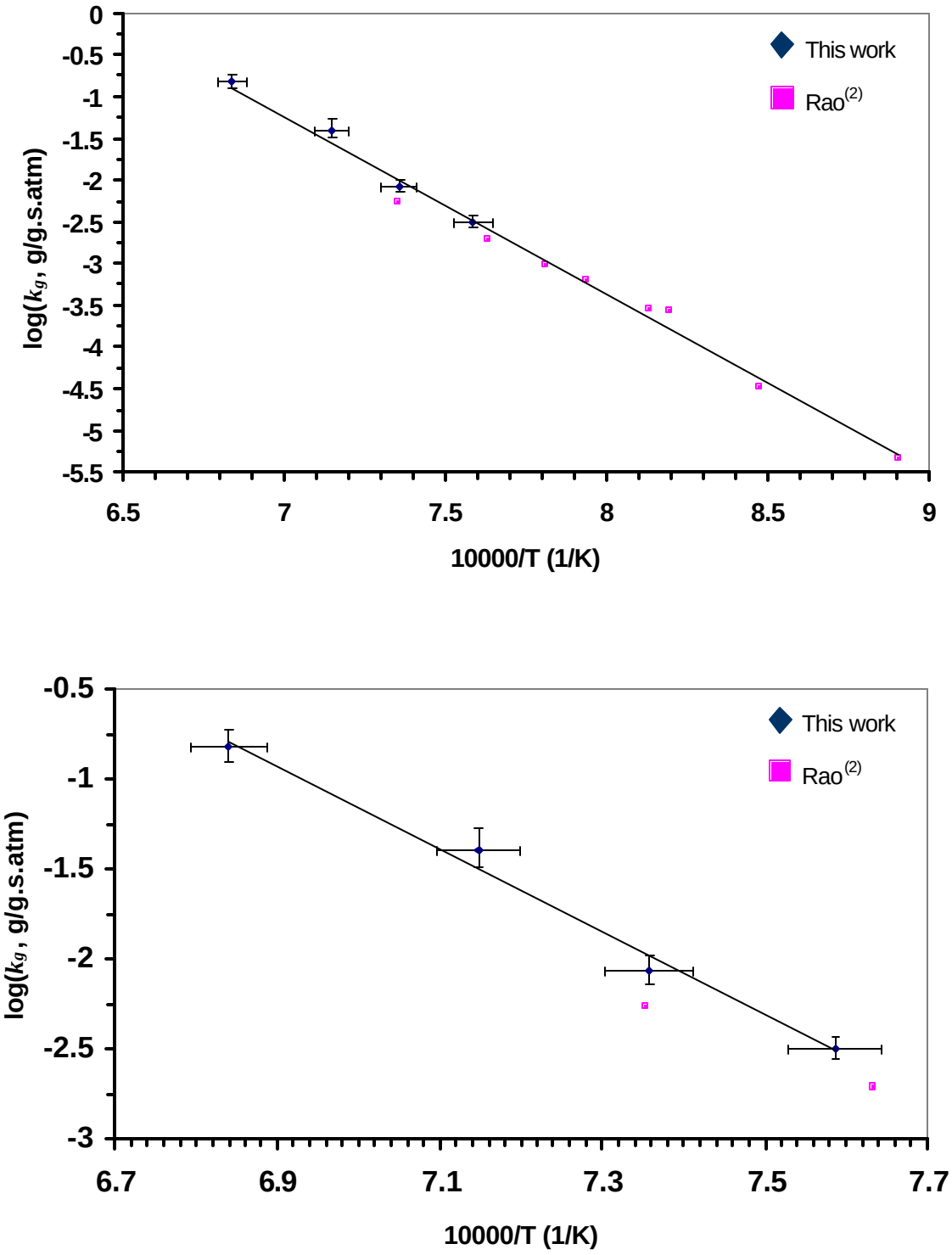

Figure 9: Temperature dependence of rate constants for oxidation of graphite. Data from Rao[2] measured using amorphous graphite.

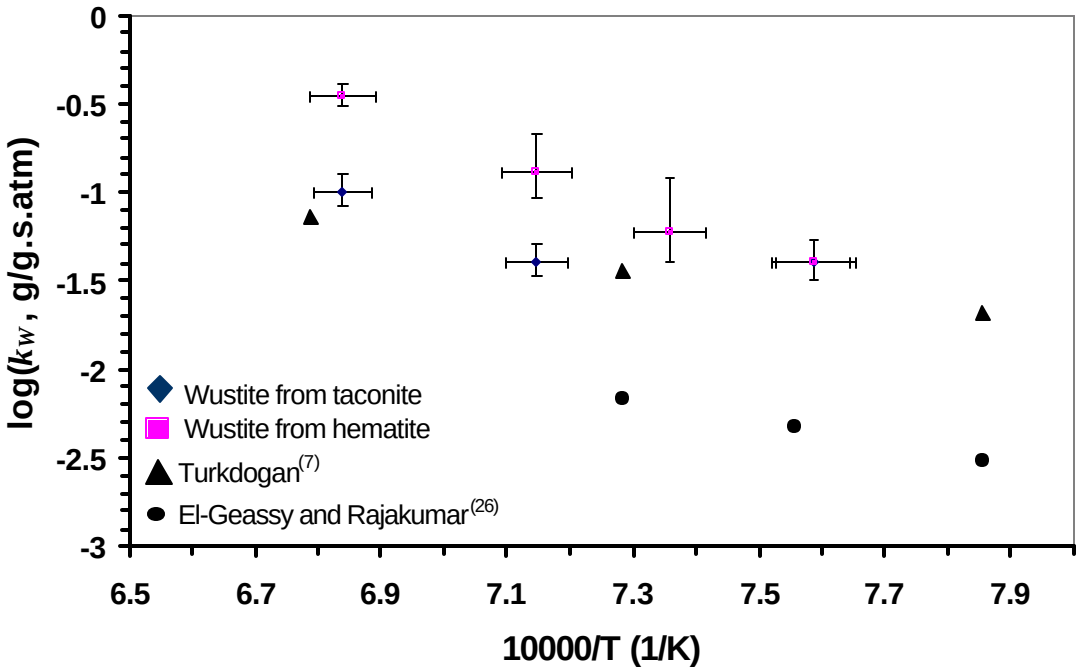

Figure 10: Comparison of intrinsic rate constants for reduction of wustite measured in this work with values from the literature.

References

5) R. J. Fruehan: *Metall. Trans. B*, 1977, vol. 8B, pp. 279-86.

6) Y. K. Rao: *Metall. Trans.*, 1971, vol. 2, pp. 1439-47.

7) S. Sun and W-K. Lu: *Iron Steel Inst. Jpn. Int.*, 1993, vol. 33, pp. 1062-69.

8) J. Gadsby et al.: Proc. Roy. Soc., 1948, vol. A193, pp. 357-376.

9) A. E. Reif: J. Phys. Chem., 1952, vol. 56, pp. 785-788.

10) S. R. Story: Post Combustion Reactions and Modeling, PhD thesis, Carnegie Mellon University, 1997.

11) E. T. Turkdogan and J.V. Vinters: *Metall. Trans.*, 1972, vol. 3, pp. 1561-74.

12) E.T. Turkdogan, R. G. Olsson and J. V. Vinters: *Carbon*, 1970, vol. 8, pp. 545-564.

13) P.L. Walker, F. Rusinko, and L.G. Austin: *Adv. Catalysis*, 1959, vol. 11, pp. 133-221.

14) O. Kubaschewski, E.L. Evans, and C.B. Alcock: *Metallurgical Thermochemistry*, Pergamon press, Oxford, 1976.

15) L. S. Darken and R. W. Gurry: *Journal of the American Chemical Society*, 1945, vol. 67, pp. 1398-412.

16) Y. K. Rao: *Chem. Eng. Sci.*, 1974, vol. 29, pp. 1435-45.

17) R. H. Tien and E. T. Turkdogan: *Metall. Trans. B*, 1977, vol. 8B, pp. 305-13.

18) J. Feinman and D. M. Rae: *Direct reduced iron technology and economics of production and use*, Iron and Steel Society, Warrendale, PA, 1999, p. 53.

19) H. K. Kohl and H-J. Engell: *Arch. Eisenhuttenwesen*, 1963, vol. 6, pp. 411-18.

20) E. T. Turkdogan and J. V. Vinters: *Carbon*, 1970, vol. 8, pp. 39-53.

21) E. W. Thiele: *Ind. Eng. Chem.*, 1939, vol. 31, pp. 916-920.

22) A. Wheeler: *Adv. Catalysis*, 1951, vol. 3, pp. 249-327.

23) S. R. Story and R. J. Fruehan: *Metall. Trans. B*, 2000, vol. 31B, pp. 43-54.

24) H.-J. Grabke: *Z. Elektrochem.*, 1965, vol. 69, pp. 48-57.

25) F. S. Pettit and J. B. Wagner: *Acta Met.*, 1964, vol. 12, pp. 35-40.

26) K. Hauffe and H. Pfeiffer: *Z. Metallk.*, 1953, vol 44, pp 27-36.

27) R. J. Fruehan and L. J. Martonik: *High Temp. Sci.*, 1971, vol. 3, no. 3, pp. 244-256.

28) S. P. Trushenski, K. Li and W. O. Philbrook: *Metall. Trans.*, 1974, vol. 5, pp. 1149-1158.

29) M. Meraikib and H. A. Friedrichs: *Arch. Eisenhuttenwesen*, 1987, vol. 58, pp. 439-445.

30) A. A. El-Geassy and V. Rajakumar: *Iron Steel Inst. Jpn. Int.*, 1985, vol. 25, pp. 1202-1211.

Appendix B – Detailed Construction of Model Combining Heat Transfer and Chemical Kinetics

Submitted for publication in Metallurgical Transactions

Rate of Reduction of Ore-Carbon Composites
Part II: Modeling of Reduction in Extended Composites

O. M. Fortini and R. J. Fruehan
Carnegie Mellon University
Pittsburgh, PA

Abstract

A new process for ironmaking was proposed using a rotary hearth furnace and an iron bath smelter to produce iron employing wood charcoal as energy source and reductant. This paper examines reactions in composite pellet samples with sizes close to sizes used in industrial practice (10 to 16mm in diameter). A model was constructed using the combined kinetic mechanism developed in Part I of this paper[1] along with equations for the computation of pellet temperature and shrinkage during the reaction. The analysis of reaction rates measured for pellets with wood charcoal showed that heat transfer plays a significant role in their overall rate of reaction at elevated temperatures. The slower rates measured in pellets containing coal char show that the intrinsic kinetics of carbon oxidation is more significant than heat transfer. Model calculations suggest that the rates are highly sensitive to the thermal conductivity of pellets containing wood charcoal and are less sensitive to the external conditions of heat transfer. It was seen that the changes in pellet surface area and diameter due to shrinkage introduce little change on reaction rates. The model developed provides an adequate description of pellets of wood charcoal up to circa 90% of reduction. Experimentally determined rates of reduction of iron oxide by wood charcoal were approximately 5 to 10 times faster than rates measured in pellets with coal char.

I. Introduction

In Part I of this paper[1], a new process for ironmaking was proposed using a rotary hearth furnace (RHF) in combination with a smelter. In the new process, composite pellets of iron oxide and carbon would be partially reduced in a rotary hearth furnace and the final reduction, melting and gangue separation would be done in the smelting unit. The rate constants for oxidation of wood charcoal and graphite by CO_2, and reduction of wustite by CO were measured at temperatures relevant to the RHF. In this paper, a model for the reduction of composite pellets is developed taking into account the combined kinetics of carbon oxidation and wustite reduction along with heat transfer and pellet shrinkage. The modeling for this system was done coupling the equations of continuity for solid and gas with an enthalpy balance applied to a control volume inside the pellet. Experimentally, measurements of mass change, pellet size, and composition of off-gas during reduction were conducted in order to validate the model. The final model will be used in a process model of the RHF.

A number of models can be found in the literature which are related to reduction in composites of iron oxides and carbon[2,3,6-9] . The main features commonly found in the reduction models are: reaction rate laws, temperature change, gas transport, and changes in size of specimen. A summary of the approaches found in the literature for each of these items is given in Table I.

Reaction rate laws: The generally accepted mechanism of reduction in composites of iron oxides and carbon consists of two elementar reaction steps: carbon oxidation and reduction of iron oxides. The two steps were discussed in Part I of this paper. Consistent with this reaction mechanism, Rao[2] and Tien and Turkdogan[3] presented models for

reduction in composites where the overall kinetics is controlled by the oxidation of carbon. This should be the case at lower temperatures, where rates of reduction of iron oxides are considerably faster than rates of carbon oxidation. Rao[2] used a rate law in the original form derived from the mechanisms of Gadsby[4] and Reif[5] while Turkdogan[3] employed a simplified version to account for the effects of poisoning by CO, namely:

$$R = \frac{k_1 P_{CO_2}}{1 + k_2 P_{CO}} \tag{1}$$

where R is the rate constant per unit mass of carbon (g/g.s), k_1 and k_2 are empirical rate constants in (g/g.s.atm) and (atm^{-1}) respectively, and P_{CO_2} and P_{CO} are the local pressures of carbon dioxide and carbon monoxide (atm). Sohn and Szekely[6] suggested the use of a form similar to that used by Turkdogan[3] with the addition of a reversible term for both steps of carbon oxidation and reduction of the iron oxides but limited their study to the interpretation of limiting cases in terms of their reaction model; no experimental work was presented for validation of the formulation suggested. In the modeling of reactions at higher temperatures, Sun and Lu[7, 8], and Donskoi and McKelwain[9] considered both steps in the reaction mechanism in the formulation of reaction rate laws. Sun and Lu[7, 8] applied a rate law for reduction of iron oxides with the form:

$$R = nS\,4p\bar{r}^{2} k_o (C_{CO} - C_{CO}^{e}) \tag{2}$$

where R is the rate of reduction per unit volume of mixture (mol/m^3.s), n is the number of particles of iron oxide per unit volume of composite (m^{-3}), S is a shape factor used to correlate the average particle radius r (m) with the surface area of one particle being determined from BET adsorption techniques and measurements of average particle radius, k_o is a specific rate constant (m/s), and C_{CO} and C_{CO}^e are the local and equilibrium concentrations of CO (mol/m^3). Sun and Lu[7, 8] also used the same form of rate law for the oxidation of carbon. In a different approach, Donskoi and McKelwain[9] used a series of "mass ratio coefficients" assuming a first order reaction, rate constants of carbon oxidation were not directly addressed. The values or procedures for determination of the "mass ratio coefficients" were not given.

Reaction sequence: Rao[2] and Sun and Lu[7, 8] assume a stepwise pattern of reduction where each step in the sequence $Fe_2O_3 \rightarrow Fe_3O_4 \rightarrow FeO \rightarrow Fe$ goes to completion before the next step is started. Turkdogan[3] and Donskoi and McKelwain[9] do not rely on this hypothesis. Some authors have observed the coexistence of more than two iron phases during reduction of composites but it is unclear whether the three phases were found in a same grain or in different locations inside the reacting mixture. The coexistence of more than two iron phases was experimentally verified by Spitzer[10] for the reduction of large specimens of iron oxides in streams of reducing gases (CO, H_2).

Temperature change: The temperature change is usually determined by means of an enthalpy balance. Simple formulations can be found in the literature[11] where no temperature gradient inside the samples is considered. In other works, such as those of Sun and Lu[7, 8] and Donskoi and McKelwain[9], the enthalpy balance is usually done considering the distribution of temperatures inside the reacting mixture or pellet. In the

early work of Sun and Lu[7] and in the work of Dosnkoi and McKelwain[9], no account is taken of the gas transport in the enthalpy balance. However, in the most recent work, Sun and Lu[9] include such transport of gas.

Gas transport: The problem of gas transport inside reacting composites has been approached in at least two different ways. In developing his reduction model, Rao[2] assumed that Knudsen diffusion was the operative mode of gas transport and derived expressions for the effective Knudsen diffusivity based on structural parameters of the reacting composite. Tien and Turkdogan[3], and Lu[8] considered the movement of gas as the result of molecular diffusion and forced flow due to the positive net rate of gas generation during reduction. Other researchers such as Donskoi and McKelwain[9] consider the transport of gas as secondary for the overall reduction process thus disregarding gaseous exchanges in their formulation.

Changes in pellet size: In previous studies, changes in size of reacting composites have been addressed essentially by means of empirical correlations as exemplified in the work of Donskoi and McKelwain[9]. In their work, Donskoi and McKelwain[9] considered the total change in size of the reacting composite as the combined result of shrinkage and swelling with proper empirical correlations derived from works of other researchers. However, it must be noticed that the empirical correlations used are obtained assuming an isothermal situation where the composite sample is at a given temperature during the whole process. Thus, the use of such correlations in cases where the samples are non-isothermal may not be strictly correct. No attempt for a more refined treatment of changes in size could be found in the literature.

II. Experimental Apparatus and Technique

The apparatus used in this research, a thermogravimetric furnace, was described in Part I of this paper. In the current work, reduction experiments were done with composite pellets of carbon and iron oxides following the same procedure described previously[1]. The samples were in the form of pellets of 10-16mm. Three different types of carbon and two types of iron oxides were employed: wood charcoal, coal, graphite, North-American ore, and reagent grade hematite. The amount of ash in the wood charcoal used was measured by burning samples of sized granules (from larger than 20 mesh down to smaller than 200 mesh) in a muffle furnace under air. In these tests, the samples were placed in crucibles and had their mass measured in intervals of 24 hours until no measurable mass loss could be registered for three consecutive intervals. These experiments showed a low amount of ash (less than 2%) in the wood charcoal. A maximum of 1.7% in mass of ash was found in the wood charcoal fraction smaller than 200 mesh. The amount of ash in the coal was significantly higher than in wood charcoal, 12.6% in mass in the fraction smaller than 200 mesh. The amount of volatiles released from the wood charcoal was measured in conditions of fast heating following the same procedure described previously. The amount of volatiles released appears evenly distributed according to the sizes of the wood charcoal used ranging from 16.8 up to 18.6%. The composition of the ore used is given in Table II.

The pellets used in reduction experiments were prepared from master mixtures of carbon and iron oxide with carbon to oxide ratios close to 0.175 by mass. Experiments were done with furnace temperatures between 900 and 1280^{o}C, as typical of RHF operations as reported by Grebe[12]. The wood charcoal and coal used were devolatilized at 1000^{o}C for 10 hours under a stream of argon prior to the preparation of the pellets. All

reactants were sized to –200mesh before mixing and agglomeration. The agglomeration of the pellets was done by addition of water followed by rolling and drying in a muffle furnace at 200^{o}C for four days. Pellets containing ore required addition of a binder (5% in mass of bentonite containing sodium) for agglomeration. The final pellets used in reduction experiments had masses ranging from 2.0 to 5.0g providing for two ranges of diameters close to 1.0 and 1.6 cm.

During the pellet reduction experiments, changes in mass were recorded with the same procedure used previously. The composition of gas leaving the furnace tube was also monitored using a mass-spectrometer linked to the gas outlet of the furnace. Changes in pellet size were measured by two different procedures. First, a caliper was used to measure the initial and final diameter of the pellets along four different directions. Changes in pellet size were also measured placing a CCD (Charge-coupled device) camera in front of the observation window at the bottom of the reaction tube. The images from the camera were continuously registered in video cassete and later analyzed with an image analyzer where the cross section area of the pellets was measured. The errors in all measurements were studied in detail and do not invalidate the conclusions.

Ancillary experiments were developed to study the heat transfer conditions from the furnace to the surface of the pellets during fast heating after loading into the furnace. Conditions of heat transfer were studied placing an optical pyrometer in front of the observation window at the bottom of the reaction tube. These experiments were done with pellets of pure hematite so that chemical reactions did not affect the analysis of the data. In these experiments, the temperature readings from the pyrometer were continuously registered in a micro-computer linked to the pyrometer. Heat transfer

conditions were summarized in terms of the radiation view factor pellet-furnace tube by best fit of the data acquired with a simple model for the heating of pellets in the absence of reactions resulting in a range of view factors from 0.6 to 1.0. The average value of 0.8 was used during the simulations of composite pellets.

IV. Model Development

In order to predict rates of reduction of composite pellets in an industrial RHF based on laboratory data and cope with the variety of reduction patterns seen during the experimental work, a model of reduction was developed following the guidelines of previous researchers. As in previous works, two equations of continuity (for gas and solids) were coupled with the enthalpy balance in a control volume inside the composite assuming spherical symmetry for simplicity. The equations used for computation of changes in mass and temperature inside the composites were:

$$\frac{\partial r_i}{\partial t} = -\frac{1}{h^2}\frac{\partial (r_i v_i h^2)}{\partial h} + r_i \tag{3}$$

$$\sum_{i=1}^{i=P}\frac{\partial r_i \overline{H_i}}{\partial t} = -\sum_{i=1}^{i=P}\frac{1}{h^2}\frac{\partial (r_i v_i h^2 \overline{H_i})}{\partial h} + \frac{1}{h^2}\frac{\partial}{\partial h}\left(k h^2 \frac{\partial T}{\partial h}\right) \tag{4}$$

where r_i represents the molar concentration of component *i* in the pellet (mol/m^3 of pellet), P represents the total number of components present in the pellet, *t* represents time (s), v_i is the velocity of species *i* along the radius of the pellet (m/s), *h* is the distance from the center of the pellet (m), r_i is the rate of formation of component *i* per unit volume of pellet (mol/m^3.s), $\overline{H_i}$ represents the molar enthalpy of compound *i* (J/mol), *k*

represents the thermal conductivity of the pellet (J/s.m.K) and *T* represents the temperature (K) of the pellet at a given position *h*. In considering the possibility of shrinkage as suggested by Gilbert[13], the identity in volume fractions of the several solids and void space inside the composite was considered:

$$g_P + \sum_{i=1}^{i=S} g_i = 1 \Rightarrow \sum_{i=1}^{i=S} g_i = 1 - g_P \tag{5}$$

where g_i represents the volume fraction of solid *i* in the mixture, S represents the total number of solid components in the mixture, and g_P represents the pore fraction of the mixture. Solid velocities could be computed by means of identity (5) and a known function for the total change in pore with time as:

$$\frac{\P g_P}{\P t} = \sum_{i=1}^{i=S} \frac{1}{y_i} \left[\frac{\P (r_i v_i)}{\P h} + r_i \right] \Rightarrow \sum_{i=1}^{i=S} \frac{1}{y_i} \frac{\P (r_i v_S)}{\P h} = \frac{\P g_P}{\P t} - \sum_{i=1}^{i=S} \frac{r_i}{y_i} \tag{6}$$

where y_i (mol/m^3) is the compact molar density of each solid in the mixture. Gas velocities were computed combining the equation of continuity for the gas phase with the ideal gas law:

$$y_i = \frac{P_i}{mT} \tag{7}$$

where P_i stands for the partial pressure of gas *i* in the mixture (Pa) and m stands for the universal gas constant (Pa.m^3/mol.K). The resulting equation for gas velocity obtained is:

$$\frac{\partial y_i g_P}{\partial t} = -\frac{\partial (y_i g_P v_i)}{\partial h} + r_i \qquad (8)$$

In computing gas velocities, a total pressure of 1atm was assumed to hold during all the process of reduction. This assumption was taken from the argument of Turkdogan[3] that significant pressure buildups should not occur inside reacting composites and the experimental measurements of Fruehan[14]. The equations obtained for changes in moles, temperature and velocities of gas and solid were discretized according to the methodology of Patankar[15]. Briefly, the equations are first integrated over finite radial distances inside the pellet and suitable approximations for the derivatives of intensive properties at the boundaries are chosen for the computation of fluxes between control volumes. The derivatives in time were dealt with employing a fully explicit scheme.

In order to define the boundary condition of heat transfer to the surface of the pellets, the contributions due to convection and radiation were estimated from literature correlations. This analysis revealed that most of heat transfer is due to radiation. Thus, the boundary condition used was defined by:

$$q = S.\varepsilon_F.\varepsilon_P.\sigma.(T_F^4 - T_P^4) \qquad (9)$$

where q is the heat flux (J/m^2.s.K) to the surface of the pellets, S is a geometric view factor ranging from 0 to 1, ε_F and ε_P are the emittances of furnace tube and pellet, σ is the Stefan-Boltzmann constant (J/m^2.s.K^4), and T_F and T_P are the

temperatures of furnace and pellet surface (K). A literature search of emittances of carbon, oxidized iron and alumina showed large ranges of values depending on specific conditions of the surfaces. Therefore, in analyzing heat transfer from the surroundings to the pellets a heat transfer coefficient (h_r) was defined as the product of emittances and view factor as:

$$h_r = S.e_F.e_P \tag{10}$$

The coefficient h_r in the experimental apparatus is in the range 0.6 to 1.0. This range was determined from the comparison of experimental results of surface temperature measurements of a pellet of pure hematite and results from the model developed. Thermal conductivies of the reacting composites were obtained from the base data of Akyiama[16] pertaining to compact iron oxides and iron, and a comparative study of values reported for carbon. It should be noticed that values reported for carbon span a considerable range from a low 0.84 for amorphous graphite up to 418 J/m.s.K in recrystallized ingots. In this work, only the upper limit of 418 J/m.s.K was used in simulations since all heat would flow along the path of highest thermal conductivity in a random aggregate of powders. The model chosen to represent the thermal conductivity of the aggregate assumed an arrangement of series resistances for the solid phases in parallel with a pore of negligible conductance based on the analogy of Maxwell. Radiation through pores was disregarded from a comparison of results from Schotte's[17] correlation and the conductivity of amorphous graphite. Finally, the contribution of interface resistances between grains suggested by Luikov[18] was also disregarded from results of experiments with samples of loose alumina powders in a uni-directional heat

transfer apparatus. The interested reader is referred elsewhere to the details of this experimentation[19].

III. Results and discussion

A. Reduction rates

Wood Charcoal: Experimental measurements of mass loss and gas composition during reduction of pellets of wood charcoal and hematite or taconite are shown in Figures 1 and 2. As can be seen in the figures, no sudden changes in slope indicating abrupt changes in reaction rates could be seen in the measurements of mass loss taken during experiments with these types of composite pellets. The absence of marked changes in reaction rates during the experiments strongly suggests that carbon oxidation is not the only rate-controlling mechanism in operation. In strict control by carbon oxidation, at least one marked change in rate should be seen corresponding to the increase in CO content of the off-gas due to the transition between the steps of reduction of magnetite to wustite and wustite to iron. Indeed, rates of reaction per unit mass of carbon or iron oxides computed from the experimental data were not constant between experiments with large and small pellets at the same temperature as should be expected from pure control by one of the two chemical steps. Instead, the best correlation found in pellets containing wood charcoal was between their initial surface area and the initial absolute rate (g/s). This empirical correlation is strong evidence that external heat transfer from the furnace tube to the samples plays a significant role in determining the overall rate of reaction. Measurements of off-gas composition showed an initial period with large generation of CO_2 followed by a short 'plateau' and final decrease towards the end of reduction. These measurements of off-gas composition support the proposition of Rao[2]

that reduction takes place following the stepwise transformation $Fe_2O_3 \rightarrow Fe_3O_4 \rightarrow "FeO" \rightarrow Fe$. A peculiarity was found in the cross-sections of partially reduced pellets containing wood charcoal as shown in Figure 3. As can be seen in Figure 3, a rim of iron close to the surface of the pellet was found in pellets of wood charcoal resembling the outer topochemical layer found in pellets of pure iron oxides. The two observations of proportionality between the initial rates of reaction and presence of an outer rim of reduced iron may be considered experimental evidence of combined control by heat transfer to the surface and within the pellet.

Graphite: Typical results of measurements of mass loss and off-gas composition for pellets containing graphite are shown in Figures 4 and 5. In these experiments, the curves of mass loss indicate the existence of three main stages of reaction marked by two changes in slope. This observation is in support of the pattern proposed by Rao[2] with the changes in rate seen between the two first reaction stages (i.e. the transformations of hematite to magnetite and magnetite to iron) explained by the change in CO concentration in the gas inside the composites; CO poisoning of carbon surfaces has been extensively reported as a cause for the retardation of rates of carbon oxidation. The increase in rate during the third reduction step indicated by the second change in slope cannot be explained by the effects of CO on the rates of carbon oxidation.

An ancillary set of experiments of graphite combustion in CO_2 was undertaken to clarify the possible existence of catalysis by iron formed during the third step of reduction as the motive for the increase in rate suggested by the second change in slope shown in Figure 4. The comparison of results from the experiments of graphite oxidation in CO_2 with the measurements of wustite reduction by graphite reported in Part I of this paper

strongly suggested that catalysis by newly formed iron could play a part in this process. Rate constants of graphite oxidation measured after all corrections for mass transfer effects were lower than measured in studies with composite samples with wustite in small crucibles. Therefore, catalysis of graphite by iron is a strong possibility to explain the rate increase observed. Another possibility for the rate increase observed during the third reduction step is the development of extra porosity in the graphite. However, experiments with pellets at lower temperatures where heat transfer should play a lesser role in determining the overall reaction rate showed increases in rate of several orders of magnitude at sharply defined instants in time as shown in Figure 6. An increase in graphite porosity of such magnitude occurring at the exact instant when the first formation of iron is expected seems unreasonable. Therefore, the catalytic activity of iron on the oxidation of graphite is the most plausible explanation to the increase in rate seen during the third stage of reduction of composite pellets.

Finally, differing from pellets with wood charcoal, no outer rim of iron could be identified in the cross sections of partially reduced pellets containing graphite as exemplified in Figure 7. Rather, reduction seems to take place evenly throughout the specimen suggesting the absence of significant gradients of gas composition and temperature.

Coal char: Results of mass loss and gas composition from experiments with pellets using coal char are shown in Figures 8 and 9. These results indicate that reaction rates of pellets containing coal char are roughly one order of magnitude slower than rates in pellets containing wood charcoal. In general, these experiments showed one change in slope indicating two main onsets of reaction. This is an indication of a reduction pattern

following the sequence $Fe_2O_3 \rightarrow Fe_3O_4 \rightarrow Fe$ similar to that proposed by Fruehan[14] instead of the pattern $Fe_2O_3 \rightarrow Fe_3O_4 \rightarrow "FeO" \rightarrow Fe$ followed in pellets with wood charcoal or graphite. This shift in reduction pattern is in agreement with the measurements of off-gas composition where an initial period with extensive formation of CO_2 is followed by a continuous decrease in the CO_2. In measurements with pellets containing coal char, no intermediate region with stable CO_2 amounts could be seen. Measurements of mass loss from pellets containing coal char did not show an increase in rate during the third stage of reaction as should be expected from any catalytic effect of iron as during reduction by graphite. Finally, it was observed that reactions in pellets containing coal char are apparently much slower than in pellets with wood charcoal or graphite as indicated by the much longer reaction times. This observation is in agreement with the observations of previous researchers that rates of coal char oxidation are slower than rates of oxidation of carbons from wood. Fractured surfaces of coal char pellets partially reduced were also examined and showed a uniform distribution of iron suggesting the absence of significant gradients of temperature and gas composition.

B. Pellet Shrikage

Owing to a considerable dispersion in the measurements of changes in diameter along the four different directions according to the placement of the pellets in the furnace tube, the extent of shrinkage among pellets of the same type was quantified in terms of a shrinkage coefficient (S_h) defined as the ratio between the final (D_F) and initial (D_o) average diameters measured along the four directions as:

$$S_h = \frac{D_F}{D_o} \tag{11}$$

The values of shrinkage coefficients are given in Table III. As can be seen in the Table, the experiments show the occurrence of some shrinkage in all types of pellets studied. The data summarized in Table III suggested that the type of iron oxide is important to the changes in size of the pellets, shrinkage being more pronounced in pellets containing hematite than in pellets containing taconite. Indeed, a more careful analysis of shrinkage in terms of the change in cross section area of the pellets during reduction showed two distinct behaviors according to the type of iron oxide used.

Shrinkage was further studied by means of the measurements of cross section area from the images registered with the CCD camera. Examples of measurements in cross section area of pellets containing wood charcoal are shown in Figure 10 in terms of the relative change in area defined as the ratio between the instantaneous cross section measured and the initial cross section of the pellets. As exemplified in Figure 10, all experiments with pellets containing hematite showed an initial period of fast shrinkage regardless of the type of carbon used. This behavior was not seen in pellets containing ore suggesting that the initial shrinkage is related to the sintering of the iron oxides. In some of the measurements of cross section area with pellets containing taconite, a small initial increase of less than 10% was observed confirming the experimental observation of Seaton at al.[20]; this initial increase could be due to the thermal expansion of the iron oxides and carbon.

In order to set a maximum limit on the possible extent of shrinkage due to the sintering of the iron oxides, results from the experiments where a pellet of pure hematite

was sintered for 20 hours in the reaction tube were used. Clearly, the long time allotted for the sintering of the hematite at the elevated temperature of the experiment would ensure the attainment of the upper limit of sintering shrinkage. For modeling purposes, an empirical correlation for the change in pore fraction of the hematite due to sintering was derived from the measurements of pellet diameter as:

$$g_P = 0.8052 \times \exp(-6.80 \times 10^{-4} T) \tag{12}$$

The correlation above was obtained assuming an exponential dependence for the volumetric fraction of pores on temperature as introduced by Seaton et al.[20]. The pore fractions of the initial and final hematite pellet were computed from the density of compact hematite and the measurements of pellet mass and diameter. Equation (12) was used in the reduction model of pellets containing hematite to account for the sintering of the iron oxides.

C. Comparison to Model

In order to evaluate the interplay among the several factors operating during the reduction of composite pellets, the model developed was first validated against experimental measurements of mass loss. Figures 11 and 12 show the comparison of results from the model with experimental results for pellets of hematite and wood charcoal or graphite with different size pellets and temperatures. The model developed was successful in simulating composites with hematite in all cases up to approximately 90% of reduction. In some cases, slower rates were measured after 90% reduction than were predicted from the model possibly due to the partial melting of the Fe-C alloys

formed during reduction of the wustite. Also, as discussed in Part I of the current paper, these deviations could be due to the changes in porosity of the carbon and iron oxides particles undergoing reactions. For illustrative purposes, Figure 11 also shows results from a calculation where heat transfer effects are disregarded (i.e. in this simulation, the pellet is assumed to reach the temperature of the furnace and there remain for the whole period of reaction). The results in Figures 11 and 12 show that heat transfer plays an important role in determining reaction rates in pellets of hematite combined with wood charcoal or graphite.

The model predictions for pellets of North-american ore in combination with wood charcoal or graphite resulted in significantly faster rates than actually measured as exemplified in Figure 13. These findings are in complete opposition to the behavior expected in the presence of the binder necessary for agglomeration. Carvalho[21] has associated the presence of sodium with the formation of highly reducible iron morphologies (whiskers) thus suggesting that intrinsic rates of reduction should increase in the presence of the bentonite used. Neither sodium nor bentonite have ever been reported to have any effect on the oxidation of carbon. Partial melting of the samples is the most probable cause of the discrepancies found. This reason should be considered as speculative in nature since a detailed thermodynamic study of the system is necessary in order to determine if low melting temperature phases would be stable in the presence of bentonite. This issue should be further studied along with the kinetics of formation of these new phases. The model developed presents good predictive results in cases where no such complex phases are present such as in the studies of pellets of hematite in combination with wood charcoal or graphite.

The importance of heat transfer does seem dominant in experiments where good agreement with model predictions is found up to almost complete reduction. That is, while deviations should be expected for the reasons of extra area available for reactions and possible melting, the agreement is sustained up to almost complete reaction indicating that other phenomena play a lesser role in determining overall reaction rates. In such cases, the agreement found suggests that intrinsic rates of reaction of carbon and iron oxides are fast enough to consume most of the heat supplied to the pellets.

In order to assess the relative importance of the two heat transfer steps to the overall rate of reaction in composites of wood charcoal and hematite, calculations were done varying the heat transfer coefficient (h_r) over the range 0.6 to 1.0 and the thermal conductivity of the pellet from 0.418 to 418 J/m.s.K. The importance of heat transfer inside the pellet to the overall reaction rate is exemplified by the results shown in Figure 14. The results shown in Figure 14 indicate that internal heat transfer has a significant role to the overall reduction rate attained. Indeed, among the factors studied, the internal condition of heat transfer was the one causing the most significant changes in model results. The evaluation of changes in the view factor representing the external condition of heat transfer showed that this parameter has little effect on the measured rates of reaction as exemplified in Figure 15. Instead, the main effect of changes in view factor seems to be the change induced in the time necessary to attain significant rates of reaction. Effects of shrinkage were evaluated by comparison of results from simulations where it is disregarded with the base case computations and experimental measurements of mass loss. This comparison showed that shrinkage introduces little changes in the rates computed from the model. The deviations between model and experimental results introduced by disregarding shrinkage are small and take place at after 70% of mass loss.

IV. Summary and Conclusions

In order to predict the rate of reduction of composite pellets of iron oxide and wood charcoal as proposed in the new process, a model of reduction for pellets was developed including the most prominent features of models reported in the literature. The model developed includes chemical kinetics, heat transfer, and effects of pellet shrinkage. The intrinsic rate constants of carbon oxidation and reduction of wustite were measured in Part I of the current paper. Experimentally, studies of reduction of composite pellets of wood charcoal, coal, and graphite in combination with hematite or North-American ore were done to validate the model. The main conclusions from this work are:

1. The assessment of compositions of off-gas during reduction confirmed the mechanism of gaseous intermediates as the main operative reaction mechanism in composite pellets;
2. The qualitative assessment of off-gas composition and mass change suggests that reduction in pellets of wood charcoal and graphite proceeds in the series $Fe_2O_3 \rightarrow Fe_3O_4 \rightarrow "FeO" \rightarrow Fe$ while in pellets with coal it proceeds in the series $Fe_2O_3 \rightarrow Fe_3O_4 \rightarrow Fe$;
3. The experimentally measured time to reach 90% reduction in pellets with coal char was 5 to 10 times longer than for pellets with wood charcoal primarily due to the faster rate of oxidation of charcoal;

4. Rates of reduction in pellets with graphite are faster than rates of reduction in pellets with coal char possibly due to the occurrence of catalysis of graphite oxidation by newly formed iron;
5. A reduction model was developed taking into account the kinetics of carbon oxidation and reduction of wustite along with heat transfer effects. This model was successfully applied to experiments done in the absence of binders;
6. Discrepancies found between results from the model and experimental measurements suggest that the presence of binder causes slower rates of reaction either by direct interaction with the reagents or by the formation of phases with low melting point;
7. For wood charcoal pellets reduced at temperatures common to RHF processes, the chemical rates of atomic recombination are fast resulting in overall reaction rates controlled mainly by heat transfer. On the other hand, for pellets of coal char the chemical rates are most probably the rate controlling step of the overall process.

Acknowledgments

The authors would like to thank very much the AISI-DOE, and the member companies of the Center for Iron and Steelmaking Research for the sponsorship and collaboration. Also, the authors are very grateful to Prof. Klaus Schwerdtfeger for all the help given in the development of the mathematical model. Finally, many thanks are due to Prof. Alan Cramb for the help given in the experimentation concerning the determination of thermal conductivities.

References

1) Fortini, O.M., and Fruehan, R.J., “Rate of reduction of ore-carbon composites. Part I: Determination of Intrinsic rate constants”, unpublished research.
2) Rao, Y.K., “A Physico-Chemical model for reactions between particulate solids occurring through gaseous intermediates – I. Reduction of Hematite by Carbon”, Chem. Eng, Sci., 1974, vol. 29, pp. 1435-1445.
3) Tien, R.H., and Turkdogan, E.T., “Mathematical Analysis of Reactions in Metal Oxide/Carbon Mixtures”, Met. Trans. B, vol. 8B, june 1977, pp. 305-313.
4) Gadsby, J., Long, F. J., Sleighton, P. and Sykes, K. W., “The mechanism of the carbon dioxide-carbon reaction”, Proceedings of the Royal Society of London, A193, 357(1948), pp. 357-376.
5) Reif, A. E., “The mechanism of the carbon dioxide-carbon reaction”, J. Phys. Chem., vol. 36, june 1952, pp. 785-788.
6) Sohn, H.Y., and Szekely, J., “Reactions between solids through gaseous intermediates – I Reactions controlled by chemical kinetics”, *Chem. Eng. Sci.*, vol. 28, 1973, pp. 1789-1801.
7) Sun, S., and Lu, W-K., “Mathematical Modeling of Reactions in Iron Ore/Coal Composites, ISIJ Int., vol. 33(1993), No. 10, pp. 1062-69.
8) Sun, S., and Lu, W.-K, “Building of a mathematical model for the reduction of iron ore in ore/coal composites”, ISIJ Int., vol. 39, 1999, no. 2, pp. 130-138.
9) Donskoi, E., and McKelwain, D.L.S., “Mathematical Modeling of non-iothermal reduction in highly swelling iron ore-coal char composite pellet”, Ironmaking and Steelmaking, vol. 28 (2001), No. 5, pp. 384-389.
10) Spitzer, R.H., Manning, F.S., and Philbrook, W.O., “Generalized Model for the Gaseous, Topochemical Reduction of Porous Hematite Spheres”, Trans. Met. Soc. AIME, vol 236, dec 1966, pp 1715-1724.
11) Wang, Q, yang, Z., Tian, J., Li, W., and Sun, J., “Reduction kinetics of iron ore-coal pellet during fast heating”, Ironmaking and Steelmaking, vol. 25(1998), No. 6, pp. 443-447
12) Grebe, K., Gunter, G., Lehmkuhler, H-J, Schmauch, H., “Die metallurgie der direkreduction von Huttenreststoffen nach dem Inmetco-Verfahren”, Stahl und Eisen 110(1990) Nr. 7, pp. 99-106.
13) Gilbert, D., “Coal based DRI: know the questions/get the answers”, Gorham Intertech Conference, Iron Ore for Alternative Iron Units, October 25-27, 1999, Charlotte, NC.

14) Fruehan, R. J., “The rate of reduction of iron oxides by carbon”, Metallurgical Transactions B, vol. 8B, june 1977, pp. 279-286.
15) Patankar, S.V., “Numerical heat transfer and fluid flow”, Taylor&Francis, New York (1980), 197 p.
16) Akyiama,T., Ohta, H., Takahashi, R., Waseda, Y., Yagi, J-i., “Measurement and Modeling of Thermal Conductivity for Dense Iron Oxide and Porous Iron ore Agglomerates in Stepwise Reduction”, ISIJ Int., vol. 32(1992), No. 7, pp. 829-837.
17) Schotte, W., “Thermal conductivity of packed beds”, *A.I.Ch.E. Journal*, vol. 6, No. 1, march 1960, pp. 63-66.
18) Luikov, A.V., Shashkov, A.G., Vasiliev, L.L., and Fraiman, Yu. E., “Thermal conductivity of porous systems”, *Int. J. Heat Mass Transfer*, vol. 11(1968), pp. 117-140.
19) O.M. Fortini, “Renewable Energy Steelmaking: On a New Process for Ironmaking”, Carnegie Mellon University, 2004.
20) Seaton, C.E., Foster, J.S., and Velasco, J., “Reduction Kinetics of Hematite and Magnetite Pellets Containing Coal Char”, Trans. ISIJ, vol. 23(1983), pp. 490-496.
21) Carvalho, R. J., Quariguasi Netto, P. G. And d’Abreu, J. C., “Kinetics of reduction of composite pellets containing iron ore and carbon”, Canadian Metallurgical Quarterly, vol. 33, No. 3, 1994, pp. 217-225.

Tables and Figures

Table I: Main characteristics of previous models of reduction in composites of iron oxides and carbon.

	Kinetic mechanism	Temperature change	Gas transport	Size changes
Sun and Lu[6]	Mixed control	Non-isothermal	Molecular diffusion and forced flow	Not addressed
Rao[2]	Carbon oxidation control	Isothermal	Knudsen diffusion	Not addressed
Tien and Turkdogan[3]	Carbon oxidation control	Isothermal	Molecular diffusion	Not addressed
Sohn and Szekely[5]	Mixed control	Isothermal	Not addressed	Not addressed
Sun and Lu[7]	Mixed control	Non-isothermal	Ergun (laminar)	Not addressed
Wang et al.[10]	Direct reduction	Non-isothermal	Not addressed	Not addressed
Donskoi and McElwain[8]	Empirical arrenius laws	Non-isothermal	Not addressed	Addressed with empirical correlations

Table II: Composition of iron ore used in this work.

Analyte	Mass percent
Total iron	70.13
MnO	0.08
SiO_2	3.38
Al_2O_3	0.12
CaO	0.13
MgO	0.13
P_2O_5	0.01

Table III: Computed values of average shrinkage coefficients for different types of composite pellets.

Mixture	S_h (± 0.04)
Wood charcoal + Taconite	0.78
Wood charcoal + Hematite	0.74
Coal char + Taconite	0.75
Coal char + Hematite	0.73
Graphite + Taconite	0.83
Graphite + Hematite	0.72

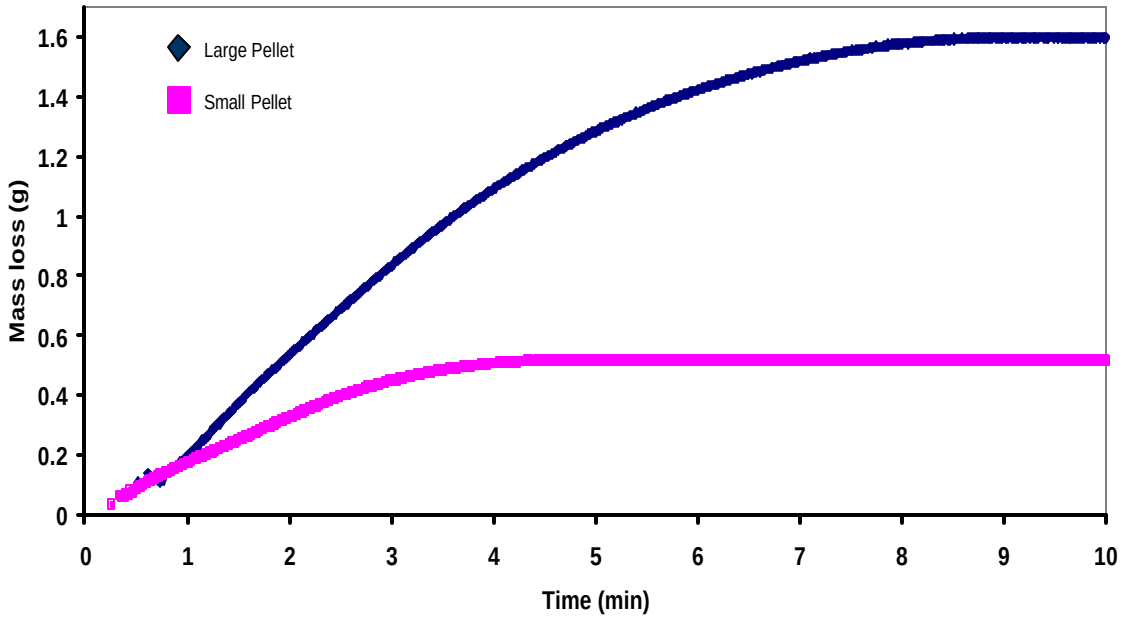

Figure 1: Typical measurements of mass loss with pellets of wood charcoal and hematite (4.04g at 1200^{o}C).

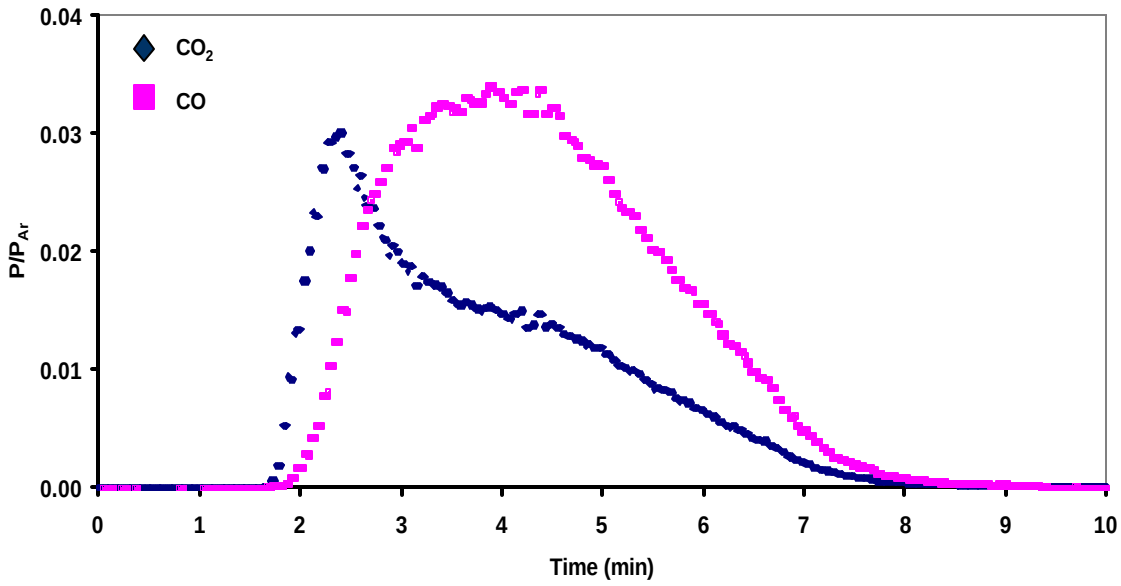

Figure 2: Off gas composition measurements from the experiment with large pellet of wood charcoal and hematite (4.04g at 1200^{o}C).

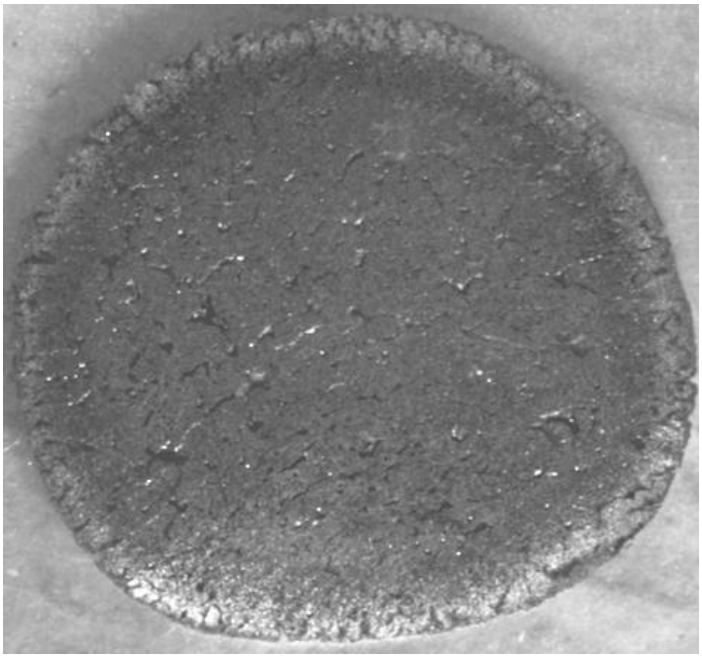

Figure 3. Fracture surface of pellet containing wood charcoal and hematite showing layer of reduced iron close to the surface.

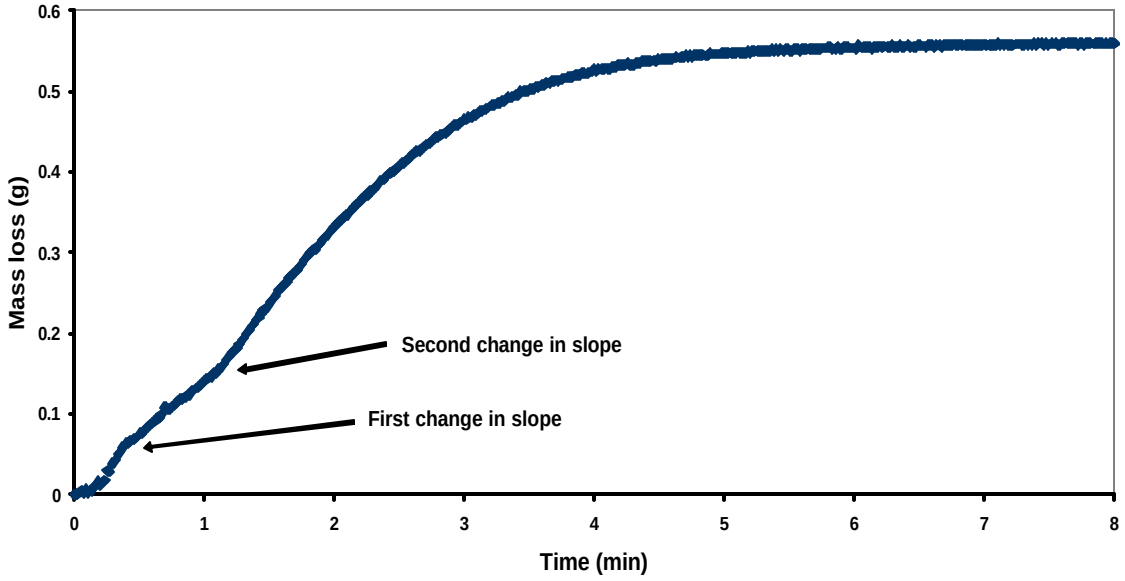

Figure 4: Typical measurements of mass loss with pellets of graphite and hematite showing two changes in reaction rate. (1.4g pellet at 1240^{o}C).

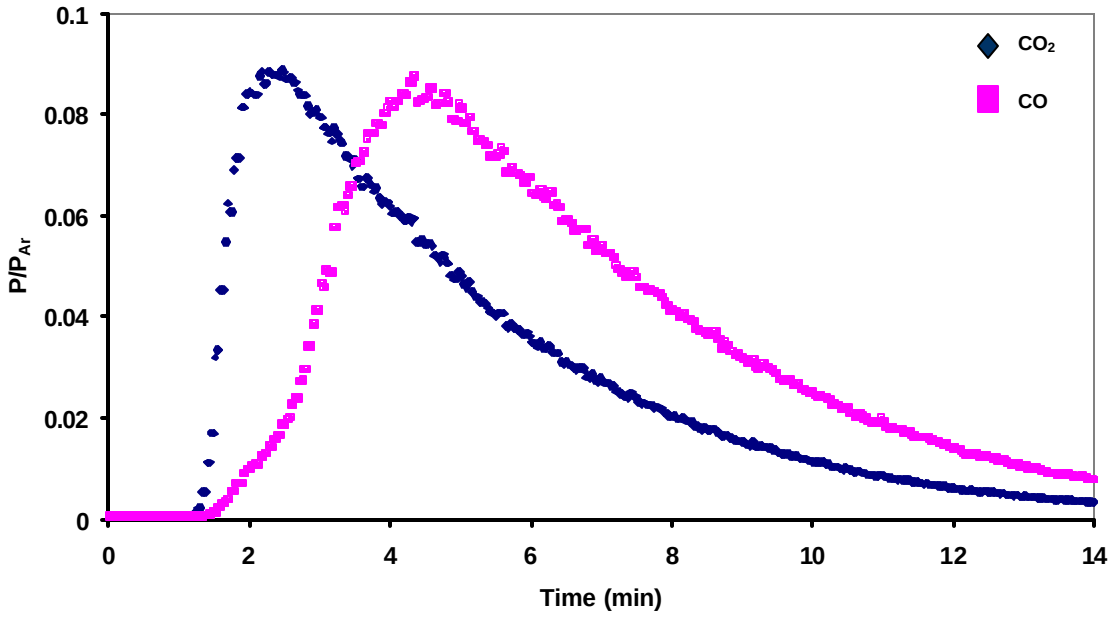

Figure 5: Off gas composition measurements from an experiment with a large pellet of graphite and hematite (3.98g at 1240^{o}C).

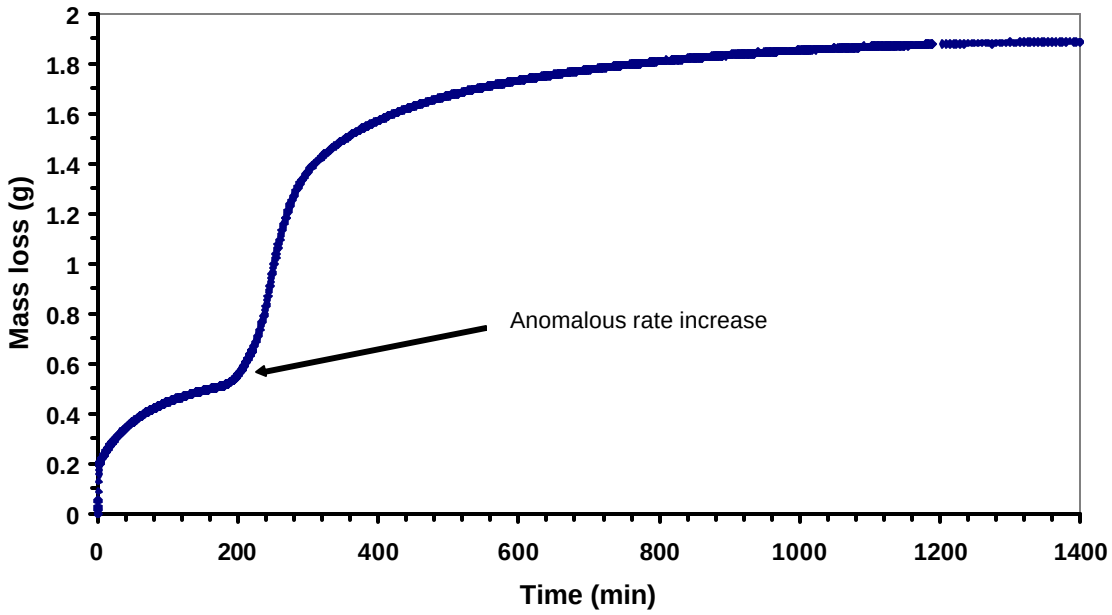

Figure 6: Mass loss measured during reduction of hematite with graphite showing anomalous rate increase. (5.28g at 900^{o}C).

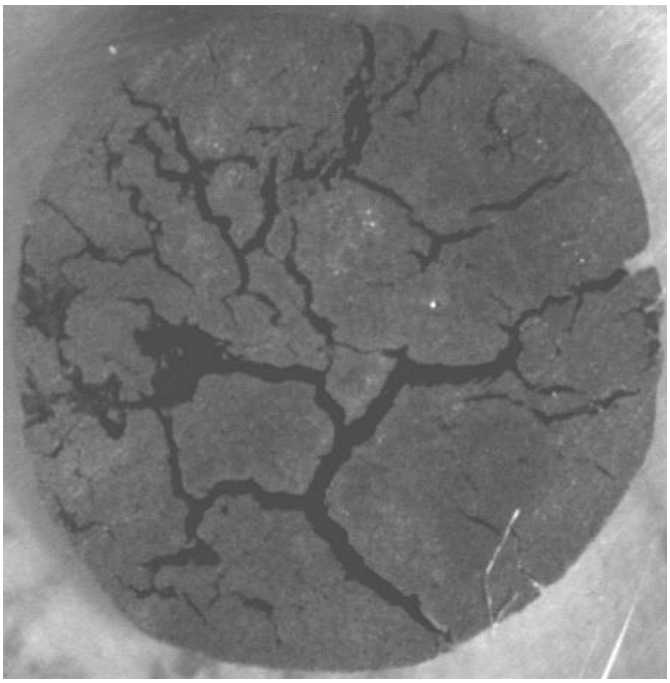

Figure 7: Fractured surface of a pellet of graphite and hematite reduced up to approximately 50% of mass loss showing no appreciable differences in reduction extent.

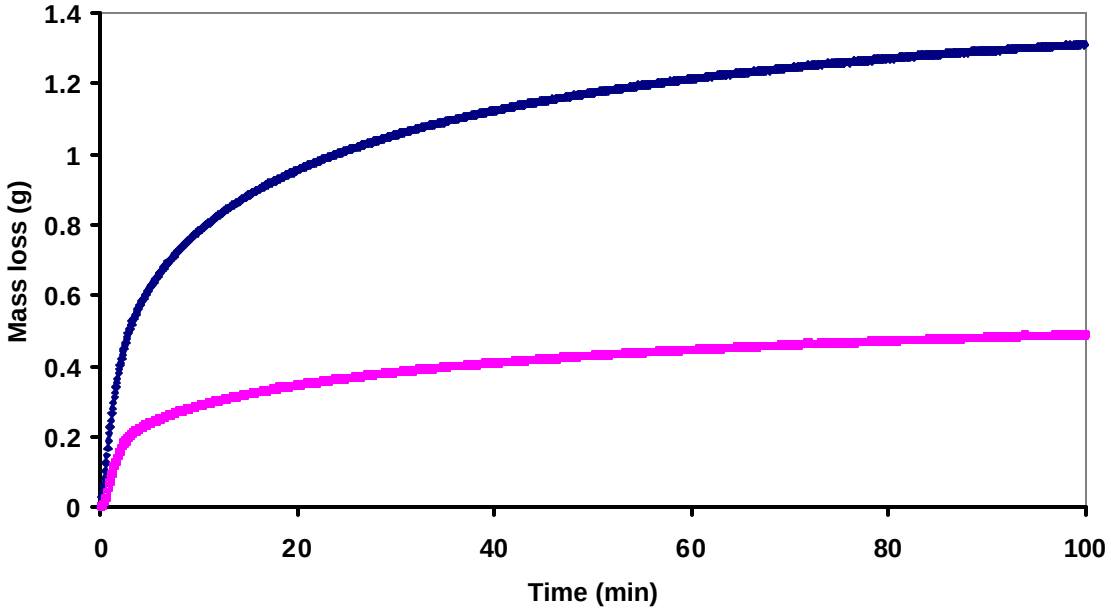

Figure 8: Typical measurements of mass loss with pellets of coal char and hematite at a mass ratio coal char/hematite of 0.177. (Pellets of 4.26 and 1.31g reduced at 1200^{o}C).

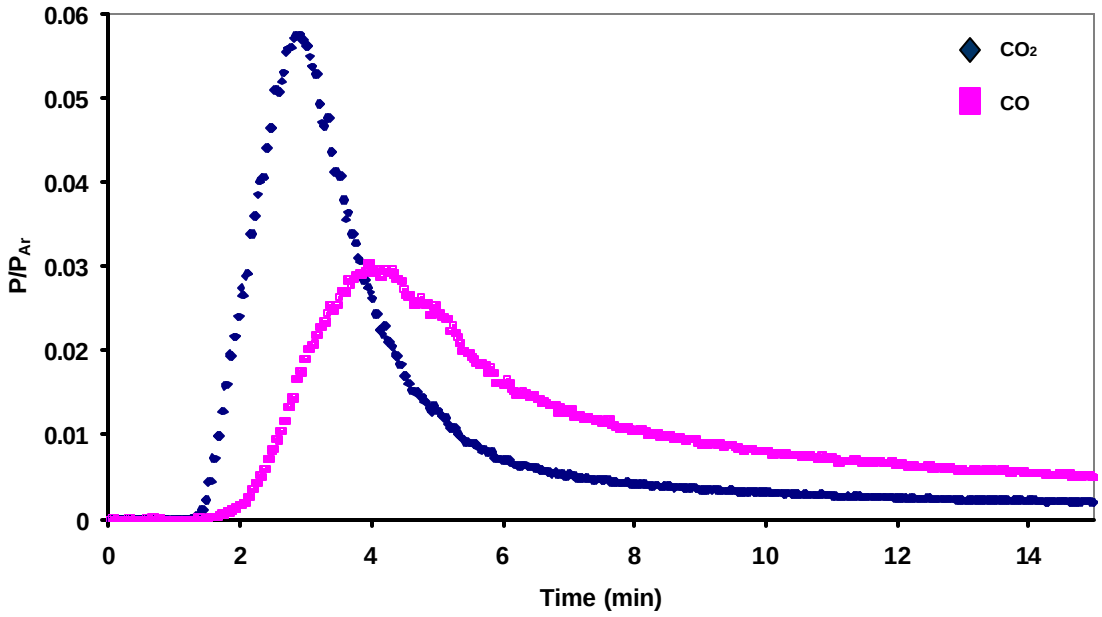

Figure 9: Off gas composition measurements from the experiment with large pellet of coal char and hematite. (4.26g at 1200^{o}C).

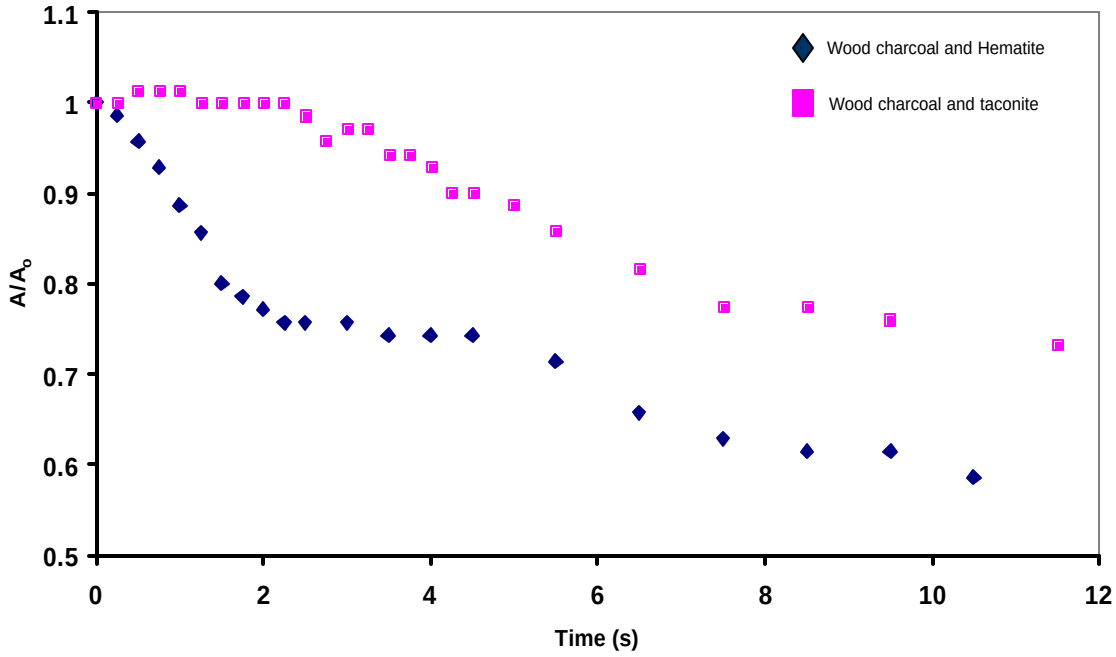

Figure 10: Measurements of cross section area of pellets of wood charcoal and hematite, and wood charcoal and North American Ore showing distinct shrinkage patterns.

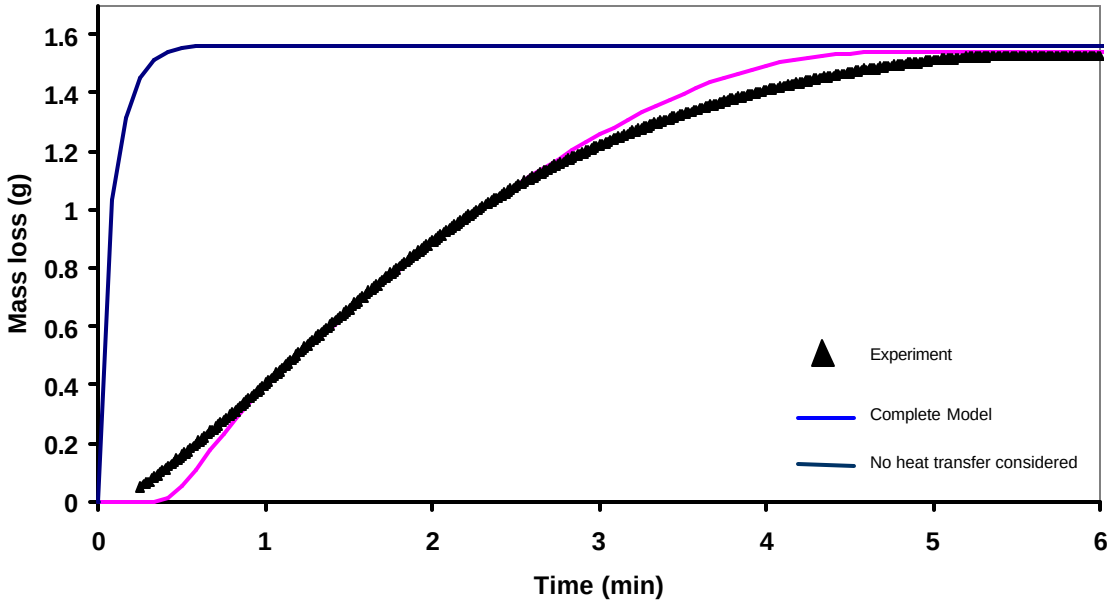

Figure 11: Comparison of experiment and pellet model for a pellet of wood charcoal and hematite. Isothermal model included for illustrative purposes. Large pellet with 3.86g reduced at 1280^{o}C. Wood charcoal/hematite mass ratio of 0.1766.

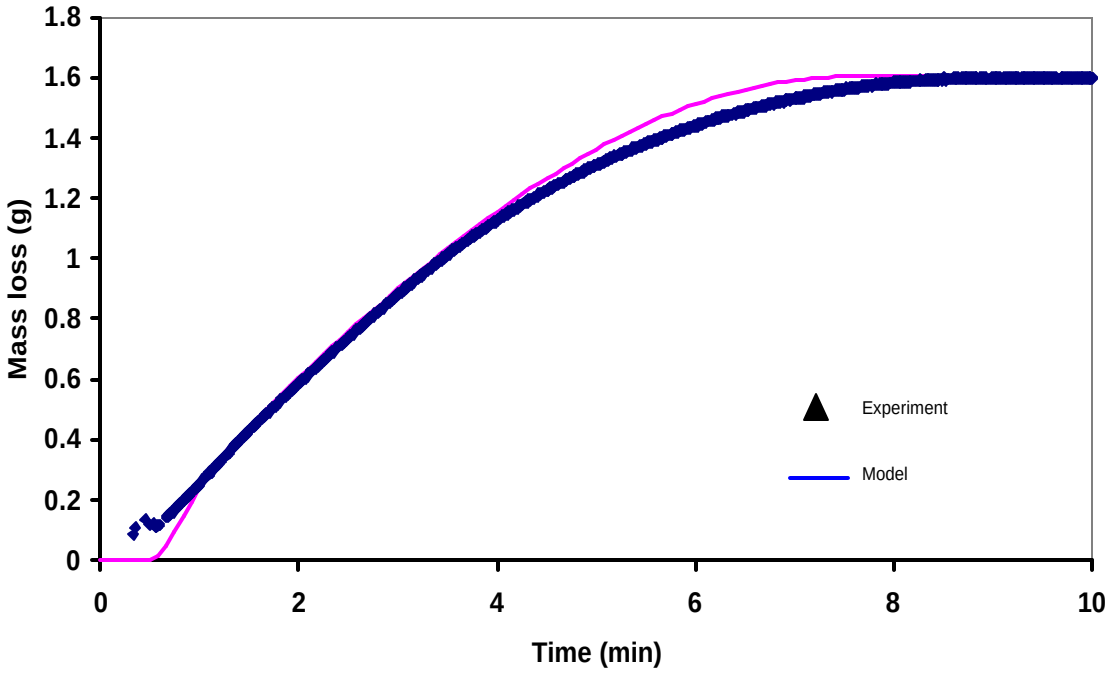

Figure 12: Comparison of experiment and pellet model for a pellet of wood charcoal and hematite. Large pellet with 4.04g reduced at 1200^{o}C. Wood charcoal/hematite mass ratio of 0.1766.

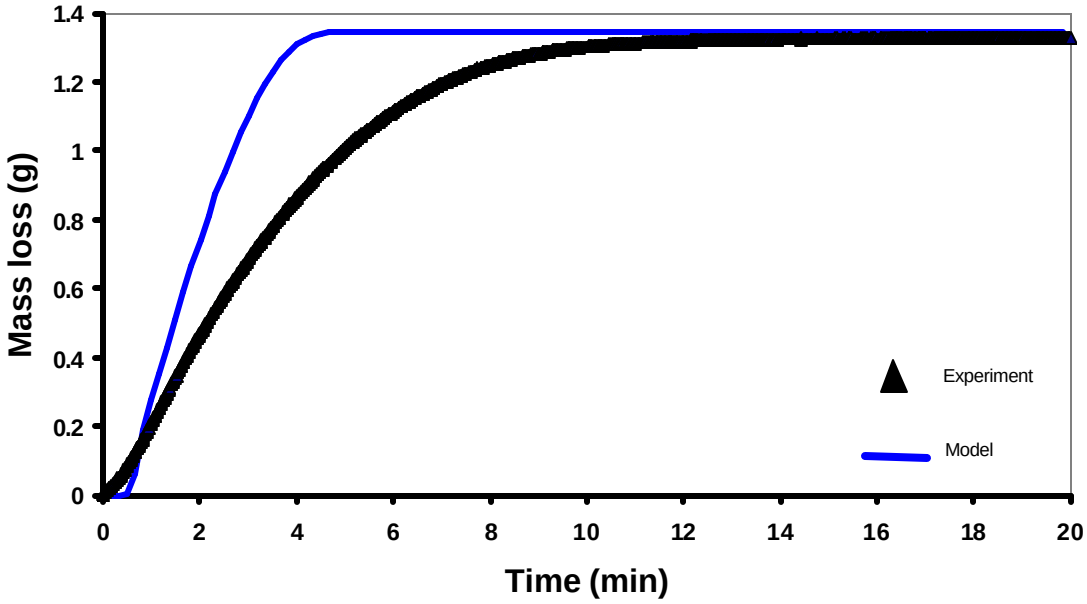

Figure 13: Comparison of experiment and pellet model for a pellet of wood charcoal and ore. Large pellet with 3.97g reduced at 1200^{o}C. Wood charcoal/ore mass ratio of 0.1769.

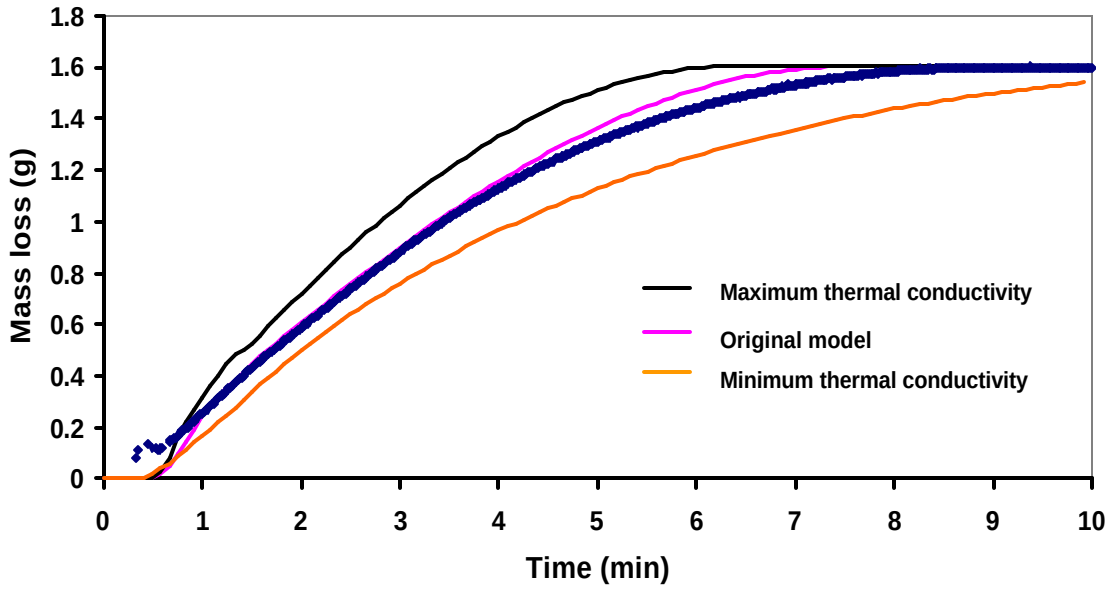

Figure 14: Effect of changes in effective thermal conductivity on model predictions for a pellet of wood charcoal and hematite (4.04g at 1200^{o}C).

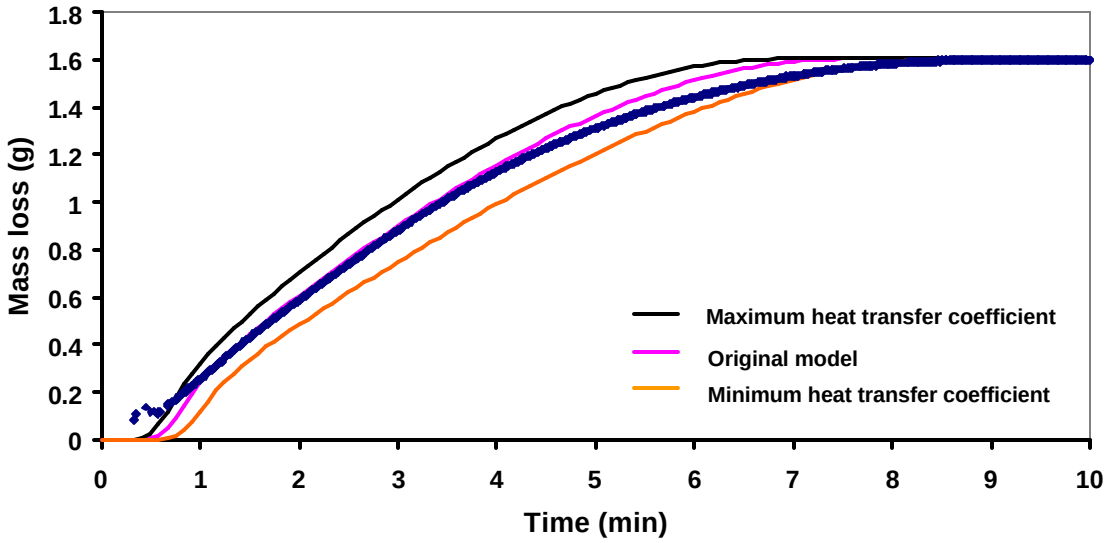

Figure 15: Effect of changes in external heat transfer coefficient on model predictions for a pellet of wood charcoal and hematite (4.04g at 1200^{o}C).

Appendix C – Estimations of RHF Productivity Change

Submitted for publication in Iron and Steel Research

Evaluation of a New Process for Ironmaking: a productivity model for the Rotary Hearth Furnace

Otavio Fortini, Ph.D., Carnegie Mellon University, USA
Richard Fruehan, Professor, Carnegie Mellon University, USA

Abstract

In order to address the key issues of capital costs and CO_2 emissions in ironmaking operations, a new process was proposed combining a Rotary Hearth Furnace (RHF) and a Bath Smelter. This paper describes the construction of a productivity model for the RHF based on previous studies concerning the reduction behavior of pellets of carbon and iron iron oxides. The model was used to estimate changes in RHF productivity according to the type of carbon used in the RHF pellets, numbers of layers of pellets, final metallization degree of the direct reduced iron (DRI) produced, and initial sizes of the pellets. The results indicate that productivity gains between 33 and 46% can be achieved replacing coal with wood charcoal, a carbon source virtually free of net CO_2 emissions. Also, the productivity of the RHF can be doubled by reducing the charge only up to 70% metallization. The model allowed the study of changes in overall energy consumption due to changes in the extent of primary oxidation of the gas at the pellet level showing that the use of wood charcoal increases the total amount of carbon consumed by less than five percent relative to operations with coal.

Keywords: ironmaking, new processes, direct reduction, direct reduced iron, rotary hearth furnace, wood charcoal, renewable energy, carbon dioxide emissions.

Introduction

Over the last fifty years, the specific energy consumption of Ironmaking operations was drastically reduced from over 40 to less than 20 GJ/t of hot metal by means of incremental improvements in conventional Blast Furnace practices. As a paradox to the early times of Ironmaking, modern large Blast Furnaces of high productivity are unsuitable for wood charcoal owing to its low strength and density of this type of carbon. Indeed, current Blast Furnaces using wood charcoal are limited to small units of 400,000 t/year or less. Thus, new ironmaking processes using wood charcoal are desirable owing to the very low net amounts of CO_2 produced using this type of carbon.

With the aim of a niche market of units ranging from 400,000 up to 1,000,000 tons of hot metal a year, a new process was proposed to replace conventional Blast Furnaces. In the new process, a Rotary Hearth Furnace (RHF) would be combined with a Bath Smelter in order to overcome problems associated with each of these two technologies separately. It was shown by practice that Rotary Hearth Furnaces suffer from low productivity in order to achieve high degrees of metallization. For Bath Smelting the hurdle is energy generation when reducing charges directly from ore. In the proposed process, composite pellets of wood charcoal and iron ore would be charged into the RHF and pre-reduced only up to about 70-80% metallization. The semi-metallized product would be taken to the smelting unit where final reduction and gangue separation could be achieved with only a fraction of the energy necessary to reduce the ores in a single step. The off-gas from the Smelter could be used to replace the secondary fuel injected through the burners in the RHF. Wood charcoal is considered as a potential fuel for the new process owing to the relative ease in milling into the powders necessary to the manufacture of the composite pellets used in the RHF. Moreover, cultivated crops of wood charcoal reduce net CO_2 emissions to less than 2% of the emissions of coal based ironmaking.

In this paper, the development of a productivity model for the Rotary Hearth Furnace using coal or wood charcoal is described. In this model, the basic phenomena of chemical kinetics and heat transfer are taken into account as significant in determining the overall rate of production of DRI in the RHF. The consequences of using different

types of carbon in the green balls are identified based on the differences in reactivity of the carbon species.

The Rotary Hearth Furnace: Rotary Hearth Furnaces are currently used in at least six ironmaking technologies: INMETCO, Redsmelt, Iron Dynamics, FASTMET, Sidcomet, and ITmk3. Among these six technologies, only ITmk3 uses the RHF as a stand-alone unit for the production of gangue free metal. In all other processes, the RHF is combined with a secondary smelting facility for gangue removal. The DRI produced is usually taken to an electric arc furnace for final reduction and gangue removal. In the traditional design of RHF technologies such as in the INMETCO and FASTMET, coal and iron oxides are first mixed into green pellets and charged in the RHF as layers of 2 to 3. The DRI produced is removed at the end of one revolution with metallization degrees ranging from 85 to over 90%. In other RHFs, such as Sidcomet, the coal and iron oxides are charged as tall beds of loose but coarser powders and remain in the RHF for considerably longer times. In this type of RHF, the materials remain in the RHF for more than one revolution and are mixed by plows improving heat transfer. In traditional RHFs, the retention time is usually under 20 minutes while in Sidcomet it is close to one hour. In Sidcomet, the final melting and reduction is also done in an electric furnace.

A schematic view of the Rotary Hearth Furnace (RHF) illustrating its main features is shown in Figure 1: a shallow bed of composite pellets on the hearth is depicted under a stream of gas moving in the opposite direction. Energy for reduction comes from the post combustion of the gas from the pellet bed and combustion of extra fuel injected through the RHF roof [1]. Overall reduction rates are determined by the intrinsic kinetics of reduction of the composite pellets along with the ease in transfer of heat from the top gas to the pellets in the reduction bed. Most researchers agree that radiation is the main mode of heat transfer from the top gas to the bed of pellets inside the RHF [2, 3].

In RHF technologies, the extent of post combustion of the upper gas is carefully controlled in order to maximize energy generation and avoid re-oxidation of the DRI [4]. Indeed, the control of the post combustion degree by regulating the amount of oxygen injected into the top gas has apparently brought about several different operational regimes. Franzen [5] described the operation of the first RHF at Elwood City with two main regions according to the degree of post-combustion of the gas. In the first part

immediately following the loading zone excess air or oxygen is injected into the upper gas so that practically all the CO and hydrogen are oxidized to CO_2 and H_2O. In the second part, close to the discharge zone, less oxygen is injected providing for a more reducing atmosphere around the pellet bed. Degel [6] describes recent RHF operation as having three main regions with decreasing oxygen potential from the loading until the discharge zones. These zones could be associated with pre-heating, intermediate reduction, and final reduction of the pellet charge. The largest number of zones and strictest control of oxygen potential in the gas is suggested by Harada et al. [7] with operations using six distinct zones.

Productivity model for the RHF

Model Development: The productivity of an industrial reactor represents the capacity of processing materials according to the size of the facilities available. The productivity of a Rotary Hearth Furnace is usually expressed in terms of the amount of DRI produced per unit time per unit area of hearth or simply Kg DRI/m^2.hour. The metallization degree of the DRI produced is controlled adjusting the speed of rotation of the moving hearth. Usually, pellets span angles close to 270 degrees in 10 to 20 minutes to achieve 90% of average metallization [8]. In this work, a model was constructed aiming at the estimation of changes in RHF productivity according to the types of carbon employed, sizes and number of layers of the pellets used, as well as with RHF operational temperatures. Following the description of Degel [6], the productivity model considers three main reaction zones assigned to the pre-heating, pre-reduction, and final reduction of the pellets. In the model, the transition of the first to the second zone was taken as the limit where the pellets attain a minimum temperature of 600^oC marking the end of pre-heating. During the evaluation of different operational scenarios, the transition between the second and third zones was taken as the first formation of iron corresponding to the end of pre-reduction of the pellets to wustite and, finally, the third zone ends when the pellet bed achieves the desired average metallization degree. Typical temperatures for the gas in each of the three zones were taken from Bauer as 1100, 1280, and 1280^oC respectively [9].

In each zone, the RHF was modeled as two separate parts constituted by the top gas and the bed of pellets. The transfer of heat from the RHF to the surface of the pellets in

the reduction bed was considered due to radiation alone. A view factor of 1 was assumed for the transfer of heat to pellets at the top layer as suggested by Gilbert [3]. Heat transfer and chemical reactions in pellets at each layer in the bed were described with a model previously developed for the reduction of a single pellet [10]. In brief, this model solves transport equations using two main sets of parameters to define reaction rates and heat transfer inside the pellets and computes the overall rates of reduction based on the external conditions of heat transfer to the surface of the pellet. In the model, the external conditions of heat transfer to the pellets are represented by the temperature of the gas in each zone and a radiation heat transfer coefficient encompassing geometric factors and the emittances of pellets and RHF gas. The model of a single pellet is explained in detail elsewhere [10] and was validated against experimental data as exemplified in Figure 2. The transient solution of the pellet model is used to determine the residence times in each zone of the RHF along with other exchange variables such as the amount of radiation heat received by the pellet bed and the amounts of gas expelled by the pellets in each zone. The determination of the residence time of pellets in each zone from the solution of the pellet model is exemplified in Figures 3, 4 and 5. In the case of two or more pellet layers, the same criteria used for the zone limits with a single layer were adopted, however considering all the pellets in the stacking. It should be stressed that, although arbitrary limits were used for the transitions between zones, their choice was made observing the relationship between the external gas atmosphere surrounding the pellets and the reduction reactions occurring inside the pellets in the bed. That is, the division of the RHF in three zones can allow the later consideration of the interplay of mass transfer from the RHF gas to the pellets and reduction reactions taking place inside the pellets. Clearly, in order to avoid reoxidation in areas close to the discharge zone, a lower oxygen potential should be maintained in the gas demanding a lower relative amount of carbon dioxide in the RHF gas.

The first set of fundamental constants used in the model for the estimation of RHF productivity are the intrinsic rate constants for oxidation of carbon in CO_2 and reduction of wustite by CO. In the light of Bodenstein's mechanism [11] of gaseous intermediates, the intrinsic kinetics of reduction of iron oxides by CO and carbon oxidation by CO_2 in composite samples were studied considering a coupled reaction mechanism where both steps are taken into account. The Arrenius parameters defining

the intrinsic reaction rates of the carbons and iron oxides were taken from our previous experimental work and the measurements of Fruehan [12, 13]. The values used in the model are given in Table I. The parameters given in Table I are relative to rate laws of carbon oxidation and reduction of the iron oxides expressed as:

$$R_C = k_C m_C (P_{CO_2} - P^e_{CO_2}) \quad (1)$$

$$R_{FeO} = k_{FeO} m_{FeO} (P_{CO} - P^e_{CO}) \quad (2)$$

where R_C and R_{FeO} are the rates of carbon oxidation and wustite reduction (g/s), k_C and k_{FeO} represent the rate constants of carbon oxidation and reduction of wustite per unit matter of reagent (g/g.s.atm), m_C and m_{FeO} represent the masses of carbon and wustite in the pellets (g), P_{CO} and P_{CO_2} are the pressures of carbon monoxide and carbon dioxide in the system, and P^e_{CO} and $P^e_{CO_2}$ stand for the equilibrium pressures of CO and CO_2 at the operational temperature and pressure. In the model, reaction rate constants for the two reaction steps are computed from the pre-exponential factors (k^o_C and k^o_{FeO}) and apparent activation energies (E_C and E_{FeO}) for the two reaction steps. Equilibrium pressures of CO and CO_2 with carbon and wustite-iron were computed using the data of Barin [14], and Darken and Gurry [15].

The second set of fundamental constants used in the productivity model defines the transport of heat inside the reacting pellets. Base values for the compact phases of iron oxides, iron and carbon were taken from the literature and used to estimate the overall thermal conductivity of the pellets by means of Maxwell's electrical analogy to account for the presence of more than one type of material. The pellet model validated against experimental data from the reduction of pellets containing wood charcoal assumed the electrical analogy of resistances in series for the solid phases in parallel with pores of negligible thermal conductivity, resulting in the following expression for the overall thermal conductivity of the aggregate [16, 17]:

$$b_o = (1 - q_P) \frac{1}{\sum_S b_i / q_i} \quad (3)$$

In (3), b_o represents the overall thermal conductivity of the pellet (cal/cm.s.K), q_P represents the pore fraction of the pellet, and b_i and q_i represent the compact thermal conductivities and volume fractions of all solids present in the pellet. The values used for the thermal conductivity of the compact solids are summarized in Table II [17]. In the calculations, the value of 0.002 cal/cm.s.K taken from an extensive comparative study among many different literature sources was used for the carbons representing values measured for coals and amorphous graphite. The volume fractions of solids and pores in the pellets were estimated from reported values of compact densities and the measurements of size of experimental pellets.

Finally, in order to account for the presence of more than one layer of pellets, it was assumed that the attenuation of radiation introduced by the presence of layers of pellets is proportional to the fraction of hearth area covered by a given layer of pellets. Under this assumption, the heat input to pellets at a given layer (l) from the top is given by:

$$\dot{q} = (1-F)^{l-1}.S.e_P.e_G.(T_G^4 - T_P^4) \qquad (4)$$

where $\dot{q}$ is the instantaneous heat flux to the surface of the pellets in layer l, F is the shielding factor representing the blocking of radiation by layers above layer l, S is the view factor from the RHF gas to the surface of the pellets at the top of the reduction bed, e_P and e_G are the emittances of the pellets and RHF gas, T_G is the temperature of the RHF gas in a given zone, and T_P is the surface temperature of the pellets in a given layer l. In agreement with Gilbert, the view factor (S) to the pellets at the top layer was taken as one. An estimation of emittances of gas inside the RHF was attempted considering mixtures of CO, CO_2, H_2, and H_2O using the measurements of Hottel [18] resulting in a range from 0.25 to 0.65. However, as noted by that author, the presence of soot materials in the gas may significantly increase its emittance. Emittances reported for iron oxides and carbon are higher than 0.8 in the range of temperatures of interest [19]. Therefore, owing to the lack of certainty regarding the emittances of gas and pellets in the RHF, a product of emittances of one was used during the simulations. This

approximation should introduce little error in the calculations as evidenced by simulations of reduction of coal pellets as discussed next. The model developed is not expected to predict the exact production rates due to the lack of certainty regarding the parameters defining the external conditions of heat transfer. However, the model should predict the relative productivity rates for different operating conditions such as the carbon type and degree of reduction required.

Comparison to operations: In order to evaluate the effectiveness of the productivity model developed, simulations of reduction of pellets with coal were done and compared to the range of 70 to 90 Kg DRI/m^2.hour at 92% metallization commonly reported in the literature. Figure 6 shows results of simulations of RHF operations using beds with different numbers of layers of coal pellets at different initial pellet sizes. As can be seen in the Figure, the model slightly overestimates the productivity of the RHF for beds with one and two layers of pellets at typical RHF operating temperatures. This slight overestimation may be due to the overestimation of the external transport of heat as mentioned in the previous paragraph. Other causes for the overestimation of production rates may be differences in reactivity of the coals used in laboratory experiments and in actual industrial practice or a change in the chemical rate controlling mechanism towards the end of reduction. Indeed, the model developed for single pellets does overpredict reaction rates above 90% reduction owing to the possible shift in rate-controlling step of the reduction mechanism. In the small powders used in the pellets (-200 mesh), the reduction of the iron oxides may become partially controlled by solid state diffusion above 90% of conversion to iron. Regardless of the cause for the slight overestimation of productivity, Figure 6 shows that the deviations found are small so that the model can be used to provide indications as to the general behavior of the RHF according to operational parameters.

Effect of operating conditions: Using the model developed, changes in productivity were estimated for operations using different carbon types, final metallization degrees, numbers of layers, and initial sizes of pellets. The effects of changing the initial pellet sizes are a good illustration of the complex interplay of heat transfer and chemical kinetics determining the overall production rate of an RHF. Figure 7 shows results from simulations of operations using one and two layers of pellets with different initial radii. As can be seen in the Figure, there is apparently a maximum production rate attained at

about 0.7 cm radius when using a monolayer of pellets of wood charcoal. In simulations with a single layer, this maximum is explained solely by the interplay of chemical kinetics and propagation of heat inside the pellets. At sizes smaller than the optimum, chemical kinetics is more important than heat transfer so that extra material can be added to the reduction bed with a beneficial effect on the production rates. On the other hand, at radii larger than 0.7 cm, the transfer of heat is hindered by the addition of extra material to the pellets resulting in lower production rates. It is interesting to notice that such maximum occurs at slightly larger radii in simulations pertaining to coal pellets, where the maximum takes place at circa 0.8 cm. This should be expected since this carbon is less reactive than wood charcoal so that larger pellets are required to increase the relative importance of heat transfer to the overall rate of reduction.

Calculations for different degrees of metallization in the final DRI were done in order to estimate possible productivity gains achieved by limiting the degree of pre-reduction in this reactor. Figure 8 summarizes the results for pellets with coal and wood charcoal. These results were obtained by taking the best operational condition according to the number of pellet layers and initial radius of the pellets at each desired final metallization degree. For instance, while RHF operations with coal are apparently always best with two layers of pellets, operations with a single layer of pellets with wood charcoal may improve the overall productivity at metallization degrees higher than 0.8. At a same final degree of metallization, productivity improvements estimated by the replacement of coal with wood charcoal are between 33 and 46% relative to the operations with coal. This productivity increase is significantly less than should be expected from the comparison of the chemical kinetics of oxidation of coal and wood charcoal; at temperatures close to the temperatures of RHF operations, the rates of oxidation of wood charcoal in CO-CO_2 are four to six times faster than the rates of oxidation of coal. The slower rates actually achieved with pellets are due to the influence of heat transfer and possibly the kinetics of reduction of the iron oxides; the productivity of the RHF is not increased fourfold when replacing coal with wood charcoal as should be expected from the comparison of their oxidation constants alone. However, the productivity gains between 33 and 46% still represent a considerable improvement over traditional coal based RHF operations. In the new process, where reduction may be done employing wood charcoal and limited to 70% of metallization, the productivity of

the RHF can effectively double in comparison with traditional coal based operations producing DRI at over 90% of metallization.

Estimating the Carbon Consumption of a Rotary Hearth Furnace

In most ironmaking operations, carbon is used as reductant as well as energy source. In an RHF, carbon in the green balls is used as reductant and extra energy provided by post-combustion of the gas coming from the pellets and also by combustion of extra fuel injected through secondary burners. While the overall carbon necessary depends on the post combustion of the top gas, the extent of primary oxidation of the gas leaving the pellets determines the amount of extra energy that must be transmitted from the top gas to the reduction bed. An estimation of the extra amounts of energy from the top gas necessary to reduce the pellets according to the extent of primary oxidation shows that about 493 KJ per mole of Fe_2O_3 must be provided if no primary oxidation is achieved (i.e. if the gas leaving the pellets is pure carbon monoxide). On the other hand, if complete primary oxidation were possible and the gas leaving the pellets were pure CO_2 only an extra 234 KJ would be necessary to reduce one mole of Fe_2O_3 to iron. That is, if the gas leaving the pellets could be completely oxidized to CO_2, only half of the extra energy necessary with no primary combustion would have to be supplied from the top gas.

The extent of primary oxidation of the gas is determined by the thermodynamics as well as by the kinetics of reduction. Thermodynamics determines the minimum relative amounts of CO in the gas inside the pellets to make reduction reactions favorable. Ultimately, the kinetic mechanism resulting from the competing reactions of carbon oxidation and reduction of the iron oxides determines the extent of primary combustion achieved. Unfortunately, the kinetics of reduction cannot be varied at will; it is determined by the rates of reaction of the carbon and iron oxide used. The relative amount of CO in the gas from the pellets increases with increasing reactivity of the carbon employed. For this reason, an analysis of the changes in the extent of primary combustion of the gas due to the replacement of coal with wood charcoal was done in order to estimate the increase in extra energy necessary when using wood charcoal. In this analysis, the oxidation degree (OD) was defined in analogy with the definition of the post combustion degree as:

$$OD = \frac{P_{CO_2}}{P_{CO_2} + P_{CO}} \quad (5)$$

where P_{CO_2} and P_{CO} are the pressures of carbon dioxide and carbon monoxide in the gas leaving the pellets. Estimated average ODs for producing DRI 90% metallized using coal were between 0.39 for a single layer of pellets up to 0.42 using three layers of pellets. At the same final degree of metallization, estimated ODs for pellets using wood charcoal were between 0.34 for a single layer and 0.36 for operations using two layers of pellets. These estimates were computed considering the total amounts of CO and CO_2 produced during the complete processing of the material in the RHF. As a general trend regardless of the carbon type used, the average OD increases with increasing initial pellet sizes and number of pellet layers used. This should be expected since the temperatures in the reduction bed will be lower with the increase in these two parameters. Figure 9 presents the comparison of average OD estimates for operations with coal and wood charcoal corresponding to the points of maximum productivity according to pellet sizes and number of layers discussed previously. Figure 9 shows that the average OD estimated for operations with wood charcoal is lower than estimated for operations using coal as the reductant. This should also be expected since larger amounts of CO are present in pellets with wood charcoal owing to the faster kinetics of wood charcoal oxidation. As seen form Figure 9, a change in OD between 10 and 16% relative to operations with coal is estimated for operations with wood charcoal at a same final degree of metallization. The change in extra amount of energy necessary in the reduction bed due to this change in primary oxidation degree can be estimated considering the overall reduction reaction:

$$Fe_2O_3 + aC \rightarrow 2Fe + bCO + cCO_2 \quad (6)$$

Where a, b and c are stoichiometric coefficients defined by the ratio of CO/CO_2 in the product gas. Disregarding the latent heats associated with the increase in gas temperature, equation (6) and the OD estimates of Figure 9 indicate that an extra 0.10 to 0.16 GJ per ton of metallic iron must be provided to the reduction bed when changing from operations using coal to operations using wood charcoal. This is a small change

compared with the total energy input necessary to the reduction bed, ranging from 2 to 4.5 GJ per ton of metallic iron produced. This range of absolute minimum extra energy necessary was computed considering only the heat involved in the reduction reaction (6) so that any other possible heat sinks introduced by the presence of gangue or heat up of gases will provide for even higher estimates. This calculation shows that the relative increases in bed energy demands substituting coal with wood charcoal is between 3 and 5% of the bed energy demands of coal. Adopting an energy equivalence of 32.72 GJ to one ton of carbon provides for rough estimates of a necessary extra 3 to 6 Kg carbon per ton of metallic iron produced, representing less than 5% of the total carbon necessary for processing pellets with coal. It should be born in mind, though, that the extra carbon actually necessary for the operations may be lower than the amount estimated considering only the increase in bed energy demands. Off-gas from the pellet bed can be post-combusted at the top of the RHF providing for better energy use. That is, while a slight increase in the energy required by the bed is brought about by the replacement of coal with wood charcoal, the overall energy necessary for the process may be the same or even lower depending on the maximum operational degree of post combustion of gas inside the RHF. The estimate of extra 3 to 6 Kg of carbon per ton of DRI represents an estimate of the maximum increase in carbon demands.

Conclusions

A productivity model was developed for the Rotary Hearth Furnace combining the chemical kinetics of reduction and heat transfer. Results from this model showed that replacing coal with wood charcoal as reductant in the RHF can provide significant productivity gains, from 33 to 46% relative to operations using coal. This gain is less than anticipated from an analysis considering only the differences in reactivity between wood charcoal and coal, but still quite significant. The model indicates that the optimum pellet sizes for maximum productivity are larger for pellets using coal than for pellets using wood charcoal. A brief analysis of the change in energy requirements of the RHF due to the change in carbon used as reductant showed that, although less CO_2 is present in the gas from the reduction bed with wood charcoal, the overall increase in energy demands of the reduction bed compared with operations using coal is small estimated as less than 5% of the total carbon necessary.

References

[1] R. Shultz, F. Piergiorgio, H. Lehmkuhler: “REDSMELT: an alternative ironmaking technology to improve economics and environmental compatibility for pig iron production”, Proceedings of the Metec Conference, July 1999, Dusseldorf.

[2] J.K. Pargeter and H-J. Lehmkuhler: “Recycling of waste and flue dust from the steel industry into hot metal, using the Inmetco process”, Proc. ISS/AIME Conf. on Disposal, Recycling and Recovery of Electric Furnace Exhaust Dust, 1987, Chicago, Illinois, pp. 121-126.

[3] D. Gilbert: “Coal based DRI: know the questions/get the answers”, Gorham Intertech Conference on Iron Ore for Alternative Iron Units, October 25-27, 1999, Charlotte, NC.

[4] R. Degel, P. Fontana, G. DeMarchi, H-J. Lehmkuhler: Stahl und Eisen 120(2000) No. 2, p. 33-40.

[5] H. Franzen, W. Reichelt, G. Rottmann, H. Vorwerk: Steel Times International, sept 1984, p. 44-48.

[6] R. Degel: Steel Times International, may 1999, p. 18.

[7] T. Harada, H. Tanaka, H. Sugiatsu, Y. Kuwata: Kobelco Technology Review, oct. 2001, No. 24, p. 26- 31.

[8] G.E. Hoffman: “A closer look at FASTMET and FASTMELT”, Proc. Electric Furnace Conference, Iron and Steel Society of AIME, 2000.

[9] K-H. Bauer, K. Grebe, H-J. Lehmkuhler, H. Vorwerk, H.G. Rosenstock, H. Schmauch: Stahl und Eisen 110(1990), No. 7, p.89-96.

[10] O.M. Fortini, and R.J. Fruehan: submitted for publication in Met. Trans. B.

[11] M. Bodenstein: Trans. Am. Electr. Soc. 51(1927), p. 365/76.

[12] O.M. Fortini, and R.J. Fruehan: submitted for publication in Met. Trans. B.

[13] R.J. Fruehan: Met. Trans. B, vol. 8B(1977), p. 279/86.

[14] I. Barin, O. Knacke, and O. Kubaschewski: “ Thermochemical properties of inorganic substances”, 1st ed., Springer-Verlag, New York, 1973.

[15] L.S. Darken, R.W. and Gurry: Jour. Am. Chem. Soc., vol. 67(1945), p. 1398-412.

[16] R.B. Bird, W.E. Stewart, and E.N. Lightfoot: ”Transport Phenomena”, 1st ed., John Wiley & Sons, New York, 1960.

[17] F. Kreith, and W. Black: “Basic Heat Transfer”, 1st ed., Harper&Row, New York, 1980.

[18] H.C. Hottel, and A.F. Sarofim: “Radiative Transfer”, 1st ed, McGraw-Hill, New York, 1967.

[19] Y.S. Touloukian: “Thermophysical Properties of High Temperature Solid Materials”, 1st ed., The MacMillan Company, New York, 1967.

Table I: Arrenius parameters used to compute rates of oxidation of carbon and reduction of wustite during simulations of reduction in the RHF.

	k_C^o (g/g.s.atm)	E_C (Kcal/mol)
Coal char	3.41×10^{12}	93.4
Wood charcoal	2.46×10^{11}	81.0

Table II: Correlations and values used for the estimation of physical properties of solids used in the modeling RHF pellets.

	C_P (cal/mol.K)	H_{298} (Kcal/mol)	Density (mol/cm^3)	Molecular mass (g/mol)	k (cal/cm.s.K)
Carbon	4.635	0.0	0.1842	12.0	0.002
Fe_2O_3	35.02	-197.3	0.03275	159.7	$12.97/T$
Fe_3O_4	50.86	-267.3	0.02233	231.55	$14.12/T$
"FeO"	13.75	62.38	0.076	71.85	$2.39 \times 10^{-3}/(2.355 \times 10^{-4}\ T + 0.1136)$
Fe	8.852	0.0	0.1407	55.85	$1.0/(2.6 \times 10^{-5}\ T + 0.00975)$

C_P: molar thermal capacity.

H_{298}: standard molar enthalpy at 298 *K*.

T: absolute temperature (*K*).

k: compact thermal conductivity.

Table III: Initial characteristics of pellets used in simulations of RHF operations.

Coal pellets		
	Radius (cm)	0.834
	Mass (g)	4.2602
	Composition (mass fraction)	Coal: 0.15
		Hematite: 0.85
Wood charcoal pellets		
	Radius (cm)	0.848
	Mass (g)	4.0426
	Composition (mass fraction)	Wood charcoal: 0.15
		Hematite: 0.85

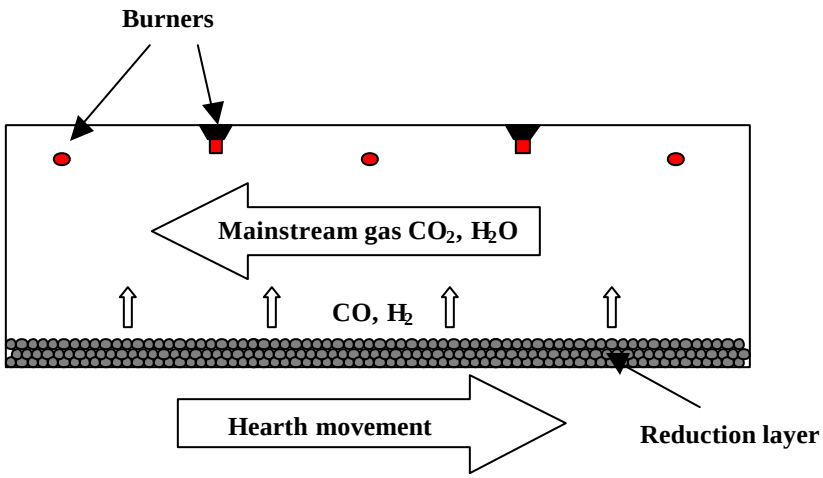

Figure 1: Rotary Hearth Furnace.

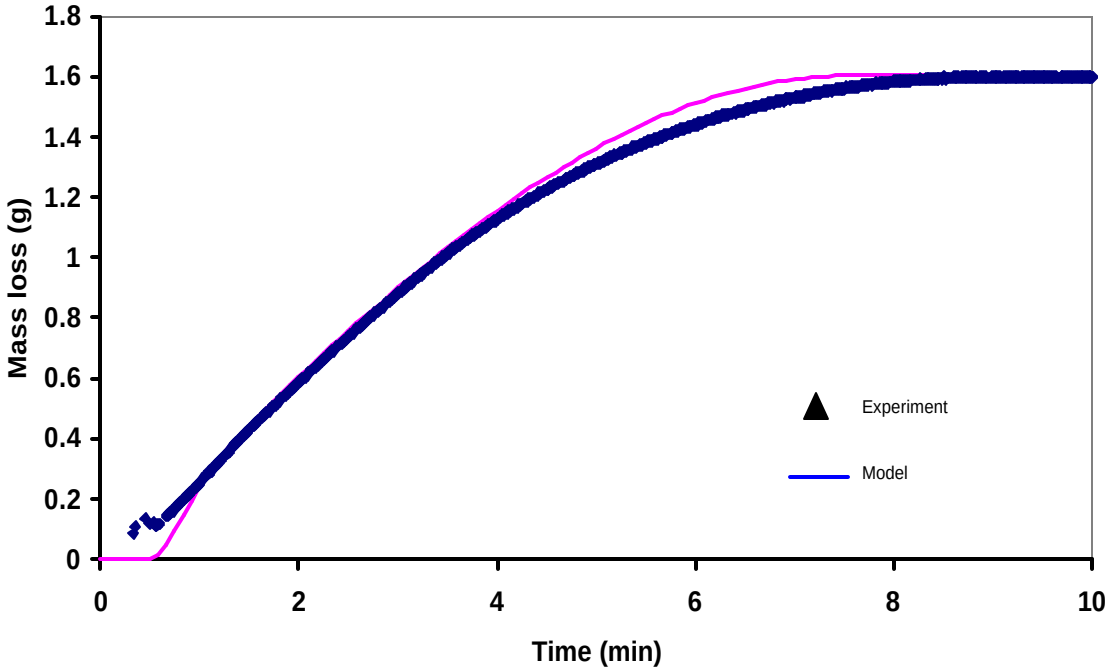

Figure 2: Example of validation of model developed for single pellets with laboratory measurements of reaction rates. Large pellet of 4.04g with wood charcoal and hematite reduced at 1200^{o}C. Wood charcoal/hematite mass ratio of 0.1766.

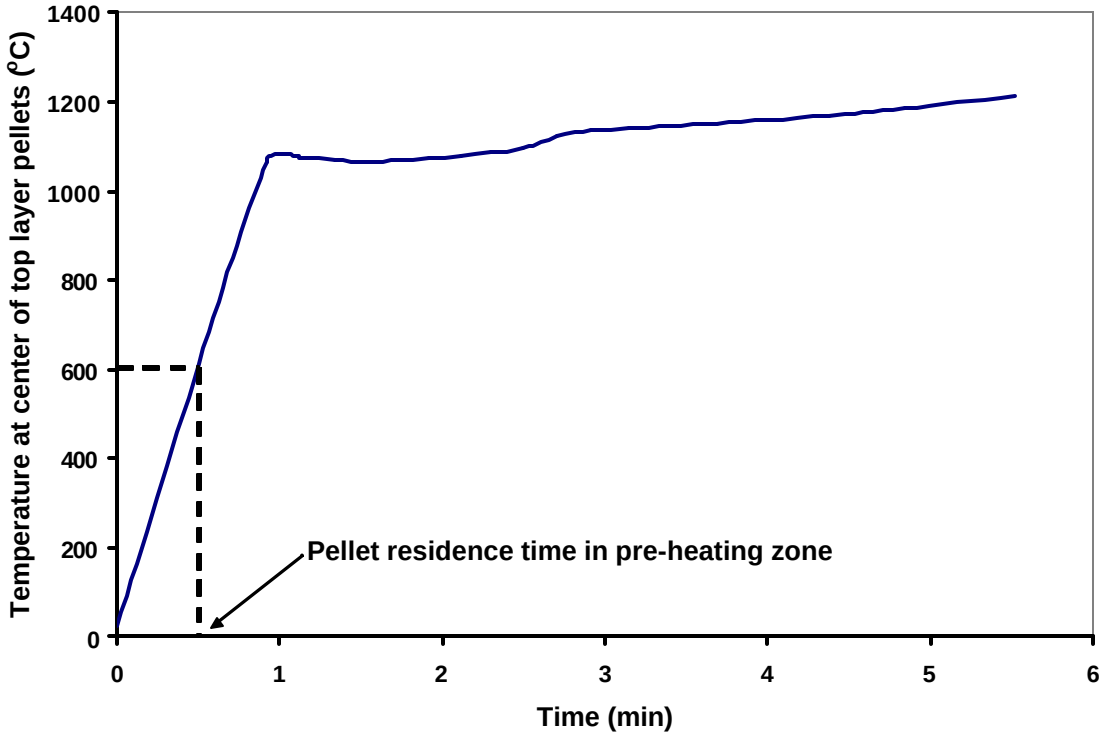

Figure 3: Example of determination of residence time in pre-heating zone considering a single layer of pellet with pre-heating temperature of 600°C.

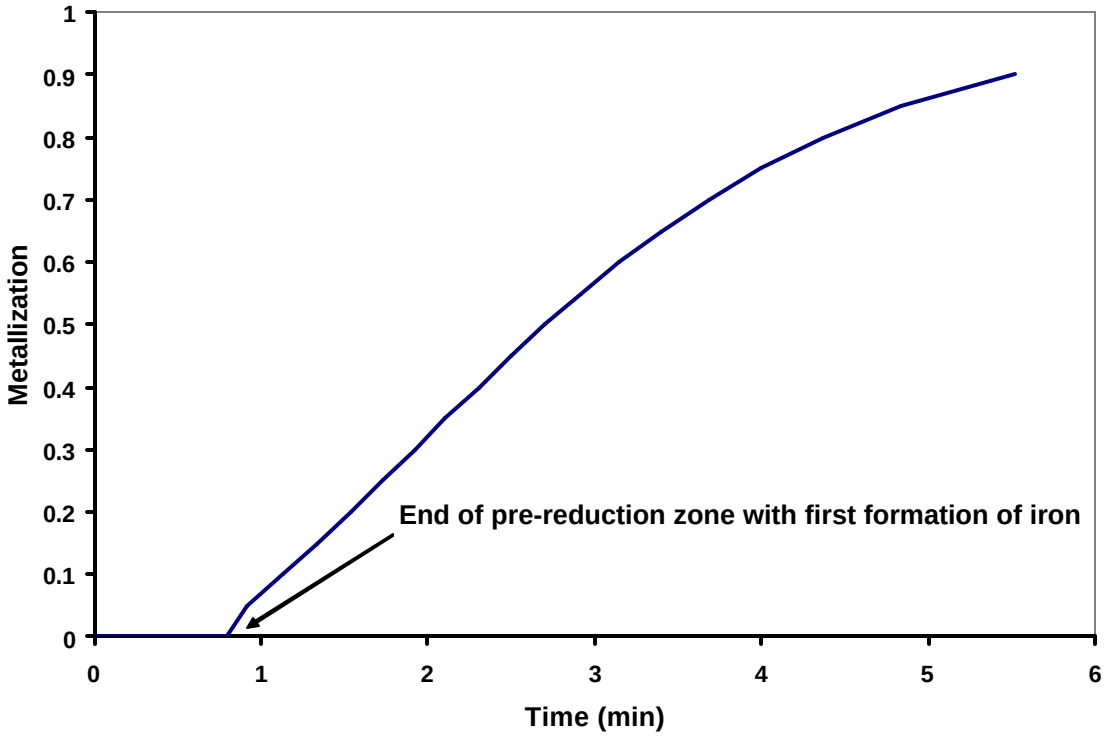

Figure 4: Determination of residence time in pre-reduction zone based on the limit of first formation of iron using a single layer of pellets containing wood charcoal and hematite.

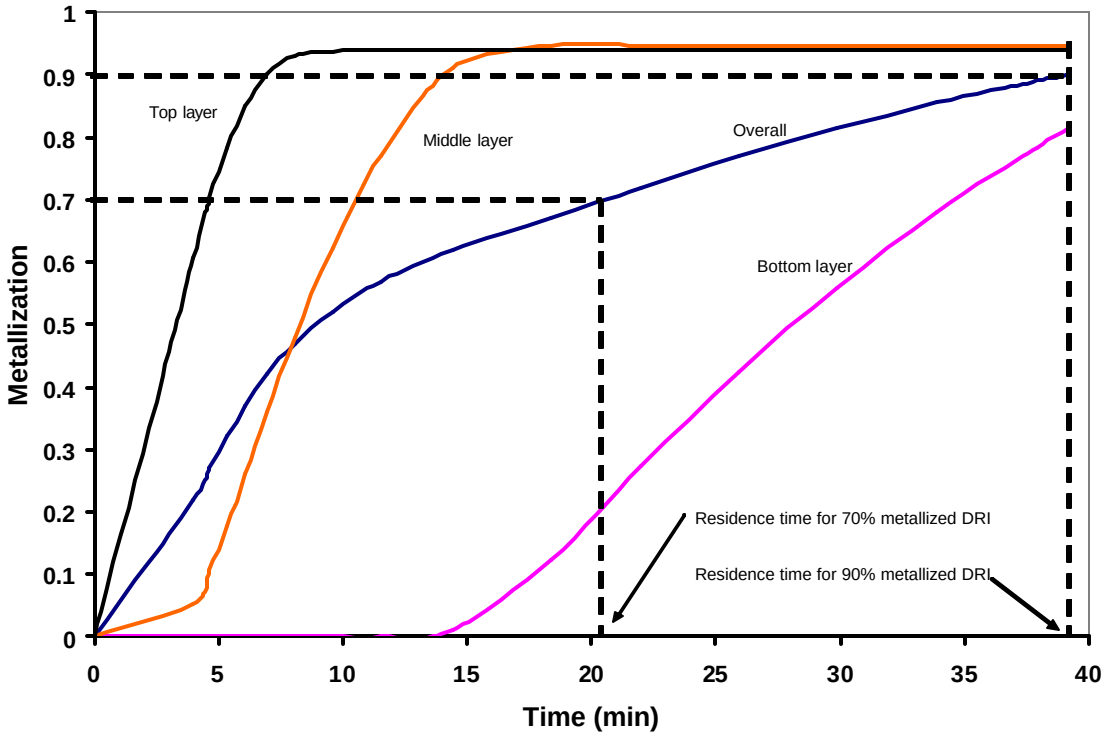

Figure 5: Example of determination of total residence time in RHF according to final metallization degree of charge considering three layers of pellets.

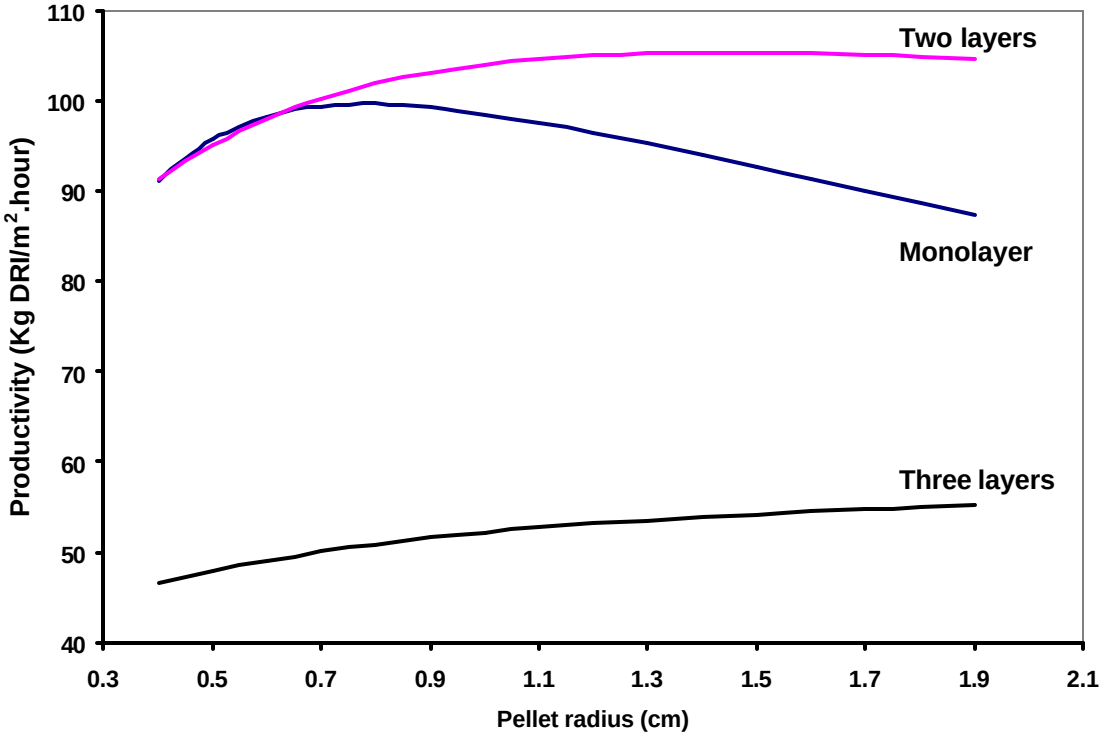

Figure 6: Predictions from the productivity model developed employing coal as reductant for typical RHF operational conditions. Reported productivities of RHF operations are usually between 70 and 90 Kg DRI/m^2.hour at 90% metallization.

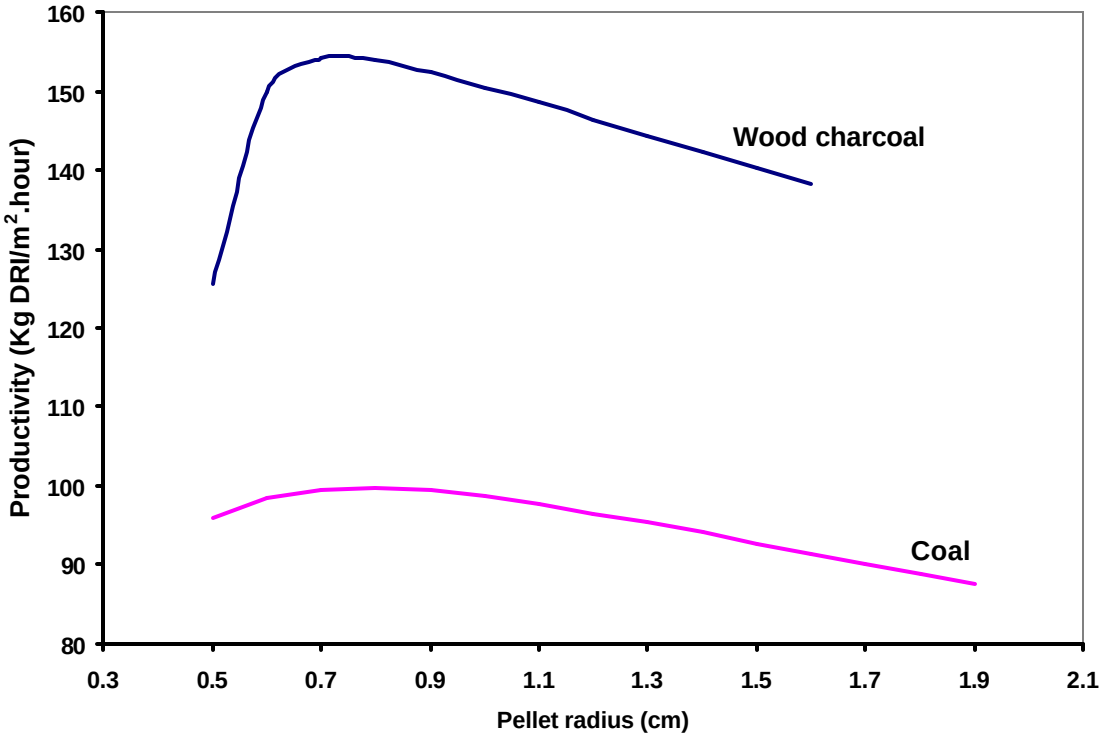

Figure 7: Results from simulations of operations using a monolayer of pellets containing coal or wood charcoal as reductant producing DRI 90% metallized.

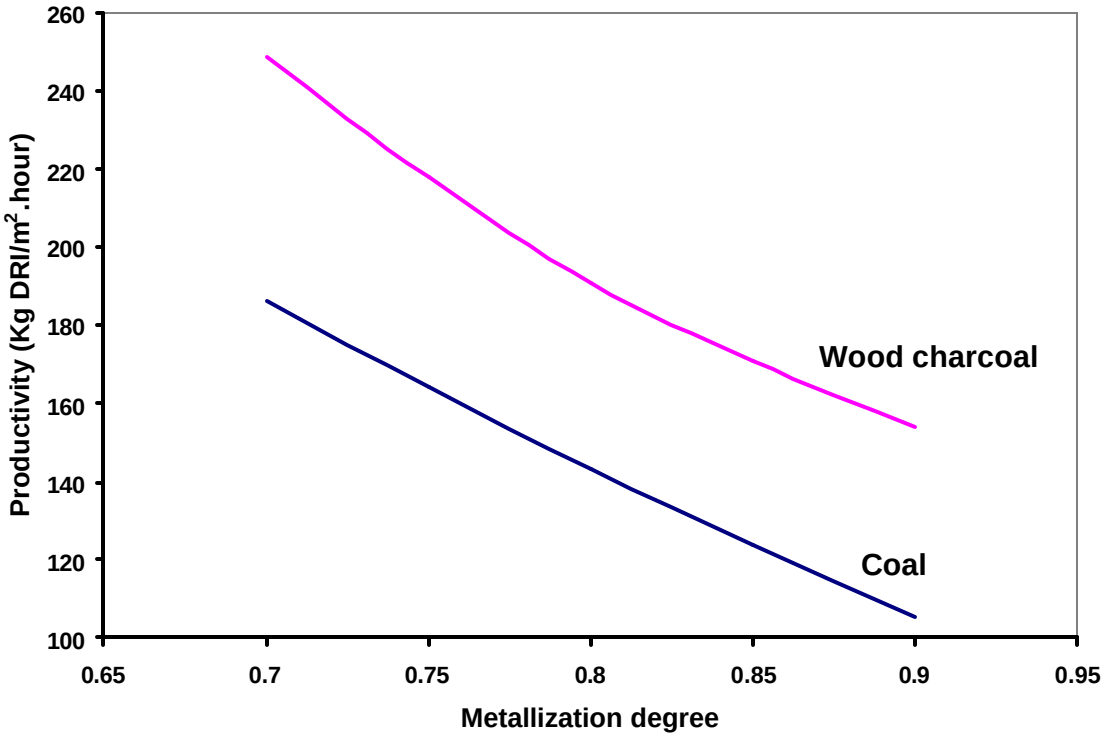

Figure 8: Estimated change in productivity of RHF operations according to metallization degree using coal or wood charcoal as reductant.

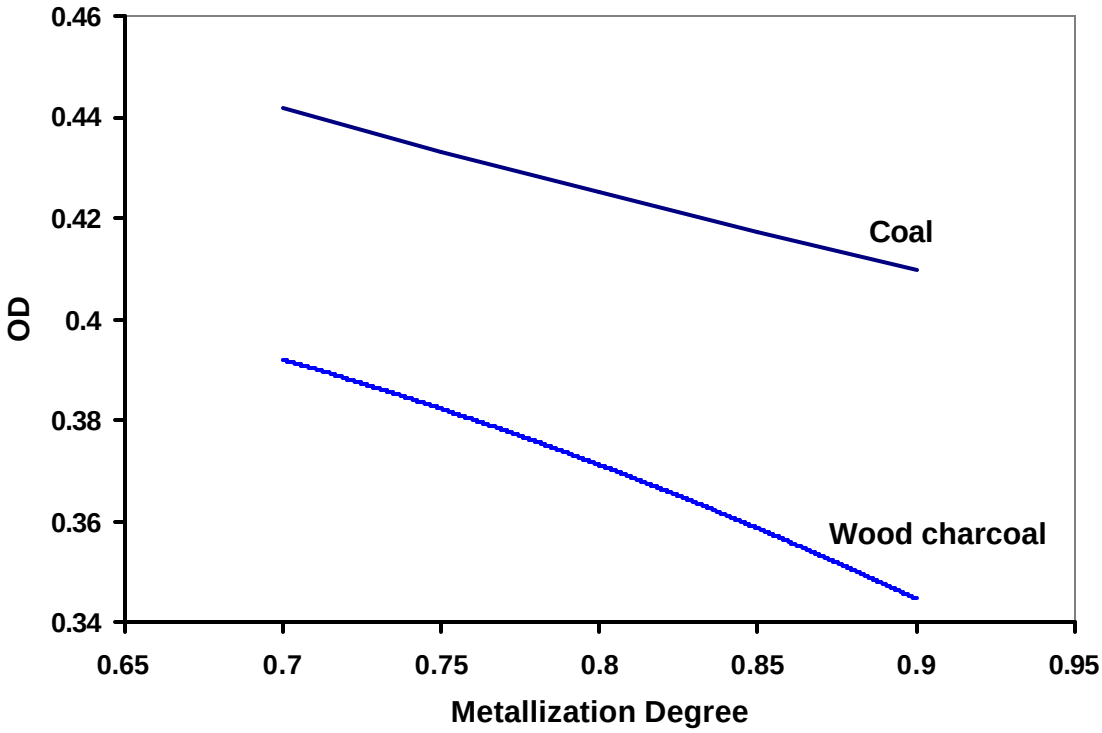

Figure 9: Comparison of estimated primary oxidation degree of gas in RHF for operations using coal and wood charcoal at optimum production rate.